TARGETING THE NEONATAL FC RECEPTOR, FCRN, TO TREAT AUTOIMMUNITY

AND ELUCIDATION OF SITES OF FCRN FUNCTION

APPROVED BY SUPERVISORY COMMITTEE

E. Sally Ward, Ph.D.

Robert Eberhart, Ph.D.

Benjamin Greenberg, M.D.

Anne B. Satterthwaite, Ph.D.

Olaf Stüve, M.D., Ph.D.

DEDICATION

To Mom and Dad

I would like to take this opportunity to acknowledge and appreciate the constant cooperation and support provided by various people without which my Ph.D. would have not been possible.

I would like to start by thanking my mentor, Dr. E. Sally Ward, who entrusted me with the research projects described in this dissertation. I also thank her for teaching me important research skills and for helping me realize the potential of FcRn-targeting and antibody engineering to treat autoimmune and other diseases. Importantly, her perseverance and patience with respect to solving research problems has been, and will continue to be, an inspiration for my research career. I would like to mention special appreciation for the freedom that Dr. Ward provided in carrying out my research. Under her mentorship, I have grown professionally as well as an individual. I wish to also thank Dr. Raimund J. Ober for the resources, scientific discussions, suggestions and support he provided during the course of my graduate studies. I am grateful to my dissertation committee members, Drs. Robert Eberhart, Benjamin Greenberg, Anne B. Satterthwaite and Olaf Stüve for dedicating their valuable time and for providing helpful suggestions and perspectives on my research.

I will be indebted for life to my parents (Mohini Venkata Nageswaramma and Ramesh Challa) and my other family members (Deepak Kumar Challa, Dinesh Kumar Challa, Pallavi Challa and Sweta Challa) for their belief in my academic abilities and for encouraging me to pursue my passion for research. I would like to thank all my family members for their unconditional love, which aided in handling the stress associated with research obstacles. I also appreciate the lessons

on hard work and ethics by my parents that have greatly helped my research. Thanks to my wife (Sai Hymavathi Challa) for being supportive with respect to my long working hours.

I would like to thank all my friends who have been around all these eight years and helped me in some or the other way. In particular, I thank my flat mates, Sandeep Kumar Ganji, Ramraj Velmurugan, Sairam Geethanath and Sarath Chandra, for creating an enjoyable living environment and for fun discussions on scientific and non-scientific topics.

Many thanks to Wentao Mi and Héctor Pérez Montoyo for training me in animal work. I would like to express my special gratitude to Ramraj Velmurugan for providing invaluable help in imaging, image processing and statistics. I thank Venkata Siva Charan Devanaboyina for assistance with BIAcore analyses. Finally, I would like to appreciate the assistance of all the past and present lab members.

TARGETING THE NEONATAL FC RECEPTOR, FCRN, TO TREAT AUTOIMMUNITY AND ELUCIDATION OF SITES OF FCRN FUNCTION

by

DILIP KUMAR CHALLA

DISSERTATION

Presented to the Faculty of the Graduate School of Biomedical Sciences

The University of Texas Southwestern Medical Center at Dallas

In Partial Fulfillment of the Requirements

For the Degree of

DOCTOR OF PHILOSOPHY

The University of Texas Southwestern Medical Center

Dallas, Texas

December, 2016

TARGETING THE NEONATAL FC RECEPTOR, FCRN, TO TREAT AUTOIMMUNITY AND ELUCIDATION OF SITES OF FCRN FUNCTION

DILIP KUMAR CHALLA, MRes

The University of Texas Southwestern Medical Center at Dallas, 2016

E. SALLY WARD OBER, Ph.D.

The neonatal Fc receptor, FcRn, is expressed in many different cell types and serves several functions, some of which are cell type-specific. A function common to most cell types that express this receptor is salvage of IgG from cellular degradation which is responsible for the long *in vivo* half-life of IgG. This property of IgG is responsible for its indispensable role in humoral immunity and also contributes to the successful use of IgGs as therapeutics. In autoimmunity, however,

autoantibodies are generated that can contribute to pathology. FcRn-mediated salvage is also responsible for the long half-life of autoreactive IgGs. Therefore, this study employed an engineered antibody (Abdeg, a novel FcRn inhibitor) that lowers endogenous IgG levels by competing for binding to FcRn, to directly assess the effect of decreased antibody levels in an autoantibody-dependent murine model of multiple sclerosis (MS), experimental autoimmune encephalomyelitis (EAE). Essentially, Abdeg delivery reduced the accumulation of autoantibodies in the target organs and ameliorated the disease.

Autoreactive $CD4^+$ T cells are also known to play an important role in the pathogenesis of autoimmune diseases. Thus, with the goal of inducing antigen-specific T cell tolerance, the current study employed immunoglobulin Fc engineering to develop a novel platform for the delivery of peptide epitopes as Fc-peptide fusions with different dynamic properties. Using very low doses of these engineered antigens to avoid anaphylactic shock, the study demonstrates that the longevity of the peptide antigen is the primary determinant of tolerance induction in a murine EAE model that is driven by autoreactive $CD4^+$ T cells. Long-lived Fc-antigen fusions are effective tolerogens in both prophylactic and therapeutic treatments, although distinct mechanisms lead to tolerance in these two settings.

Further, to identify the FcRn-expressing cell types that mediate the effects of Abdegs and Fc-antigen fusions on autoantibodies and autoreactive T cells, respectively, cre-loxp technology was used to generate multiple cell type-specific FcRn knockout mice. This study indicates that macrophages are the primary sites among hematopoietic cells where IgG homeostasis occurs. Collectively, these studies have led to an improved understanding of FcRn function at both the level of its sites of functional activity and targeting this receptor for therapy.

TABLE OF CONTENTS

PRIOR PUBLICATIONS

1. **Challa, D.K.**, Mi, W., Lo, S.T., Ober, R.J. & Ward, E.S. Antigen dynamics govern the induction of $CD4^+$ T cell tolerance during autoimmunity. *J. Autoimmun.* **72**, 84-94 (2016).

2. Velmurugan, R., **Challa, D.K.**, Ram, S., Ober, R.J. & Ward, E.S. Macrophage-mediated trogocytosis leads to death of antibody-opsonized tumor cells. *Mol. Cancer Ther.* **15**, 1879-1889 (2016).

3. **Challa, D.K.**, Velmurugan, R., Ober, R.J. & Sally Ward, E. FcRn: from molecular interactions to regulation of IgG pharmacokinetics and functions. *Curr. Top. Microbiol. Immunol.* **382**, 249-272 (2014).

4. Swiercz, R., Chiguru, S., Tahmasbi, A., Ramezani, S.M., Hao, G.Y., **Challa, D.K.**, Lewis, M.A., Kulkarni, P.V., Sun, X.K., Ober, R.J., Mason, R.P. & Ward, E.S. Use of Fc-engineered antibodies as clearing agents to increase contrast during PET. *J. Nucl. Med.* **55**, 1204-1207 (2014).

5. **Challa, D.K.**, Bussmeyer, U., Khan, T., Montoyo, H.P., Bansal, P., Ober, R.J. & Ward, E.S. Autoantibody depletion ameliorates disease in murine experimental autoimmune encephalomyelitis. *mAbs* **5**, 655-659 (2013).

6. Bansal, P., Khan, T., Bussmeyer, U., **Challa, D.K.**, Swiercz, R., Velmurugan, R., Ober, R.J. & Ward, E.S. The encephalitogenic, human myelin oligodendrocyte glycoprotein-induced antibody repertoire is directed toward multiple epitopes in C57BL/6-immunized mice. *J. Immunol.* **191**, 1091-1101 (2013).

7. Patel, D.A., Puig-Canto, A., **Challa, D.K.**, Perez Montoyo, H., Ober, R.J. & Ward, E.S. Neonatal Fc receptor blockade by Fc engineering ameliorates arthritis in a murine model. *J. Immunol.* **187**, 1015-1022 (2011).

LIST OF FIGURES

LIST OF TABLES

LIST OF ABBREVIATIONS

APCs: antigen presenting cells

AUC: area under the curve

β_2m: $\beta_2$microglobulin

CIS: clinically isolated syndrome

CNS: central nervous system

CSF: cerebrospinal fluid

DCs: dendritic cells

EAE: experimental autoimmune encephalomyelitis

ECs: endothelial cells

ELF: epithelial lining fluid

EMPs: erythro-myeloid precursors

FcRn: neonatal Fc receptor

GBM: glomerular basement membrane

HBSS: Hank's Balanced Salt Solution

HCs: hematopoietic cells

HSC: hematopoietic stem cell

ICs: immune complexes

Ig: immunoglobulin

IgG: immunoglobulin G

IVIG: intravenous immunoglobulins

KO: knock out

LNs: lymph nodes

mAbs: monoclonal antibodies

MaFIA: macrophage Fas-induced apoptosis

MBP: myelin basic protein

MHC: major histocompatibility

mIgG1: mouse immunoglobulin G1

MOG: myelin oligodendrocyte glycoprotein

MS: multiple sclerosis

Myo Vb: motor myosin Vb

OVA: ovalbumin

PBS: phosphate-buffered saline

PCT: proximal convoluted tubule

PPMS: primary progressive multiple sclerosis

RRMS: relapsing-remitting multiple sclerosis

SPMS: secondary progressive multiple sclerosis

TCR: T cell receptor

TCs: transport carriers

TLR: toll-like receptor

WT: wild type

CHAPTER ONE
General Introduction

Few sections in this chapter have been published in the journal *Current Topics in Microbiology and Immunology* [Challa, D.K., Velmurugan, R., Ober, R.J. & Sally Ward, E. FcRn: from molecular interactions to regulation of IgG pharmacokinetics and functions. *Curr. Top. Microbiol. Immunol.* 382, 249-272 (2014)]. These sections are reproduced here with permission from Springer (License number: 3940470310628).

1.1 INTRODUCTION TO DISSERTATION

The neonatal Fc receptor, FcRn, as the name implies, belongs to the family of Fc receptors. Unlike the 'classical' Fc receptors, the primary functions of FcRn include salvage of IgG (and albumin) from lysosomal degradation through the recycling and transcytosis of IgG within cells[1, 2]. Considering the critical role of FcRn in regulating the levels of IgG, many therapies (mostly IgG-based) have been developed that target FcRn, and have shown promise in treating animal models of autoimmune diseases and cancer[2]. One particular class of FcRn-targeting therapies includes agents that deplete endogenous antibodies which have applications in antibody-mediated pathologies. The first major aim (chapter II) of the project is to use one such recently developed FcRn-targeting agent, Abdegs (for "antibodies that enhance IgG degradation")[3], to treat an antibody-dependent murine experimental autoimmune encephalomyelitis (EAE) model of multiple sclerosis (MS). Although MS has been considered a T cell-mediated disease, much data support a role for CNS antigen-specific antibodies in the pathogenesis of MS in a subgroup of patients[4, 5]. Hence, these studies have direct relevance to the development of a new potential

treatment for MS and other antibody-dependent autoimmune diseases such as neuromyelitis optica and myasthenia gravis.

The second major aim (chapter III) of the project is concerned with the exploitation of IgG-salvage function of FcRn to treat T cell-mediated murine EAE. It is well established that the aberrant activation of autoreactive $CD4^+$ T cells is a driver of autoimmune disorders such as MS[6]. The existing therapies for T cell-mediated autoimmune diseases are non-specific and can result in adverse side effects such as systemic toxicities and increased risk for infection or cancer[7]. Consequently, a need for the development of tolerizing agents to selectively target autoreactive T cells persists. The use of soluble immunodominant peptides to induce T cell deletion or anergy has been successful in treating many animal models of MS[8-14], but suffers from lack of efficacy in MS patients[15, 16]. Further, the requirement to use relatively high doses of these peptides (necessitated by rapid renal clearance[17]) increases the possibility of adverse events[18, 19]. Thus, the aim of this project is to define the properties of antigen in a low dose setting that lead to tolerance using engineered Fc-antigen fusions and consequently, develop low dose T cell tolerogens that are effective in ameliorating EAE. These studies have direct relevance to the development of novel, efficient and safer therapies for T cell-mediated pathologies like MS.

FcRn is expressed in many different cell types, and endothelial cells (ECs) and hematopoietic cells (HCs) are the dominant cell types involved in IgG homeostasis *in vivo*[20]. Among HCs, in both humans and mice, monocytes, macrophages, dendritic cells (DCs) and B cells express FcRn[20, 21]. However, it is not clear in which HCs FcRn is crucial for persistence of IgG. This information is necessary to define the cell types that contribute to the activity of Abdegs and Fc-antigen fusions. In addition, such information is required to understand and predict the

pharmacokinetic behaviors of IgG-based drugs. Therefore, the third major aim (chapter IV) of the project is to identify the cells types among HCs that are crucial for FcRn-mediated IgG recycling.

1.2 FcRn

The neonatal Fc receptor (FcRn), as the name indicates, was first described for its role in the transfer of immunoglobulin G (IgG) from mother's milk across the neonatal gut epithelial barrier into the neonatal blood stream[22]. It is also referred to as a major histocompatibility (MHC) class I-related receptor since it shares structural similarity with MHC class I[23]. FcRn belongs to the class of Fc receptors that bind to IgG. However, FcRn differs from other members (collectively referred as FcγRs) of this class in multiple ways: 1) FcRn is expressed in hematopoietic cells (HCs) as well as non-HCs[20, 21, 24, 25], whereas FcγR expression is primarily confined to cells of hematopoietic origin[26, 27]; 2) the cytoplasmic domain of FcRn lacks the ability to signal intracellularly[28], whereas FcγRs (except human FcγRIIIB) or their subunit (γ chain) have immunoreceptor tyrosine-based activatory or inhibitory motifs (ITAMs or ITIMs) in their cytoplasmic domains which can mediate intracellular signaling[26, 27]; 3) the key function of FcRn involves recycling and transcytosis of monomeric IgG, leading to prolonged *in vivo* half-life and transport of IgG to sites of initial pathogen encounter (mucosal surfaces), respectively[1, 29, 30], whilst FcγRs regulate the immune complex-mediated effector functions of innate immune cells[26, 27].

Two primary and very well studied functions of FcRn include the regulation of IgG homeostasis and IgG transport across cellular barriers[1]. FcRn is expressed in many different cell types, some of which can be found in all organs of the body[20, 24]. As a result, the functions of FcRn are not localized to a single organ or cell type, an attribute required for regulating the homeostasis and transport of the ubiquitous immune molecule, IgG. FcRn also regulates the homeostasis of albumin[31], although the binding site on FcRn is different for the two molecules[32, 33] and hence they do not compete with each other for FcRn binding. Recently, FcRn has been shown to also play an

important role in the regulation of renal filtration[34, 35] and antigen presentation[36, 37]. The data that elucidates the mechanisms through which FcRn performs these multiple functions is discussed in the following sections. The well-defined role of antibodies in autoimmunity[38] and the emergence of IgG-based therapeutics[39, 40] have motivated the development of many FcRn-targeting therapies that have shown promise in pre-clinical studies, which are presented in section 1.2.4.

1.2.1 Molecular biology of FcRn

FcRn exists as a heterodimer of the MHC class I-like heavy chain and $\beta_2$microglobulin (β_2m), which are non-covalently associated[23]. Association with β_2m is required for the expression and normal functioning of FcRn[41]. The MHC class I-like heavy chain includes glycosylated α1-3 domains, a transmembrane domain and a ~ 42 amino acid cytoplasmic tail[28]. Crystallographic studies of a rat FcRn-rat Fc (IgG2a) complex revealed that the α2 domain residues (Glu117, Glu118, Glu132, Trp133, Glu135, and Asp137) and Ile1 of β_2m combined with the carbohydrate of rat FcRn interacts with residues (Ile253, His310, His435, and minor role for His436) at the CH2-CH3 interface of rat Fc[42]. The role of His433 of the Fc region in these interactions is contentious[43-46]. The stoichiometry of the interaction between FcRn and Fc or IgG is 2:1, as shown by equilibrium gel filtration or sedimentation equilibrium assays[47, 48]. The FcRn:Fc (or IgG):FcRn interaction is asymmetric, with dissociation constants for the two binding sites differing by almost 50 fold[48]. This, combined with a recent three dimensional structure of human FcRn bound to an engineered human IgG1[33], indicate that occupancy of the 'first' site on IgG results in conformational changes that reduce the affinity of FcRn for the second site. Further, the FcRn-IgG interaction is highly pH-dependent, with relatively high affinity binding at acidic pH (< 6.5) and no detectable binding at physiological pH (7.4)[49, 50]. Site-directed mutagenesis studies have shown

that the pH-dependence is imparted by His310 and His435 of human Fc[43] (or His310, His435 and His436 of rodent Fc[50]) which get protonated at acidic pH. These positively charged histidines can then form a salt bridge with the corresponding residues of the FcRn heavy chain[42]. However, the crystal structure of the complex of human FcRn bound to an engineered human Fc fragment (M252Y/S254T/T256E) was recently solved which indicates that His310 of human Fc is the most important histidine residue for pH-dependent binding[33].

1.2.2 Cell biology of FcRn

Studies using mutated versions of FcRn have localized the endocytosis and transcytosis signals within the cytoplasmic tail of FcRn which include the conserved motifs tryptophan (Trp311) and dileucine (Leu322, Leu323)[51]. A calmodulin-binding site in the membrane proximal region of human FcRn has also been identified that controls the transcytosis and half-life of FcRn in epithelial cells in a calcium-dependent manner[52]. Also, rodent FcRn has three extracellular N-glycan moieties that are absent in human FcRn, which has only one N-linked glycan common to both human and rodent FcRn[28]. Interestingly, when human FcRn is rodentized in terms of N-glycan moieties, its steady state distribution changes (from basolateral) to the apical membrane and its predominant direction of transcytosis (basolateral to apical) is reversed, resulting in the transport of IgG from apical to basolateral side[28].

Although recent data suggests a slightly different picture (refer to section 1.2.3.1), in the past it was hypothesized that FcRn in vascular endothelial cells (ECs) is most important for recycling of IgG, since these cells form a large surface area that is in contact with the bloodstream. Therefore, FcRn trafficking with respect to IgG recycling has been extensively studied in ECs[53-56]. Specifically, the recycling process has been characterized in human FcRn-Green Fluorescent

Protein (GFP)-transfected human microvasculature ECs (HMEC-1), using live-cell fluorescence imaging[54]. In these studies, fluorescently labeled wild type (WT) human IgG1 was used to trace the path of recycling IgG, and a mutated variant (H435A), which binds to FcRn with negligible affinity at both physiological and acidic pH, was used to track IgG that does not bind to FcRn. Based on the results from these and subsequent studies[53, 55-57], a model for FcRn recycling/transcytosis has been constructed which can be summarized in three steps (Fig. 1-1): 1) Cells non-specifically pinocytose extracellular fluid including IgG into adaptor protein containing pH domain, PTB domain and leucine zipper motif 1 positive ($APPL1^+$) vesicular transport carriers (TCs), which then fuse with sorting endosomes. The acidic environment in these compartments facilitates IgG binding to FcRn. 2) FcRn-IgG complexes are sorted into recycling or transcytotic TCs. These TCs subsequently fuse with the plasma membrane, followed by the release of IgG into the serum or interstitial space due to the physiological (near-neutral) pH. 3) Meanwhile, the sorting endosomes mature to late endosomes, which deliver their luminal contents to lysosomes, resulting in the degradation of any IgG that failed to be recycled by FcRn.

FcRn-mediated transcytosis has also been extensively studied using Madin–Darby canine kidney (MDCK) cells[58, 59], which form polarized monolayers when cultured *in vitro*, a property necessary for studying transcytosis. In human FcRn-transfected MDCK cells, FcRn localizes predominantly to apical intracellular compartments, with surface expression primarily on the basolateral side. Importantly, FcRn was demonstrated to transcytose IgG in both basolateral to apical and apical to basolateral directions, the latter being dominant[58]. What factors define whether IgG is recycled or transcytosed? Although this question has not been answered completely, studies have identified molecular effectors for these processes which include Rab GTPases and motor myosin Vb (Myo Vb). Rab GTPases are regulated by GTP-GDP exchange cycles, and in

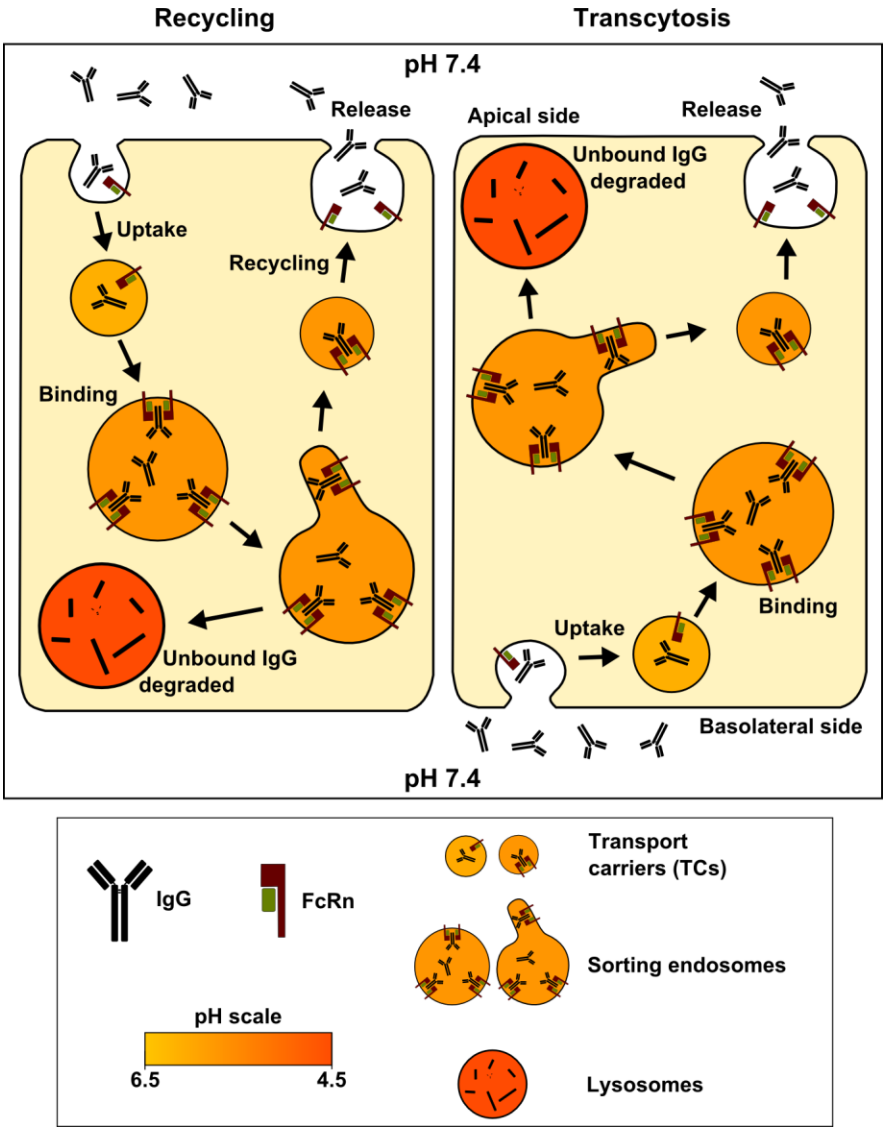

Figure 1-1. FcRn-mediated recycling and transcytosis of IgG. Cells internalize IgG through fluid-phase pinocytosis into tubulovesicular transport carriers (TCs), which subsequently fuse with sorting endosomes. The acidic pH in these compartments favors the binding of IgG to FcRn. FcRn with bound IgG sorts into TCs, which either recycle or transcytose to the plasma membrane. The near-neutral pH on the plasma membrane results in the release of IgG from FcRn into the extracellular fluid.

combination with soluble NSF attachment protein receptors (SNAREs) can regulate the merging of different organellar membranes[60-62]. Also, when active, Rab GTPases can activate or recruit effector molecules such as kinases, phosphatases, motors, etc. Consequently, these proteins control multiple intracellular trafficking processes[63, 64]. On the other hand, myosin motors are mechanical, enzymatic motors which generate energy by hydrolyzing ATP to drive cargo along actin filaments[65]. Rab11 GTPase associates with FcRn during recycling in HMEC-1 cells[66], and regulates recycling in MDCK cells[67], whereas Myo Vb and Rab25 GTPase are involved in bi-directional transcytosis in MDCK cells[67].

1.2.3 Functions of FcRn

1.2.3.1 IgG homeostasis

IgG and albumin constitute ~ 80% of total serum protein, with mean concentrations as high as 10 mg/ml and 40 mg/ml, respectively[68]. The primary reason for the high abundance of these proteins is their extraordinarily long serum half-life. IgG has a serum half-life of ~ 22 days in humans[69] and ~ 8 days in mice[70, 71]. Multiple studies have convincingly shown that the extended half-life of IgG (and albumin) is FcRn-mediated. The first *in vivo* evidence for this came from studies using β_2m-deficient (knockout, KO) mice, which do not express functional FcRn in addition to having other defects such as $CD8^+$ T cell deficiency. In these mice, IgG has an extremely short half-life[71-73]. Later, similar conclusions were obtained using FcRn KO mice[74], which are more specific tools than β_2m KO mice for studying FcRn biology. In addition, based on archived blood samples a study has identified two deceased humans (with familial hypercatabolic hypoproteinemia) who were analogous to β_2m KO mice i.e., β_2m expression was almost completely inhibited in these patients (soluble β_2m levels in their serum were < 1% of normal) due

to a point mutation in the leader peptide of their β_2m gene[75]. IgG and albumin levels were abnormally low in their serum, also indicating a role for FcRn in humans in protecting IgG and albumin from catabolism.

As mentioned earlier, FcRn is expressed in many different cell types across the body. In adult humans, FcRn expression can be found in skin microvasculature, retinal and placental ECs[54, 76, 77], monocytes, macrophages, dendritic cells (DCs)[21], T and B lymphocytes[78], keratinocytes[79], hepatocytes[80], epithelial cells of intestine[81, 82], mammary gland[83], kidney[84], lung[85], eye[77] and the female genital tract[86]. In adult mice, FcRn has been localized to vascular ECs of some but not all organs[24], macrophages, DCs[20, 24], B cells[20] and epithelial cells of kidney[34], alveolus[85], intestine[24], choroid plexus[24], eye[87] and the female genital tract[86]. It is not clear in which cell type(s)/organ(s) FcRn is crucial for persistence of IgG (and albumin). Elucidation of these sites is necessary to discern the pharmacokinetics, tissue localization and side effects associated with IgG-based therapeutics, which have become some of the most effective drugs to treat various types of cancers, autoimmune and infectious diseases[39, 40, 88-90]. Further, this information can aid in better understanding the pathophysiology of synthesis-independent hypoalbuminemia, which is observed in various medical conditions and can have serious clinical consequences[91]. Experiments using bone marrow chimeras of wild type (WT) and FcRn KO mice revealed that FcRn in both HCs and non-HCs is important for IgG homeostasis[24, 36, 88, 92]. Subsequent studies using Cre-loxp technology-based cell type-specific FcRn KO mice demonstrated that FcRn-expressing ECs and HCs are the major sites of IgG homeostasis[20].

The relative contribution of different cell types to IgG recycling depends on many factors, including the number of FcRn-expressing cells within each group, FcRn expression levels, the rate of pinocytic/phagocytic activity and the concentration of IgG in the respective microenvironments.

Also, the relative contribution of cells might change during inflammation, since toll-like receptor (TLR) ligands and pro-inflammatory cytokines have been shown to modulate FcRn expression. In particular, CpG oligodeoxynucleotide (TLR9 ligand), *lipopolysaccharide* (TLR4 ligand), tumor necrosis factor (TNF)-α and interleukin-1β have been shown to upregulate FcRn expression in intestinal epithelial cells and/or monocytes[93]. By contrast, interferon-γ has been shown to downregulate FcRn expression in intestinal epithelial cells and monocytes[94]. Determining the contribution of each cell type to IgG protection, and how this changes under inflammatory conditions, will aid in developing accurate pharmacokinetic-modeling tools required for optimizing the delivery of IgG-based therapeutics.

1.2.3.2 IgG transfer from mother to fetus or neonate

IgG is the only immunoglobulin subclass that is actively transported from mother to fetus/neonate. Although both mother-to-fetus and mother-to-neonate transfer of IgG can occur in rodents and humans, the former is dominant in humans while the latter plays a major role in rodents.

In mice, FcRn expression in the yolk sac mediates the maternofetal transfer of IgG[95]. However, at birth, the concentration of IgG in the serum of neonatal mice is only 20-30% of that in adult mice[96] and hence, IgG transport during gestation in mice is considered to be of relatively low importance. In rodents, the transfer of passive immunity in the form of IgG primarily occurs postnatally[96]. Upon ingestion of IgG-containing maternal milk, IgG and other milk proteins reach the proximal small intestine (the stomach is less acidic in neonates). Acidic pH in the duodenum allows IgG to be selectively endocytosed by enterocytes in an FcRn-dependent fashion[97-99]. Internalized IgG is then transcytosed across the cell to the basolateral membrane, where the

physiological, near-neutral pH results in the release of IgG from FcRn into the intestinal tissue. IgG can subsequently transfer into the blood through the lymphatics. Coincidentally, in rodents, FcRn expression in enterocytes rapidly decreases at around weaning age[24, 100].

In newborn infants, the concentration of IgG in the serum is at levels similar to those observed in mothers[101]. This indicates that maternofetal transport of IgG (during the third trimester of pregnancy) is extremely efficient in humans. The transport is mediated by FcRn expressed in syncytiotrophoblasts[102-104], which constitute the continuous, multinucleate epithelium separating the mother from fetus. On the apical side, the brush border surface of syncytiotrophoblast is bathed in maternal blood, whilst the basolateral membrane faces fetal blood capillaries. In brief, the maternal serum containing IgG is pinocytosed into the endosomes of syncytiotrophoblasts, followed by IgG transcytosis to the fetal side (basolateral membrane), where the near-neutral pH enables IgG dissociation from FcRn.

1.2.3.3 Maintenance and regulation of renal filtration

Blood is filtered in nephrons, the functional units of kidneys, to form urine. Nephrons are made up of different kinds of tubules, each performing a different function (Fig. 1-2A). The head portion of the nephron, called the glomerular capsule, performs filtration, and the following proximal convoluted tubule (PCT) performs reabsorption of salt, water, glucose, albumin, etc. Blood, destined for filtration flows into glomerular capillaries (enclosed by the glomerular capsule), where filtration occurs, and the resultant filtrate flows into the lumen of the glomerular capsule. For filtration to occur, the plasma has to pass through three layers of filters (Fig. 1-2B) with increasing size selectivity[105]. The first filtration barrier is formed by fenestrated endothelial cells of glomerular capillaries. These fenestrae are large but charged, which may prevent bulky

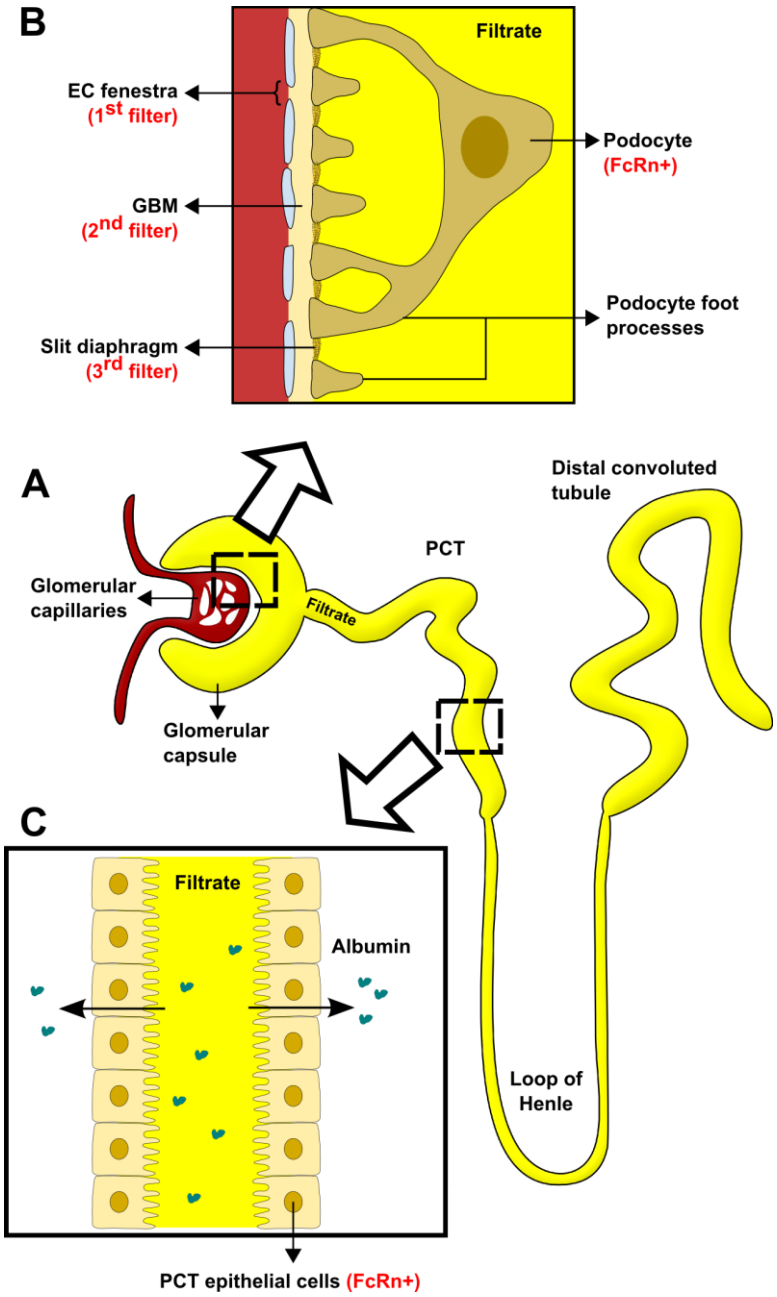

Figure 1-2. FcRn-mediated functions in the kidney. (A) Schematic structure of nephron. (B) Plasma from glomerular capillaries passes through three different filters before flowing into the lumen of glomerular capsule. During this process, IgG and albumin accumulate at the glomerular basement membrane (GBM) or slit diaphragm and IgG (and possibly albumin) is cleared by FcRn in podocytes. (C) The filtrate that forms in the glomerular capsule contains significant amounts of albumin and flows into the lumen of proximal convoluted tubule (PCT), where FcRn in epithelial cells mediates transcytosis of albumin from the filtrate into the interstitial space in the kidney.

proteins from crossing the barrier. The second barrier is formed by the glomerular basement membrane (GBM), which has small and charged pores and lies immediately below the glomerular capillaries. Underneath the GBM lie specialized epithelial cells called podocytes, which have long extensions (foot processes) that wrap around the GBM. The foot processes interdigitate forming narrow slits, and are bridged by extracellular structures, referred to as slit diaphragms[106]. The foot processes of podocytes along with associated slit diaphragms constitute the third filtration barrier. The pore size of the slit diaphragm is equal to or less than the size of albumin[107].

Considering the fact that ~ 180 L of glomerular filtrate is generated per day, it is very likely that albumin and IgG (which constitute ~ 80% of serum proteins) accumulate at the GBM and/or slit diaphragm, resulting in the clogging of these biological filters. Hence, it has been hypothesized that a mechanism is in place to clear the filters of these accumulated proteins. In this context, a study has shown that FcRn in podocytes function to remove accumulated IgG at the GBM[34]. The role of renal FcRn in this process was confirmed primarily based on the observation that age-dependent glomerular accumulation of IgG is higher in FcRn KO mice by comparison with WT mice, despite the fact that serum IgG levels are significantly lower in FcRn KO mice. Based on the pattern of IgG accumulation observed in the glomerulus, podocytes were suggested to be the primary cells that clear the accumulated IgG. Also, the study shows that the protein-elimination function of podocytes is saturable. This finding might explain how immune complex deposition occurs in the kidneys of systemic lupus erythematosus (SLE) patients which leads to nephritis.

The glomerular filtrate flowing into the PCT contains significant amounts of albumin, most of which is reclaimed by PCT epithelial cells[108]. Importantly, these epithelial cells express high levels of FcRn[24]. It has now become clear that FcRn in PCT cells is responsible for retrieval of albumin (Fig. 1-2C). The role of FcRn in this process is primarily based on two observations[35].

Firstly, FcRn KO mice excrete more albumin in urine than WT mice. Secondly, in FcRn KO mice that were transplanted with one WT kidney (after nephrectomy of one native kidney) serum albumin levels increased, whereas WT mice transplanted with a KO kidney developed hypoalbuminemia. Also, based on the localization of exogenously added, labeled albumin in the kidneys of unmanipulated mice and transplant chimeras, it was suggested that albumin is reclaimed by the epithelial cells of PCT. In this context, FcRn performs bidirectional transcytosis in human proximal tubular epithelial cells[109]. Hence, it is logical to assume that albumin reclaimed by the cells of the PCT would be transcytosed into the interstitium of kidneys, followed by drainage of albumin into the lymphatics and entry into the circulation. In addition, in the same study[35], experiments using kidney transplant chimeras showed that renal FcRn aids elimination of IgG from plasma into urine. However, the mechanism through which IgG elimination occurs is unclear.

1.2.3.4 Role in antigen presentation

Professional APCs (DCs, macrophages and B cells) can present antigens to $CD8^+$ and $CD4^+$ T cells in the context of MHC class I and MHC class II, respectively. In general, intracellular antigens are proteasomally processed and presented on MHC class I molecules, and extracellularly-derived antigens are processed in late endosomes or lysosomes and presented on MHC class II molecules[110]. Under some circumstances, extracellular antigens are processed by proteasomes or within endosomes or phagosomes and presented on MHC class I molecules[111, 112]. This type of antigen presentation can only be carried out by DCs[113] and possibly macrophages[114, 115] and is referred to as cross-presentation.

Importantly, all professional APCs in both mice and humans express FcRn[20, 21, 78]. Professional APCs, except B cells, also express activating FcγRs, which in the presence of IgG-

based immune complexes (ICs) mediate activation of APCs[26, 27, 116]. Further, antigens in the form of ICs are more efficiently internalized (through activating FcγRs) by APCs than soluble antigens and hence lead to more efficient T cell activation. With respect to this, a role similar to that played by FcγRs has been shown to be performed by FcRn[36, 92]. In one such study[36], multimeric ovalbumin (OVA) ICs containing either WT IgG or a mutated IgG (IHH, no binding to FcRn at physiological and acidic pH, but no change in binding to FcγRs) were used in *in vitro* mouse $CD4^+$ T cell proliferation assays in the presence of either WT or FcRn KO DCs. In these assays, the proliferation of OVA-specific $CD4^+$ T cells decreased when DCs lacked FcRn or when ICs comprising IHH antibodies were used by comparison with that observed using WT DCs or ICs containing WT antibodies, respectively. Similar observations were made using human cells, and when *in vitro*-loaded (with ICs containing WT or IHH antibodies) WT or FcRn KO DCs were injected into WT mice. These observations indicate a role for FcRn in IC-mediated antigen presentation. Specifically, based on the observed trafficking patterns of ICs and FcRn, it was demonstrated that FcRn rapidly transports WT ICs to lysosomes, leading to enhanced antigen presentation and T cell proliferation. In the assays described above, it is possible that some ICs would presumably cross-link FcγRs, leading to DC activation and cytokine secretion, which in turn would upregulate MHC class II and the associated invariant chain[116, 117]. Invariant chain has been shown to also associate with FcRn and target it to late endosomes or lysosomal compartments[118]. Hence, the invariant chain might have a role to play in diverting FcRn-bound ICs to lysosomes in APCs.

Recently, FcRn has also been shown to play a role in cross-presentation of IC-derived antigens[37]. In this study, mouse DCs pulsed with ICs comprising WT or IHH antibodies complexed with OVA (similar to those described above) were injected into WT mice that had also received

labeled OVA-specific $CD8^+$ T cells. The antigen in this case is exogenous and hence $CD8^+$ T cells will only be stimulated if the antigen is cross-presented. The proliferation of $CD8^+$ T cells was found to be many fold higher when WT IgG ICs were used in comparison to the proliferation observed with IHH IgG ICs, highlighting the importance of FcRn in IC-mediated cross-presentation. Interestingly, only $CD8^-CD11b^+$ DCs, but not $CD8^+CD11b^-$ DCs (shown to be the major mediators of cross-presentation of soluble and tumor antigens[119]) were able to efficiently cross-present IC-derived antigen to $CD8^+$ T cells. Using IgG-opsonized, OVA-containing beads (IC-beads), it was also shown that the $FcRn^+$ phagosomes formed upon WT IgG IC-bead internalization by DCs had many features that facilitated cross-presentation by comparison with phagosomes formed by IHH IgG IC-beads. The features included lower pH, persistence of antigen in the phagosomes and enrichment of components of the cross-presentation machinery such as the transporter associated with antigen processing 1 (TAP1) and MHC class I. Finally, the authors suggest that ICs are internalized by DCs in an FcγR-dependent fashion, followed by the transfer of ICs from FcγRs to FcRn in acidic, endosomal compartments followed by cross-presentation. Taken together, FcRn is indicated to be important for the presentation of IC-derived antigen to both $CD4^+$ and $CD8^+$ T cells.

1.2.4 FcRn-targeted therapies

Monoclonal antibodies (mAbs), due to their specificity and long half-lives, are considered to be one of the most effective and safe therapies for many diseases. Currently, there are almost 350 mAbs that are either in early development or Food and Drug Administration (FDA)-approved for the treatment of inflammatory disorders, cancers, infectious diseases and solid organ transplant rejection[120, 121]. As mentioned in the previous sections, FcRn functions to regulate the levels and

many functional activities of IgGs. As a result, many therapies (mostly IgG-based) have been developed that target FcRn, and have shown promise in treating animal models of autoimmune diseases and cancer. FcRn-targeting therapies can be broadly classified into two distinct categories: 1) mAbs with extended half-life which will have applications in any disease where mAbs can be used therapeutically and 2) agents that deplete endogenous antibodies which will have applications in antibody-mediated pathologies and other situations in which antibody clearance is indicated.

During the last decade or so, a significant component of Fc-engineering efforts has focused on developing IgG mutants that vary in their binding to FcRn and have enhanced *in vivo* half-life, with an aim to boost the efficacy and/or reduce the dosing frequency of IgG-based therapies. The first report demonstrating that Fc engineering can be used to generate IgGs with increased *in vivo* persistence came from a report in which a mutated mouse IgG1 Fc (T252L/T254S/T256F) was produced using random mutagenesis and phage display. This mutated Fc fragment has increased binding to mouse FcRn at acidic pH, but negligible binding at physiological pH, resulting in an extended half-life in mice by comparison with WT mouse IgG1-derived Fc[122]. Subsequently, many engineered human IgGs have been developed with increased *in vivo* half-life, as validated in non-human primates[123-126]. Among these mutants, YTE (human IgG1 - M252Y/S254T/T256E), exhibits ~ 4 fold increase in half-life relative to WT human IgG1 in non-human primates which is the longest half-life extension reported to date[123]. Another mutant, HN (human IgG1 - H433K/N434F), with increased pH-dependent binding to (human) FcRn has been shown to be more efficient than WT human IgG1 in FcRn-mediated transcytosis across the *ex vivo* human placenta[127]. Importantly, IgG with enhanced half-life has been demonstrated to have increased anti-tumor activity than WT IgG in tumor xenograft studies in mice[128]. Finally, based on the *in vivo* half-lives of various IgG mutants that were Fc-engineered with respect to their FcRn binding,

it is clear that while an increase in IgG affinity towards FcRn at acidic pH is important, retention of low affinity at physiological pH is equally important to allow exocytic release from cells[55] and consequent persistence of an IgG[126, 127, 129].

Autoantibodies lead to pathology in autoimmune diseases such as SLE, neuromyelitis optica, myasthenia gravis and multiple sclerosis[130-133]. Also, antibodies can mediate rejection of organ allografts[134]. Currently, approved treatments for depleting antibodies in such diseases, in a non-specific manner, include plasmapheresis and high dose intravenous immunoglobulin (IVIG)[135, 136]. Both these treatment modalities may lead to side effects or complications, but more importantly, the cost of these treatments is high[137, 138]. Hence, efforts have been undertaken to develop alternatives. IVIG lowers endogenous or pathogenic antibody levels only when used in high doses, which is essential for saturating FcRn[139, 140]. Alternatively, FcRn can be saturated or blocked using low doses of agents that bind to FcRn with very high affinity. In the case of half-life extension, retention of low affinity towards FcRn at physiological pH limits the extent to which the affinity at acidic pH can be increased[1, 126]. Such a limitation is not relevant to the generation of effective FcRn blockers, and in fact, high affinity binding to FcRn at physiological pH is desirable in this case since it will enable the engineered antibody to be efficiently endocytosed by FcRn-mediated uptake into cells[3, 55]. This in turn will result in increased competition with endogenous antibodies with respect to FcRn binding. One such Fc-engineered antibody is MST-HN (M252Y/S254T/T256E/H433K/N434F). Antibodies of this class have been shown to rapidly decrease endogenous antibody levels in mice and are called Abdegs (for antibodies that enhance IgG degradation)[3]. In a serum transfer model of arthritis in mice, Abdegs were able to reduce swelling and inflammation in the joints in both therapeutic and prophylactic disease settings[141]. Importantly, by comparison with Abdegs, 25-50 times higher amounts of IVIG were required to

achieve similar therapeutic effects. Recently, as a part of this dissertation work (chapter II), Abdegs were also shown to ameliorate disease in a passive model of antibody-mediated experimental autoimmune encephalomyelitis by mediating both the rapid clearance and reducing the accumulation of encephalitogenic antibodies in the CNS[142]. Abdegs have been lately shown to also have applications in immuno–positron emission tomography (PET) – Abdeg delivery following the administration of radiolabeled (non-residualizing ^{124}I) tumor-targeting antibody to mice bearing tumor xenograft resulted in rapid degradation of circulating radiolabeled antibody, consequently, leading to increased contrast during PET and significantly reduced systemic exposure to radiation[143].

Antibodies that bind to FcRn through their variable domains have also been developed that can block FcRn-mediated recycling of IgGs. Anti-rat (4C9) and anti-human (DVN24) antibodies specific for FcRn were shown to reduce the levels of exogenously administered tracer antibody in rats and human FcRn transgenic mice, respectively[144, 145]. Similarly, another anti-rat FcRn IgG, 1G3, was shown to reduce pathogenic antibody levels and disease symptoms in both passive and active models of myasthenia gravis in rats[146]. On the downside, FcRn blockers of this class have short *in vivo* half-lives due to strong binding to FcRn at physiological pH which results in increased accumulation in FcRn-expressing cells and reduced exocytic release[20, 127, 129, 146]. Peptide-based FcRn blockers have also been developed. In particular, SYN1436, a dimer of FcRn-binding peptide was able to significantly reduce the levels of exogenously added human IgG in human FcRn transgenic mice and endogenous antibody in non-human primates[147]. These peptide-based agents would be expected to exhibit an *in vivo* half-life that is lower than that of antibody-based FcRn blockers, primarily due to renal-mediated clearance. As a result, PEGylation has been

employed to improve the *in vivo* pharmacokinetics and efficacy of such peptide-based FcRn blockers[148].

1.3 MULTIPLE SCLEROSIS

Multiple sclerosis (MS) is a chronic, inflammatory demyelinating neurodegenerative disease[133, 149]. MS affects around 2.5 million people around the world with higher incidence in northern and central Europe, northern United States, Canada and southeastern Australia[150], and the disease is three times more common in women than in men[151, 152]. MS mainly affects young people with a mean age of onset of 30 years and is a common cause of serious physical disability in young adults[153] – 25 years post diagnosis, ~50% of the patients require permanent use of a wheelchair[6]. The etiology of MS is not known, but both environmental and genetic factors are important in the development of MS[154]. The clinical presentation of the disease can include sensory and visual disturbances, motor impairments, fatigue, pain and/or cognitive deficits[153]. The disease in young adults typically starts as a clinically isolated syndrome (CIS), a first clinical episode with features suggestive of MS, with pathological changes localized to optic nerves, the brainstem or the spinal cord[155]. Only 30-70% of the patients with CIS develop MS, but in 85% of MS patients the disease onset is CIS[155].

1.3.1 MS subtypes

The disease course in MS is heterogeneous. Based on the patterns of disease presentation, three major disease subtypes have been recognized[156] – i) relapsing-remitting MS (RRMS), ii) secondary progressive MS (SPMS) and iii) primary progressive MS (PPMS). 80-85% of the patients with MS are diagnosed with RRMS, in which episodes of clinical symptoms alternate with periods of complete or partial remission and lack of disease progression between disease relapses. Over 25 years post diagnosis, approximately 90% of RRMS patients convert to SPMS[157], which

is characterized by progressive neurological disease (after an initial RR disease) with or without minor remissions and plateaus[150]. In 10-15% of patients, MS manifests as PPMS, which is similar to SPMS in clinical presentation except that this form does not follow RRMS. In addition, a patient with PPMS who has an acute attack is considered to be PP–active, whereas a PPMS patient with no acute attacks and no new MRI lesions is considered as PP–not active[156]. Additional rarer MS subtypes include Marburg variant of acute MS, Balo's concentric sclerosis, and tumefactive MS[158].

1.3.2 Immunology of MS

MS is an autoimmune disease - an as yet unknown factor(s) is believed to trigger an autoimmune response, which drives disease progression and relapses. Myelin-reactive T cells are observed in the peripheral blood of both MS patients and healthy controls[159-162], presumably due to failure of thymic central tolerance. Further, mechanisms of peripheral T cell tolerance to self-antigens are ineffective or defective in MS patients since myelin-reactive T cells from these patients are more activated and have a memory phenotype compared to the phenotype of those from healthy controls[159, 163, 164]. Further, the activation of autoreactive T cells could be a result of molecular mimicry[165-167], bystander activation or presence of T cells with dual T cell receptor (TCR) specificities[168] – one to an autoantigen and other to a pathogen. The (aberrant) activation of autoreactive T lymphocytes in the periphery license them to enter the CNS by crossing blood-brain, blood-cerebrospinal fluid (CSF) or blood-leptomeningeal barriers[169]. Alternatively, although less likely, the entry of autoreactive lymphocytes into the CNS could be a result of CNS-intrinsic events such as an infection or primary neurodegeneration. The activation or reactivation of autoreactive T lymphocytes in the CNS initiates an inflammatory feed-forward response (involving $CD4^+$, $CD8^+$ T cells, B cells and innate immune cells) in this organ, leading to

demyelination, neuroaxonal loss and disruption of neuronal signaling and ultimately leading to MS symptoms[6].

1.3.3 MS immunopatterns

An important pathological hallmark of MS includes lesions or plaques characterized by gliosis, inflammation and relative axonal preservation. The plaques are disseminated throughout white and grey matter of brain and spinal cord, but are mainly found in subpial spinal cord, optic nerves, brainstem, cerebellum, and periventricular white matter regions[133]. Inflammation is a characteristic feature of these plaques which is more pronounced in acute phases of the disease than in chronic phases[6]. There exists profound heterogeneity in the pathology of early active plaques among different MS patients, but are identical among multiple active lesions analyzed within a given patient[170]. As such, MS lesions have been classified into four immunopatterns based on loss of specific myelin protein, oligodendrocyte destruction, plaque topography and immunoglobulin and complement deposition[133]. Pattern I lesions (found in 15% of MS patients) are mainly characterized by T cell inflammation, active demyelination with many activated microglia and myelin-laden macrophages, and absence of immunoglobulin and complement deposition. Pattern II lesions (found in 58% of MS patients) are similar to pattern I except that immunoglobulin and complement deposition is observed at sites of active demyelination. Pattern III lesions (found in 26% of MS patients) are characterized by oligodendrocyte apoptosis, T cell inflammation, activation of microglia and macrophages, and early preferential loss of myelin-associated glycoprotein (MAG), whereas other myelin proteins are partially preserved (indicates metabolically stressed oligodendrocyte). In addition, no deposition of immunoglobulin and complement is observed. Pattern IV lesions (found in only 1% of MS patients) are defined by

nonapoptotic death of oligodendrocytes in periplaque non-demyelinated white matter. This data thus indicates (but does not prove) a pathogenic role for T cells, macrophages and antibodies along with complement in majority of MS patients. In addition, this classification underscores the importance of considering interindividual heterogeneity while designing therapeutics.

CHAPTER TWO
FcRn-targeted antibody engineering to treat disease in an antibody-dependent animal model of multiple sclerosis

This study has been published in the journal *mAbs* [Challa, D.K., Bussmeyer, U., Khan, T., Montoyo, H.P., Bansal, P., Ober, R.J. & Ward, E.S. Autoantibody depletion ameliorates disease in murine experimental autoimmune encephalomyelitis. *mAbs* 5, 655-659 (2013)]. It is reprinted here with permission from Taylor & Francis LLC (Reference number: P092116-01).

2.1 INTRODUCTION

Multiple sclerosis (MS) is a demyelinating, neurodegenerative disease involving autoreactive T and B cells[133, 149]. Evidence to support the involvement of antibodies in the pathogenesis of this disease include multiple clinical and preclinical observations. The presence of oligoclonal immunoglobulin G (IgG) bands (OBs) in the cerebrospinal fluid (CSF) of MS patients was one of the first evidence pointing to the role of antibodies in this autoimmune disease. Separation of MS patient-derived CSF proteins by electrophoresis reveals two or more sharp bands corresponding to immunoglobulins (Ig) in ~80-95% of these patients[171, 172]. The OBs are not found in the corresponding serum samples (where IgG is polyclonal), indicating local accumulation of IgG specificities in the CSF. In other words, specific B cell clones in the CNS (upon stimulation) differentiated into Ig-producing plasma cells, each clone producing IgG of highly restricted mobility on electrophoresis. In agreement with this, CSF and CNS lesions in MS patients were shown to contain clonotypic B and plasma cells with restricted Ig receptor repertoire[173-177]. Further, higher numbers of B cells and plasma cells are observed in the CNS of patients with pathologically

active progressive MS compared with normal controls, and active and slowly expanding lesions contain greater number of B cells and plasma cells than the normal white matter in MS patients[178]. Importantly, antibodies in the serum and CSF of MS patients have been shown to bind CNS antigens such as myelin oligodendrocyte glycoprotein (MOG), myelin basic protein (MBP), proteolipid protein (PLP), Myelin-associated glycoprotein (MAG) and neuroaxonal proteins[179-182].

A more convincing demonstration of the pathogenic potential of MS autoantibodies is derived from clinical observations involving therapeutic application of plasma exchange and immunoadsorption. Plasma exchange involves removal of plasma from patient blood and its replacement with human albumin or donor plasma, whereas immunoadsorption involves specific removal of antibodies from patient blood. Therapeutic application of either of these apheresis techniques have been shown to provide clinical benefit in steroid-unresponsive MS patients[183-186]. Importantly, in a retrospective study, therapeutic plasma exchange was shown to improve the neurological functioning in MS patients with pattern II lesions (characterized by immunoglobulin and complement deposition) but not in patients with pattern I or III lesions[187, 188]. Another study tested the encephalitogenicity or pathogenic potential of IgG purified from a MS patient responsive to immunoadsorption using an animal model of MS, experimental autoimmune encephalomyelitis (EAE), which was induced by immunizing SJL/J mice with a low dose of proteolipid protein (PLP)139-151 peptide. Administration of patient-derived IgG to immunized mice on the day of disease onset exacerbated the disease symptoms and increased demyelination and inflammation in the CNS, however, such effects were absent when control IgG was administered to the mice[189].

Autoantibodies targeting nearly all CNS cell types are formed in MS[182], however, MOG is considered as one of the most important target of autoantibodies in MS, due to its favorable (for antibody binding) localization in the outermost layers of the myelin sheath as well as the cell body

and processes of mature oligodendrocytes[190, 191]. Importantly, demyelinating antibodies specific for MOG can contribute to pathogenesis in MS and EAE models[5, 182]. For example, in an *in vitro* study, incubation of MS patient-derived serum (positive for anti-MOG antibody) with a glioblastoma cell line, which has been transduced using a lentiviral vector to stably express MOG, strongly decreased the cell number, but such an effect was not seen when cells transduced with an empty vector were used[179]. In addition, transfer of concentrated anti-MOG antibody-containing MS patient sera into MBP72-85-immunized rats on the day of disease onset did not affect the EAE score but significantly increased demyelination and axonal loss[179]. Correspondingly, transfer of mouse monoclonal (8-18C5) or polyclonal anti-MOG antibody into SJL/J mice immunized with a low dose of PLP139-151 led to significant increase in EAE severity[192].

The above observations indicate that agents that specifically lower IgG levels *in vivo* could be potential therapies for MS. Several different classes of reagents that decrease antibody levels *in vivo* by inhibiting the MHC Class I-related receptor, FcRn, have been described[3, 30, 140, 144, 146, 147, 193]. Although these agents have been shown to be efficacious in animal models of autoantibody-dependent myasthenia gravis[146] and rheumatoid arthritis[141, 193], it is unknown whether these FcRn-targeted agents can ameliorate EAE. Therefore, the current study is directed towards analyzing the therapeutic effects of an FcRn inhibitor in a mouse model of EAE that is both T cell and antibody dependent[194].

Neonatal Fc receptor, FcRn, regulates the levels and transport of antibodies by binding and recycling or by transcytosing IgG molecules, thereby preventing their lysosomal degradation[1, 2]. Thereby, FcRn blockade (inhibiting its binding to IgG) leads to degradation of IgG that has been taken up into cells by fluid phase pinocytosis[1, 2]. With this aim, a novel class of antibody-based inhibitors of FcRn were generated that are engineered to bind FcRn through their Fc regions with

increased affinity in the pH range of 6.0-7.4[3]. These inhibitors, called Abdegs ('antibodies that enhance IgG degradation'), can efficiently enter the cells in a FcRn-dependent fashion and compete with endogenous IgGs for binding to FcRn, thus diverting them to the degradative, lysosomal pathway within cells[3, 56] (Fig. 2-1). Consequently, Abdegs can be used to induce a rapid decrease in endogenous IgG levels in the body[3, 127, 141]. As such, in the current study, Abedgs were shown to reduce the levels of an exogenously delivered encephalitogenic antibody in mice with EAE. This effect translated to decreased accumulation of autoantibody in the CNS which in turn led to reduced disease severity.

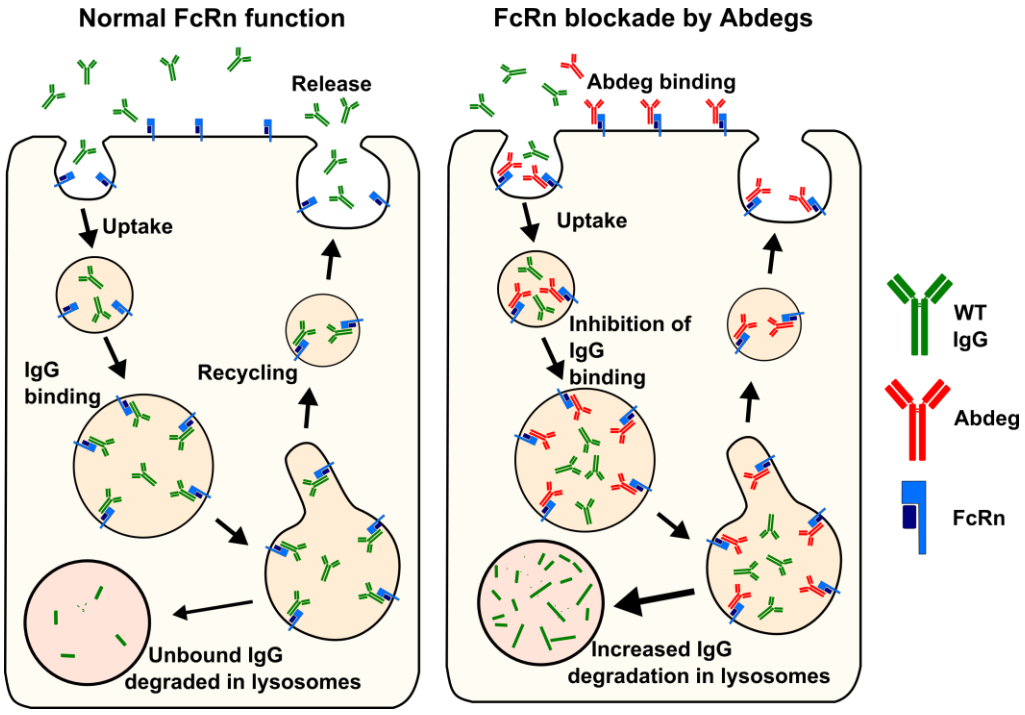

Figure 2-1. Abdeg-mediated degradation of endogenous IgG. In the absence of Abdegs (normal FcRn function; left panel), endocytosed wild type (WT) IgG binds to FcRn in the endosomes and is subsequently recycled to the cell surface where WT IgG is released from FcRn into the extracellular fluid. In contrast, in the presence of Abdegs (right panel), the interaction of endocytosed WT IgG with FcRn in the endosomes is blocked and consequently, unbound WT IgG is trafficked to the lysosomes for degradation. The stoichiometry of the interaction between FcRn and IgG is 2:1 (refer to section 1.2.1), however, for simplicity a stoichiometry of 1:1 is shown in the figure.

2.2 RESULTS

2.2.1 Development and characterization of an antibody-dependent EAE model

To study the effect of (auto)antibody depletion on EAE, we used a model recently developed in our laboratory in which encephalitogenic anti-MOG antibodies exacerbate EAE[194]. This model involves the immunization of wild type (WT)[194], rather than B cell deficient[195], mice with a weakly encephalitogenic peptide (residues 35-55 of human MOG, hMOG35-55), followed by the transfer of the demyelinating, MOG-specific monoclonal antibody (mAb), 8-18C5[196, 197]. Delivery of 8-18C5 into hMOG35-55 immunized mice at day 15 post-immunization exacerbates EAE relative to the disease activity observed in phosphate-buffered saline (PBS) vehicle-treated mice (Fig. 2-2A). In addition, treatment with isotype control (mouse IgG1), anti-lysozyme antibody D1.3[198] does not exacerbate EAE[194]. In order to confirm and determine the dynamics of localization of 8-18C5 in the CNS following its administration into immunized mice, fluorescently labeled 8-18C5 was employed. Following injection, the accumulation and binding of 8-18C5 can be detected in spinal cord sections at two hours post-delivery, and the levels of this mAb in the CNS increase at six hours post-delivery (Fig. 2-2B). This EAE model is therefore instructive for the analysis of the effects of decreasing (auto)antibody levels *in vivo*.

2.2.2 Abdegs efficiently deplete administered autoantibody from blood, whole body and CNS tissues

To investigate the effects of MST-HN (M252Y/S254T/T256E/ H433K/N434F) Abdeg[3] delivery on the clearance of 8-18C5 in mice with EAE, hMOG35-55 immunized mice were divided into equivalent groups with similar mean and median clinical scores and injected with radiolabeled

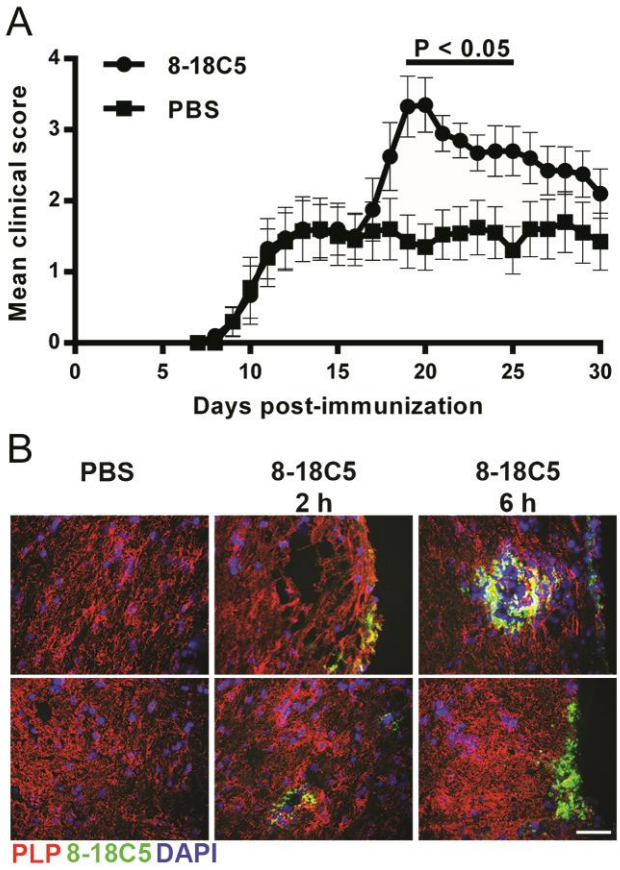

Figure 2-2. Exacerbation of EAE by transfer of 8-18C5 mAb into hMOG35-55-immunized C57BL/6J mice. C57BL/6J mice were immunized with hMOG35-55 and treated with 200 ng pertussis toxin on days 0 and 2. (A) On day 15, mice were sorted into equivalent groups (n = 10 mice/group; mean disease score of ~1.5) and were injected intravenously with 200 μg 8-18C5 or PBS vehicle. Mice were scored daily. Error bars indicate SEM. Significant differences ($p < 0.05$; two-tailed Student's *t*-test for pairwise comparison of groups) between 8-18C5 and PBS treated mice are indicated by a bar. (B) On day 15, mice were sorted into equivalent groups (n = 6 mice/group for 8-18C5 and 2 mice/group for PBS) and were treated as in (A), except that 200 μg Alexa 647-labeled 8-18C5 or PBS vehicle was injected on day 15. Spinal cords were harvested at 2 or 6 hours post-delivery of 8-18C5 or PBS, stained with anti-PLP antibody (pseudocolored red) and imaged. Cropped images of representative data are shown. Alexa 647-labeled 8-18C5 and DAPI stained nuclei are pseudocolored green and blue, respectively. For the PBS-injected group the upper and lower images correspond to spinal cord harvested at 2 hours and 6 hours post-delivery, respectively. The upper and lower panels in the 8-18C5 treated groups correspond to spinal cord harvested at either 2 hours (middle column) or 6 hours (right column) post-delivery. Bar = 50 μm.

(^{125}I) 8-18C5 on day 17 post-immunization. The mean clinical score for each mouse group at the time of 8-18C5 injection was ~1.5. Two hours later, mice were injected with Abdeg (human IgG1-derived) or, as controls, WT human IgG1 or PBS vehicle. A dose of 1.5 mg Abdeg (or WT IgG1) per mouse was chosen since the delivery of 1-2 mg MST-HN Abdeg per mouse induces a maximum decrease in endogenous IgG levels[141]. The levels of labeled 8-18C5 remaining in the mice were determined by measuring radioactivity in blood samples, CNS tissue and whole body (Fig. 2-3A,B). Abdeg delivery induces a rapid decrease in ^{125}I-labeled 8-18C5 levels in the blood and whole body relative to the slower clearance observed in control mice treated with WT IgG1 or PBS vehicle. Importantly, ^{125}I-labeled 8-18C5 levels in the spinal cord and brain were also lower in mice following Abdeg delivery relative to those in WT IgG1-treated mice (Fig. 2-3C). Thus, Abdegs are effective in reducing accumulation of this encephalitogenic mAb in the CNS.

2.2.3 Abdegs ameliorate autoantibody-induced exacerbation of EAE symptoms

We next assessed the effect of Abdeg delivery on 8-18C5-mediated exacerbation of EAE. In initial experiments, the anti-lysozyme human IgG1 antibody[3] that differs from the Abdeg at the MST-HN mutation sites was used as a control. In contrast with our earlier studies in an arthritis model[141], however, delivery of this antibody resulted in a slight exacerbation of disease relative to control, vehicle-treated mice (data not shown). Trastuzumab, a human IgG1 anti-HER2 mAb that does not recognize mouse HER2, was therefore used as a WT IgG1 control. Mice were immunized with 100 μg hMOG35-55 and, at day 15, divided into groups with similar mean and median clinical scores (mean clinical score for each group ~2) and disease history prior to day 15. Two hours following the delivery of 8-18C5, when this mAb is detectable in the CNS (Fig. 2-2B), mice were treated with 1.5 mg MST-HN, or as controls, WT IgG1 or PBS vehicle. The data presented in

Figure 2-4 demonstrate that Abdeg delivery results in amelioration of EAE. The positive effect of the Abdeg on disease activity is rapid and is observed within one day of treatment, consistent with the dynamics of Abdeg-mediated clearance of 8-18C5 (Fig. 2-3). Although the delivery of WT IgG1 into mice results in reduced disease activity relative to vehicle-treated mice, possibly due to anti-inflammatory effects analogous to those described for high dose intravenous immunoglobulins (IVIG)[199, 200], the differences between WT IgG1- and PBS-treated mouse groups are not significant for the majority of days post-treatment (Fig. 2-4).

Figure 2-3

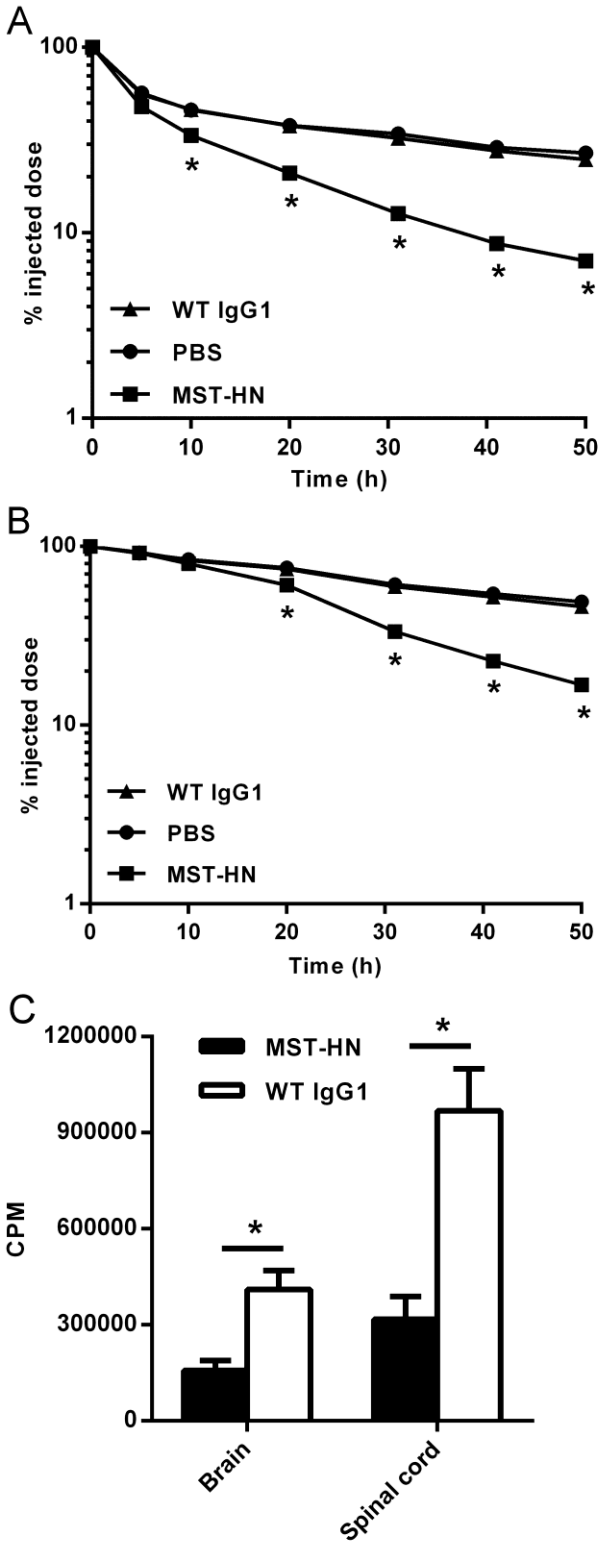
A
100
10
1
% injected dose
WT IgG1
PBS
MST-HN
0
10
20
30
40
50
Time (h)
B
100
10
1
% injected dose
WT IgG1
PBS
MST-HN
0
10
20
30
40
50
Time (h)
C
1200000
900000
600000
300000
0
CPM
MST-HN
WT IgG1
Brain
Spinal cord

Figure 2-3. MST-HN Abdeg treatment induces a rapid decrease in the levels of 8-18C5 mAb *in vivo*. Mice were immunized with hMOG35-55 as in Figure 2-2, sorted into equivalent groups (n = 4-6 mice/group; mean disease score ~1.5) on day 17 and injected with a mixture of ^{125}I-labeled 8-18C5 and unlabeled 8-18C5 (total of 200 μg mAb/mouse). Two hours later, mice were injected with 1.5 mg MST-HN, 1.5 mg WT IgG1 or PBS. Radioactivity levels were analyzed in blood (A) or by whole body counting (B) at the indicated times. (C) 48 hours post-delivery of MST-HN or WT IgG1, mice were perfused with heparin/PBS and CNS tissue (brains and spinal cords) isolated. Radioactivity levels in these tissues were determined and mean values for each group are shown. Error bars indicate SEM and in panels (A) and (B) are obscured by the symbols. Significant differences ($p < 0.05$; two-tailed Student's *t*-test for pairwise comparison of groups) between MST-HN and WT IgG1/PBS treated mice are indicated by *****.

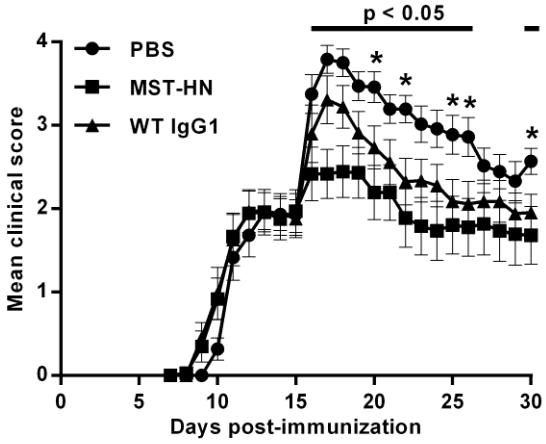

Figure 2-4. Delivery of the MST-HN Abdeg ameliorates EAE. Mice were immunized with hMOG35-55 as in Figure 2-2, sorted into equivalent groups (n = 8-9 mice/group; mean disease score ~2) on day 15 and injected with 200 μg 8-18C5. Two hours later, mice in each group were treated with 1.5 mg MST-HN, 1.5 mg WT IgG1 or PBS vehicle. Mice were scored daily for disease activity. Data are combined from two independent experiments, totaling 17-18 mice for each treatment group. Error bars indicate SEM. Significant differences ($p < 0.05$; two-tailed Student's *t*-test for pairwise comparison of groups) are indicated by bars (MST-HN vs. PBS treated mice) and ***** (WT IgG1 vs. PBS treated mice).

2.3 DISCUSSION AND CONCLUSION

This work has demonstrated that inhibition of FcRn function reduces the accumulation of (auto)antibodies in the CNS and ameliorates disease in a mouse model of EAE in which antibodies contribute to pathogenesis. Our studies indicate that FcRn blockade could have beneficial effects in MS, given the evidence to support a role for antibodies in pathogenesis[5, 185, 187]. Currently available treatments that lower IgG levels are the use of IVIG[199-201], plasmapheresis[135] and immunoadsorption[202]. IVIG contains enriched preparations of serum IgG derived from several human donors and it induces degradation of endogenous IgG by saturating FcRn[199, 200]. However, the relatively low competitive activity of IVIG for FcRn necessitates the use of doses approaching the whole body load of IgG (i.e. ~1-2 g/Kg body weight)[140, 203]. By contrast, Abdegs inhibit FcRn at comparatively low doses (~50-100 mg/Kg)[3, 141] due to their increased binding affinity for this receptor. Further, IVIG is limited by supply[204]. Both plasmapheresis and immunoadsorption can lead to side effects such as catheter-related bloodstream infections, catheter occlusion, deep vein thrombosis and internal bleeding[205-207]. Immunoadsorption can be modified to remove only antigen-specific antibodies from the patient serum, however, this approach has been shown to suffer from several issues such as inefficient (adsorption) column due to low affinity of autoantibodies, presence of autoantibodies that are specific to unidentified antigen or epitope, etc[202]. Although B cells are the source for plasma cells that produce antibodies, B cell-depleting anti-CD20 antibodies (rituximab and ocrelizumab), which have shown efficacy in treating MS, do not delete long-lived, CD20-negative plasma cells and antibody levels remain unaffected[208-212].

Several engineered or monoclonal IgG-based therapies that target FcRn have been developed and have shown promise in treating animal models of autoimmune diseases. These can

be classified into three categories based on their binding properties for FcRn at physiological and acidic pH. One category includes Fc-engineered IgG that binds to FcRn with increased affinity at acidic or endosomal pH, but has low affinity (comparable to WT antibody) towards FcRn at near neutral or physiological pH. One such engineered IgG was shown to reduce ankle swelling in a mouse model of arthritis, which was induced by administering human plasma from an RA patient[193]. Antibodies belonging to this category do not enter the endosomes efficiently (i.e., poor FcRn-mediated uptake into cells) due to low affinity for FcRn at physiological pH, as a result, offer limited competition for binding to FcRn in the endosomes and require high or frequent dosing to be efficacious[193]. A second category of FcRn blockers includes monoclonal antibodies that block FcRn through their Fragment antigen binding (Fab) arms and inhibit recycling or salvage of IgGs. Antibodies belonging to this category bind to FcRn with similarly high affinity at both acidic and physiological pH[144-146]. 1G3 is one such anti-FcRn antibody that has been shown to block disease development and reduce disease symptoms in a passive and active rat model of myasthenia gravis, respectively[146]. However, due to its high affinity towards FcRn at physiological pH, 1G3 has very short serum half-life (< 24 hours) in rats[146]. In contrast, Abdegs, which belong to the third category of FcRn blockers, retain high but significantly lower affinity (higher than antibodies in the first category but lower than antibodies in the second category) at pH 7.4 in comparison to pH 6.0[3]. In addition, Abdegs exhibit tight binding to FcRn at pH 6.0[3], similar to the antibodies in the other two categories. These properties aid Abdegs to efficiently reach endosomes and compete with endogenous WT IgG and also retain relatively long half-life (~ 40 hours)[20] in comparison to the antibodies that block FcRn through their Fab arms.

In the EAE model employed in this study, the disease exacerbation observed after antibody administration is both anti-MOG antibody- and MOG-specific T cell-mediated – i) administration

of anti-MOG antibody into ovalbumin-immunized mice does not induce EAE[213] (Priyanka Khare, E. Sally Ward, unpublished) and ii) anti-MOG antibodies that show binding to mouse CNS sections exacerbate the disease and the ones that do not recognize MOG in CNS sections are unable to exacerbate the disease in this model[194]. It is currently not known whether the T cells are required for increasing the permeability of the blood-brain barrier to facilitate the entry of anti-MOG antibodies into the CNS or for recruiting innate immune cells into the CNS that can mediate antibody-dependent demyelination or both. An alternative, but not mutually exclusive mechanism includes antibody-mediated activation or reactivation (in the CNS) of T cells. This mechanism is supported by two recent reports[214, 215]. Specifically, anti-MOG antibodies have been demonstrated to facilitate uptake of extremely low levels of endogenous MOG into antigen presenting cells (APCs) in an Fc-dependent manner resulting in activation of MOG-specific T cells and EAE[214]. Similarly, anti-MOG antibodies following diffusion into the CNS have been shown to enhance antigen presentation by CNS-resident APCs, consequently leading to enhanced activation of incoming effector T cells which in turn boosted immune cell recruitment and aggravated the clinical disease[215]. It will be of interest to analyze the effects of Abdeg-mediated autoantibody depletion on T cell activation and immune cell infiltration into the CNS in EAE.

In conclusion, inhibition of FcRn using Abdegs provides a new potential treatment for MS that, in combination with T cell-targeted treatments, could hold considerable promise for ameliorating this complex disease.

2.4 MATERIALS AND METHODS

2.4.1 Mice

Female C57BL/6J mice were purchased from the Jackson Laboratory and used at 9-10 weeks of age. Mice were housed in the animal facility at University of Texas (UT) Southwestern Medical Center and handled according to protocols approved by the Institutional Animal Care and Use Committee.

2.4.2 Recombinant antibodies and MOG

Clinical grade WT human IgG1 trastuzumab (Herceptin®) was obtained from the pharmacy at UT Southwestern Medical Center. NS0 transfectants expressing WT humanized (IgG1) anti-hen egg lysozyme antibody[216] and the MST-HN mutant derivative[3] (M252Y/S254T/T256E/ H433K/N434F) were cultured and antibodies were purified using lysozyme-Sepharose as described previously[216]. The MST-HN mutant was also scaled up in a bioreactor by BioXCell (West Lebanon, NH). Mouse IgG1 (anti-hen egg lysozyme, D1.3[198]) was purified using lysozyme-Sepharose from hybridoma culture supernatants.

The V_H and V_L domain genes of the 8-18C5 mAb (PDB code, 1PKQ)[217] were synthesized (Genscript USA, Piscataway, NJ) and used to generate full-length (mouse IgG1, kappa) expression constructs with codons encoding the leader peptide of the immunoglobulin heavy (MAVLVLFLCLVAFPSCVLS) and light (MKLPVRLLVLMFWIPASSS) chain genes of the anti-lysozyme D1.3 hybridoma[198] appended by PCR to the 5' ends of the V_H and V_L genes, respectively. PCR products encoding the complete 8-18C5 heavy and light chain genes were

cloned into pOptiVEC-TOPO and pcDNA 3.3-TOPO (OptiCHO™ antibody express kit, Life Technologies, Grand Island, NY), respectively.

Stable CHO DG44 transfectants were generated by first transfecting the 8-18C5 light chain expression construct and selecting the clone expressing the highest levels of light chain by ELISA. This clone was then transfected with the 8-18C5 heavy chain expression plasmid. Stably transfected clones were selected in Opti-CHO medium (Life Technologies, Grand Island, NY) containing 500 μg/ml geneticin. The CHO DG44 clones expressing the highest levels of antibody were identified by ELISAs using 96-well plates coated with recombinant mouse MOG and rabbit anti-mouse immunoglobulin conjugated to HRPO (Life Technologies, Grand Island, NY) for detection, and cultured in increasing concentrations of methotrexate (MTX, 50 nM-4 μM). For large scale production of 8-18C5 mAb, transfectants were expanded and antibody purified using protein G-Sepharose by BioXCell (West Lebanon, NH).

The extracellular domain (residues 1-121) of mouse MOG was expressed in recombinant form in baculovirus-infected High Five™ insect cells (Life Technologies, Grand Island, NY) using an analogous construct design to that described previously for the production of recombinant human MOG[12, 218], except that codons encoding the honey bee melittin leader peptide sequence[219] were appended to the 5' end of the gene.

2.4.3 Antibody labeling

The 8-18C5 mAb was labeled with Alexa Fluor 647 (Alexa 647) carboxylic acid (succinimidyl ester; Life Technologies, Grand Island, NY) using methods recommended by the manufacturer. Iodination (^{125}I) of 8-18C5 was carried out using Iodogen as previously described[220].

The activity of the labeled 8-18C5 was verified by carrying out surface plasmon resonance (BIAcore) analyses.

2.4.4 EAE exacerbation, pharmacokinetics and treatment

C57BL/6J mice were immunized subcutaneously at four sites in the flanks with 100 μg hMOG35-55 peptide (MEVGWYRPPFSRVVHLYRNGK; CS Bio, Menlo Park, CA) emulsified with complete Freund's adjuvant (Sigma-Aldrich, St. Louis, MO) containing an additional 4 mg/ml heat-inactivated *Mycobacterium tuberculosis* (strain H37Ra, Becton-Dickinson, San Jose, CA). 200 ng of pertussis toxin (List Biological Laboratories, Campbell, CA) was injected *i.p.* on days 0 and 2 to disrupt the blood-brain barrier. Mice were monitored daily for disease, and at day 15 were sorted into equivalent groups using a cost function (implemented in MATLAB) based on EAE scores prior to and including day 15. This cost function takes into account the similarity (in average scores and covariance) and the standard deviation of the disease scores. On day 15, mice were injected intravenously with 200 μg of Alexa 647-labeled or unlabeled 8-18C5 for immunofluorescence and treatment, respectively. For immunofluorescence, one group of mice was also injected with PBS as a control. Two or six hours later, mice in both groups were perfused with heparin/PBS and spinal cords isolated. For treatment, groups of mice were injected 2 hours following 8-18C5 delivery with MST-HN (1.5 mg/mouse), WT human IgG1 (1.5 mg/mouse) or PBS vehicle. Clinical signs of EAE were assessed for up to 30 days after immunization. Scoring of disease activity was as follows: 0, no paralysis; 1, limp tail; 2, moderate hind limb weakness; 3, severe hind limb weakness; 4, complete hind limb paralysis; 5, quadriplegia; and 6, death due to disease.

To analyze the effects of MST-HN delivery on the levels of 8-18C5, mice were immunized as above and were fed 0.1% Lugol (Sigma-Aldrich, St. Louis, MO) in water from day 14 onwards. At day 17, the mice were sorted into equivalent groups and each mouse injected with a mixture of 15 μg ^{125}I-labeled 8-18C5 and 185 μg unlabeled 8-18C5. Two hours later, groups of mice were injected with MST-HN (1.5 mg/mouse), WT human IgG1 (trastuzumab; 1.5 mg/mouse) or PBS vehicle. Levels of radioactivity were determined at the indicated times in 10 μl blood samples by gamma counting and by whole body counting using Atom Lab 100 dose calibrator (Biodex Medical Systems, Shirley, NY). To determine the levels of radioactivity in the CNS, mice were perfused with heparin/PBS 48 hours following the delivery of MST-HN or WT human IgG1. Following perfusion, brains and spinal cords were isolated and the levels of ^{125}I-labeled 8-18C5 in these tissues were determined by gamma counting.

2.4.5 Immunofluorescence analyses

Spinal cord tissue was embedded in Tissue-Tek® OCT compound (Sakura Finetek USA, Torrance, CA), sectioned (5 μm thick) using a Leica cryotome and stored at -80ºC. Frozen sections were fixed in acetone (-20˚C) and air-dried overnight. After washing with PBS, sections were blocked using 5% goat serum, followed by incubation with polyclonal rabbit anti-mouse proteolipid protein (PLP) antibody (Abcam, Cambridge, MA). Bound anti-PLP antibody was detected using Alexa 555-labeled goat anti-rabbit IgG (Life Technologies, Grand Island, NY). Following washing, coverslips were mounted using Vectashield mounting medium containing DAPI (Vector Laboratories, Burlingame, CA).

Sections were imaged using a Zeiss Axiovert 200M inverted microscope equipped with a Zeiss 20X, 0.5 NA Plan-Neofluar objective and an ORCA CCD camera (Hamamatsu). Images

were acquired with filtersets specific for Alexa 555 Fluor (TRITC-B-000-ZERO; Semrock), Alexa 647 Fluor (Cy5-4040C-ZERO; Semrock) and DAPI (Part No 31013v2; Chroma Technologies). The data were processed and displayed using the microscopy image analysis tool (MIATool) software package (www4.utsouthwestern.edu/wardlab/miatool.asp) in MATLAB (Mathworks, Natick, MA). The acquired images were embedded in 16-bit grayscale format and overlaid for presentation. For comparative purposes, the intensities of the Alexa 647 Fluor channel were adjusted in an analogous manner across the datasets. Images were exported into Adobe Photoshop CS6 for final composition of the figures.

2.4.6 Statistical analyses

Statistical analyses were carried out using two-tailed Student's *t*-test in the statistics toolbox of MATLAB (Mathworks, Natick, MA). *p* values of less than 0.05 were taken to be significant.

CHAPTER THREE
FcRn-targeted antibody engineering to treat disease in a T cell-dependent animal model of multiple sclerosis

This study has been published in the *Journal of Autoimmunity* [Challa, D.K., Mi, W., Lo, S.T., Ober, R.J. & Ward, E.S. Antigen dynamics govern the induction of $CD4^+$ T cell tolerance during autoimmunity. *J. Autoimmun.* 72, 84-94 (2016)].

3.1 INTRODUCTION

Multiple sclerosis (MS) is a chronic, demyelinating disease of the central nervous system (CNS) that represents a major cause of physical disability in young adults[153]. It is well established that the aberrant activation of autoreactive $CD4^+$ T cells is a driver of MS[6]. Currently approved therapies for MS that broadly target such cells include the depletion of lymphocyte subsets, the targeting of lymphocyte activation and proliferation or the inhibition of leukocyte trafficking[7, 221]. However, these approaches can result in adverse side effects such as systemic toxicities and increased risk for infection or cancer[7, 221]. Consequently, a need for the development of treatments, such as tolerance induction, to selectively target autoantigen-specific T cells persists.

Induction of antigen-specific $CD4^+$ T cell tolerance involves the presentation or exposure of the antigen (usually immunodominant peptides from the autoantigenic protein) to T cells in tolerogenic rather than immunogenic conditions. Different protocols have been employed in the past to achieve peptide-specific T cell tolerance. Altered peptide ligand (APL)-induced tolerance is one such protocol, in which altered versions of native autoantigenic peptides are employed as

tolerogens. APLs act as antagonist or partial agonist for native autoantigen-specific $CD4^+$ T cells, leading to T cell anergy or immune deviation from highly encephalitogenic T helper (Th)1 or Th17 to poorly encephalitogenic Th2 responses, respectively[222, 223]. Consequently, APLs have been shown to prevent or ameliorate disease in multiple animal models of MS[224-227]. However, two separate MS phase II clinical trials of myelin basic protein (MBP)83-99 were discontinued due to severe adverse reactions, which either included exacerbations of MS or hypersensitivity reactions[228, 229]. Another protocol for inducing antigen-specific $CD4^+$ T cell tolerance involves the administration of native autoantigenic peptides through mucosal (oral or nasal) route. Oral administration of high dose of antigen into mice results in anergy or deletion of antigen-specific $CD4^+$ T cells[230, 231], whereas administration of low dose of antigen leads to bystander suppression or activation of regulatory T cells (Tregs), which secrete suppressive cytokines such as transforming growth factor-β (TGFβ), IL-4 and IL-10[232-234]. In contrast, intranasal delivery of single dose of antigen results in (incomplete) deletion of antigen-specific $CD4^+$ T cells and multiple intranasal doses downregulate the capacity of antigen-specific $CD4^+$ T cells to produce IL-2, interferon (IFN)-γ and IL-4, but increases the production of IL-10 by these T cells[235]. In both prophylactic and therapeutic EAE studies, oral delivery of high or low dose of antigen has been shown to suppress EAE in few studies, but not in other studies[236-241]. In contrast, nasal delivery of single or multiple doses of antigen before EAE induction had a protective effect in most studies[235, 240-244], however, treatment of ongoing EAE with nasal delivery of antigen has provided mixed results including exacerbation of EAE[241, 243]. Importantly, in MS clinical trials, oral administration of whole bovine MBP provided no clinical benefit in comparison with the placebo group[245, 246].

An alternative cell-based protocol for inducing antigen-specific $CD4^+$ T cell tolerance is the intravenous administration of antigen-coupled, ethylene carbodiimide (ECDI)-fixed splenocytes,

referred to as antigen-coupled cells (Ag-SPs). Protein or peptide fixation to splenocytes using ECDI involves the formation of peptide bonds between free amino and carboxyl groups[247]. Multiple mechanisms have been shown to contribute to Ag-SP-induced tolerance. Peptide-coupled Ag-SPs can directly present peptide:major histocompatibility complex (MHC) class II complexes to target $CD4^+$ T cells in the absence of costimulation to induce anergy[248]. Further, it was demonstrated that uptake of intravenously delivered Ag-SPs by splenic marginal zone macrophages induces production of IL-10, which upregulates the expression of the immunomodulatory co-inhibitory molecule programmed death-ligand 1 (PD-L1)[249]. Ag-SP delivery also induces the generation of Tregs[249]. Consequently, Ag-SPs were found to prevent onset of EAE and ameliorate ongoing EAE[248, 249]. However, due to difficulties associated with isolating isologous leukocytes and peptide coupling under good manufacturing practices, polystyrene and poly(lactide-*co*-glycolide) (PLG) microparticles bearing encephalitogenic peptides have been developed[250]. Upon intravenous delivery, microparticles coupled to encephalitogenic myelin epitopes are taken up by splenic marginal zone $MARCO^+$ macrophages, subsequently resulting in antigen-specific T-cell anergy and generation of Tregs, thereby preventing and treating EAE[250]. Although microparticle-based approach is a promising strategy for T cell tolerance induction, it is associated with several limitations that are discussed later in this chapter.

One of the most extensively explored protocol for the induction of antigen-specific $CD4^+$ T cell tolerance is to use multiple high doses (few micrograms to milligrams) of soluble immunodominant peptides to delete or anergize autoreactive T cells in mice[15, 251]. Exposure of T cells to cognate antigen induces them to proliferate, but further T cell receptor (TCR) engagement can stimulate the T cells to proliferate, become nonresponsive to antigen (anergic), or to

apoptose/die (activation-induced cell death). The latter two prevail at high concentrations of antigen[8, 10, 252]. Several studies have shown efficacy of multiple high doses of antigen in protecting against disease onset or reducing disease in animal models of MS[8-14], however, the translation of such therapies into humans has been unsuccessful[15, 16]. For example, in a phase II trial using an MBP peptide in relapsing-remitting MS (RRMS) patients, the treatment showed no significant benefit over the placebo-treatment, except for a subset of patients who were HLA $DR2^+$ and/or $DR4^+$[253]. In a phase III study with the same MBP peptide in secondary progressive multiple sclerosis (SPMS) patients (HLA $DR2^+$ or $DR4^+$), the treatment did not provide clinical benefit compared with placebo[254]. Further, there are significant safety concerns due to reports of fatal anaphylaxis in many animal models of MS following the delivery of relatively high doses (necessitated by rapid renal clearance[17]) of autoantigenic peptides during ongoing disease[18, 19]. A longstanding, unsolved challenge is therefore to develop effective tolerizing agents that are safe for the therapy of autoimmunity.

Chronic exposure to autoantigens during autoimmunity results in reduced disease severity, with mouse studies indicating that this phenomenon results from Treg activation[255]. In addition, low dose, persistent antigen presentation during chronic viral infections can lead to $CD4^+$ T cell exhaustion or dysfunction in an antigen-specific manner[256]. We therefore reasoned that the development of delivery vehicles to enable persistence of low levels of antigen could represent an effective approach to induce antigen-specific T cell tolerance. However, the generation of antigen delivery strategies to achieve such immune homeostasis is challenging due to the limited understanding of the complex interplay between antigen longevity and intracellular trafficking behavior, which in turn determine the efficiency of antigen presentation by APCs.

Our Fc engineering studies indicate that antigenic peptide epitopes expressed as immunoglobulin Fc-epitope fusions can be tuned to have different pharmacokinetics by modulating their binding properties for the neonatal Fc receptor (FcRn)[257]. The majority of naturally occurring antibodies of the immunoglobulin G (IgG) class bind to FcRn at acidic pH (pH 6.0) but with an affinity that is negligible at near neutral pH[1]. Consequently, following entry into cells bathed at pH 7.3-7.4 by fluid phase processes, IgG can bind to FcRn in early acidic endosomes and undergo recycling or transcytosis[1, 41, 54]. These endosomal sorting pathways regulate the homeostasis and transport of IgG in the body. Further, FcRn is expressed in all professional APCs and is involved in antigen presentation[258]. In the current study, this knowledge has been used to inform the design of a panel of Fc-epitope fusions comprising the N-terminal epitope of myelin basic protein (MBP1-9) linked to engineered Fc regions with the goal of defining the requirements for tolerance induction in a low antigen dose setting. Specifically, we have generated a panel of Fc-MBP fusions with different subcellular trafficking behavior and *in vivo* clearance properties. The effects of these engineered proteins on both the prophylactic blockade and treatment of disease in an EAE model involving the immunization of B10.PL (H-2^u) mice with the immunodominant epitope, MBP1-9 (with N-terminal acetylation) have been investigated.

By using Fc-engineering to tune antigen dynamics, we have established the design requirements for antigen delivery vehicles that result in T cell tolerance and amelioration of ongoing autoimmune disease. Importantly, these studies have been carried out using doses (1 μg/mouse; ~50 μg/kg) that are at least ~450-fold lower than those used previously as either soluble antigen or peptides coupled to microparticles for the treatment of autoimmunity[8-14, 250], reducing the risk of anaphylactic shock. Our analyses have defined a remarkably stringent threshold of antigen persistence that is necessary to induce tolerance prior to disease induction and during

ongoing disease. In these two settings, although the threshold for antigen persistence is the same, the pathways of tolerance induction are mechanistically distinct: under prophylactic conditions, antigen-specific T cells are deleted or anergized whereas during ongoing EAE, tolerance involves the downregulation of T-bet and CD40L on antigen-specific T cells, combined with the induction of regulatory $Foxp3^+$ T cells. Our studies demonstrate that the delivery of low doses of Fc-epitope fusions represents a promising strategy for the treatment of autoimmunity and other pathological, T cell-mediated conditions.

3.2 RESULTS

3.2.1 Generation of Fc-antigen fusion proteins with different *in vivo* dynamics

The binding of WT mouse IgG1 or corresponding Fc fragment to mouse FcRn is highly pH-dependent, with binding at pH 5.5 - 6 (early-late endosomes) that becomes negligible at pH 7 - 7.4[1]. Engineered IgGs with higher binding affinity than WT IgG1 for FcRn at both acidic and near-neutral pH confers increased (receptor-mediated) uptake of the antibody, limited exocytic release during recycling, entry into lysosomes and reduced persistence[3, 20]. Two sets of Fc mutations that alter FcRn binding were selected for this study: mutation-set (m-set)-1 (T252L/T254S/T256F/ E380A/H433K/N434F)[44, 122, 127] and m-set-2 (T252Y/T256E/H433K/N434F)[3]. Based on the effects of these mutations on the equilibrium dissociation constants (K_Ds) of the interactions of mouse IgG1-derived Fc-hinge fragments with mouse FcRn (Table 3-1), Fc fragments or IgG molecules harboring m-set-1 and m-set-2 mutations would be predicted to have distinct dynamic properties *in vivo*[1]. To confirm this, the pharmacokinetics of full length mouse IgG1 molecules harboring m-set-1 and m-set-2 mutations were compared with their WT counterpart in mice (Fig. 3-1A). The exposure to these proteins (area under the curve, or AUC, of injected dose vs. time) decreases in the following order: WT >> m-set-1 > m-set-2 (Fig. 3-1B).

We next generated Fc-MBP fusions comprising WT or mutated Fc fragments linked to MBP1-9. Although multiple studies have demonstrated that this MBP peptide requires N-terminal acetylation for T cell recognition, the replacement of the acetyl group with glycine generates an analogous epitope[259]. Further, the fusion proteins contain the '4Y' analog [MBP1-9(4Y)] of this peptide, in which lysine at position 4 is substituted by tyrosine. This analog has higher binding affinity for I-A^u than its parent peptide whilst retaining recognition by autoreactive T cells[259, 260].

Table 3-1. Binding properties of mouse Fc fragments

Fc fragment	Binding to FcRn (K_D, nM)	
	pH 6.0	pH 7.4
WT	218.2	N.B.*
m-set-1	2.6	114.6
m-set-2	1.1	20.4

*N.B. = no detectable binding.

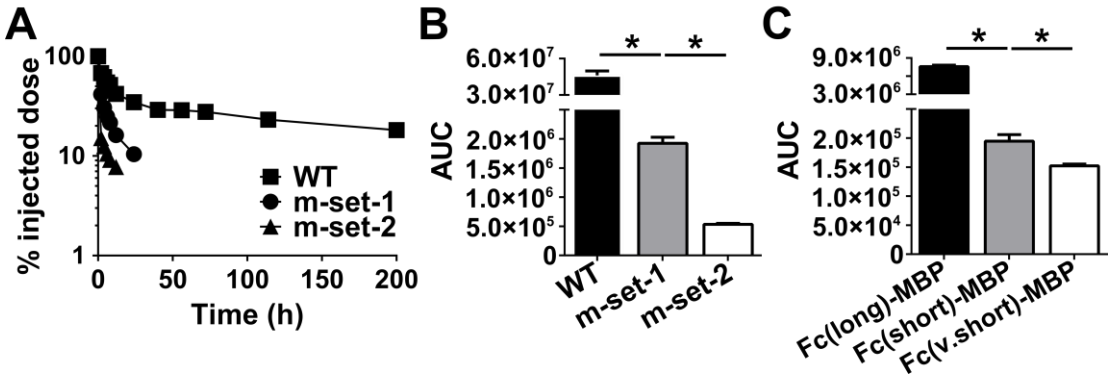

Figure 3-1. IgGs or Fc-MBP fusions containing m-set-1 and m-set-2 mutations are cleared more rapidly in mice compared with their WT counterparts. B10.PL mice (n = 4-5 mice/group) were injected with ^{125}I-labeled IgGs (A, B) or Fc-MBP fusion (C). (A) Remaining radioactivity levels in blood samples. (B, C) Areas under the curve (AUCs, cpm h), calculated for fitted data following extrapolation to 1% injected dose. Error bars indicate SEM and significant differences ($p < 0.05$; two-tailed Student's *t*-test) are indicated by *****.

The pharmacokinetics of the Fc-MBP fusions were analyzed in mice (Fig. 3-1C). Despite the lower persistence of the Fc fusions compared with the corresponding parent IgGs, most likely due to the binding of the epitope extending from the CH3 domain of the Fc fragment to the MHC Class II molecule, I-A^{u} [261], the *in vivo* exposure (AUC) to the proteins decreased in the same order (Fig. 3-1C). Throughout these studies, fusion proteins containing WT or Fc fragments with m-set-1 and m-set-2 mutations were therefore designated Fc(long)-MBP, Fc(short)-MBP and Fc(v.short)-MBP, respectively. Although the difference in exposure (AUC) between Fc(short)-MBP and Fc(v.short)-MBP was significant, this difference was much lower than that for Fc(short)-MBP compared with Fc(long)-MBP (Fig. 3-1C). Consistent with the differences in exposure for the Fc-MBP fusions, the percentage remaining of the injected dose after one hour was 16.33 ± 0.63% and 9.62 ± 0.28 % for Fc(short)-MBP and Fc(v.short)-MBP, respectively, whereas for Fc(long)-MBP, 10.54 ± 0.5 % of the injected dose remained after 118 hours.

3.2.2 Antigen persistence affects the proliferation of antigen-specific T cells *in vivo*

The effect of the distinct properties of the Fc-MBP fusions on the *in vivo* proliferation of MBP1-9:I-A^{u}-specific $CD4^{+}$ T cells was next investigated. CFSE-labeled, purified $CD4^{+}$ T cells isolated from MBP1-9:I-A^{u}-specific TCR ($V\beta8^{+}$) transgenic mice were used in adoptive transfers. Prior to T cell transfer into WT B10.PL (I-A^{u}) mice, 1 μg Fc-MBP fusion was injected into recipients on different days (day -5, -3 and 0, referring to 5, 3 and 0 days before the cell transfer, respectively, Fig. 3-2A). The percentage of divided $CD4^{+}CFSE^{+}V\beta8^{+}$ T cells was assessed in the spleen and lymph nodes (LNs) three days following T cell transfer. As a control throughout these studies, an Fc-MBP fusion in which the T cell contact residues, Gln3 and Pro6, of the MBP peptide[262] are replaced by Ala [Fc(long)-MBP(3A6A)] was used. Fc(long)-MBP induced higher

levels of proliferation in the spleens and LNs than Fc(short)-MBP for all treatments (Fig. 3-2B). We have previously characterized the properties of Fc(v.short)-MBP in analogous assays[257], and the behavior of Fc(short)-MBP is very similar (Fig. 3-2B). As expected, Fc(long)-MBP(3A6A) induced no detectable proliferative response. Collectively, the data indicate that the increased affinity for FcRn at near neutral pH of Fc(short)-MBP and Fc(v.short)-MBP confers decreased *in vivo* persistence relative to Fc(long)-MBP, which in turn results in lower T cell responses *in vivo* (Fig. 3-2B).

3.2.3 The induction of tolerance under prophylactic conditions is regulated by antigen persistence

We next investigated the activity of low doses (1 μg/mouse; ~50 μg/kg) of the Fc-MBP fusions in inducing T cell tolerance in a prophylactic setting. These low doses of fusion protein do not affect the activity of FcRn in regulating IgG half-life (Fig. 3-3). B10.PL mice were pretreated with 1 μg Fc-MBP fusion and immunized 7 days later to induce EAE. Fc(long)-MBP(3A6A) was used as a control. The majority of mice developed either no, or low grade, disease following pretreatment with Fc(long)-MBP (Fig. 3-4A). Treatment of mice with Fc(short)-MBP was less effective in ameliorating EAE, whereas Fc(v.short)-MBP treatment had no protective effect (Fig. 3-4A). Thus, low dose antigen induces prophylactic tolerance, but only if antigen persists above a threshold level.

In addition to the shorter half-life of Fc(v.short)-MBP, the inability of Fc(v.short)-MBP to induce tolerance (Fig. 3-4A) could be due to differences between this fusion and Fc(long)-MBP in endolysosomal trafficking behavior which influences antigen presentation by FcRn-expressing APCs[36, 257]. Specifically, the binding of engineered Fc fragments to FcRn at near neutral pH results in efficient receptor (FcRn)-mediated uptake and accumulation in the endolysosomal pathway in

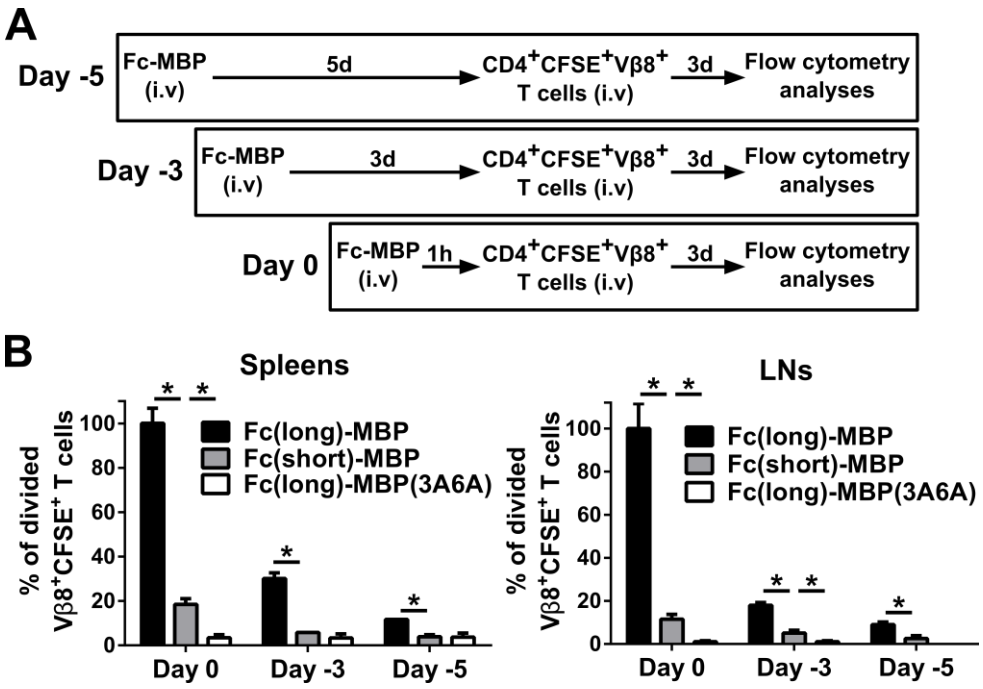

Figure 3-2. *In vivo* persistence governs the response of cognate T cells to Fc-MBP fusions. (A) Flow chart describing the experimental design. B10.PL mice were injected with 1 μg Fc-MBP fusion 0, 3 and 5 days before the transfer of CFSE-labeled antigen-specific ($V\beta8^+$) T cells. $CD4^+CFSE^+V\beta8^+$ T cell proliferation was analyzed three days later by flow cytometry. (B) % divided $V\beta8^+CFSE^+$ T cells of total $CD4^+$ cells in spleens and LNs for the different treatments, normalized to the group injected with Fc(long)-MBP on day 0. Data are combined from at least two independent experiments (n = 3-4 mice/group). Error bars indicate SEM and significant differences ($p < 0.05$; two-tailed Student's *t*-test) are indicated by *****.

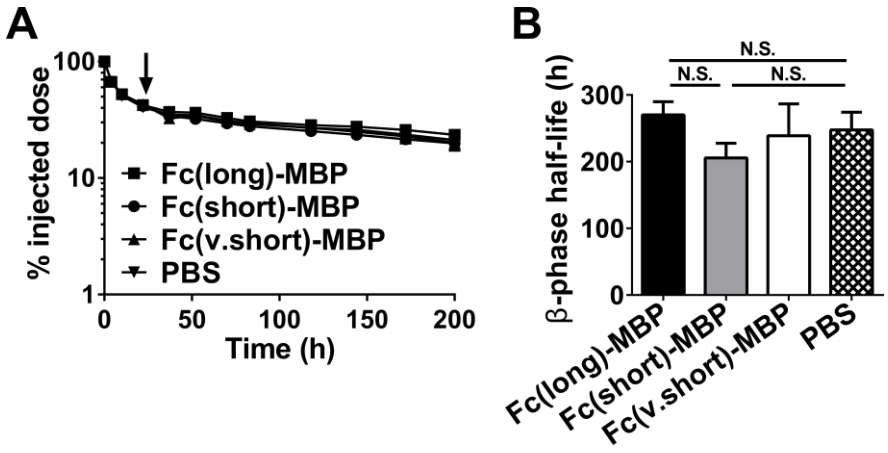

Figure 3-3. Fc-MBP fusions do not affect the clearance rate of mouse IgG1. B10.PL mice (n = 4-5 mice/group) were injected with ^{125}I-labeled mouse IgG1. 24 hours later (indicated by arrow in panel A), the mice were injected with DPBS or 1 μg Fc-MBP fusion. (A) Remaining radioactivity levels in blood samples. (B) β-phase half-lives of mouse IgG1, calculated for fitted data. Error bars indicate SEM. N.S., no significant difference ($p > 0.05$; two-tailed Student's *t*-test).

FcRn-expressing cells, by contrast with WT Fc fragments that enter cells by fluid-phase pinocytic processes[1]. Consequently, using FcRn-transfected B lymphoblastoid (PL8:FcRn)[257] cells as APCs, Fc(short)-MBP induced significantly higher IL-2 production by cognate T cell hybridoma (#46[263]) cells than Fc(long)-MBP (Fig. 3-4B), whereas in the presence of PL8 cells (that do not express FcRn), the Fc-MBP fusions induced similar levels of cytokine production (Fig. 3-4B;[257]). Analogously, in earlier studies we observed that Fc(v.short)-MBP stimulates T cells at around 600-3,000 fold lower concentrations than Fc(long)-MBP in the presence of PL8:FcRn cells[257]. To investigate whether this behavior contributed to the inability of a single dose of Fc(v.short)-MBP to induce tolerance (Fig. 3-4A), we therefore compared the tolerogenic activity of five doses of 1 μg Fc(v.short)-MBP at 36 hour intervals, starting at 7 days prior to immunization, with a single, equivalent bolus dose (5 μg) delivered at 7 days prior to EAE induction. Importantly, treatment with multiple doses of Fc(v.short)-MBP offered partial protection against EAE, whereas bolus administration of a five-fold higher dose of this Fc-MBP fusion did not affect disease activity (Fig. 3-4C). These observations indicate that antigen longevity, rather than endolysosomal trafficking behavior, is a dominant factor governing T cell tolerance. In addition, given the relatively small difference in the pharmacokinetic behavior of Fc(short)-MBP and Fc(v.short)-MBP in mice (Fig. 3-1C), the threshold of antigen persistence necessary for effective prophylaxis is stringent.

3.2.4 Antigen specific T cell numbers are reduced during prophylactic T cell tolerance

To investigate the mechanism of prophylactic tolerance induction, Fc-MBP fusions were delivered prophylactically and splenic antigen-specific T cells quantitated using fluorescently labeled MBP1-9(4Y)-I-A^u tetramers[219] ten days following immunization with MBP1-9. Antigen-specific T cell numbers in the treated mice decreased in the order: Fc(v.short)-MBP (similar to

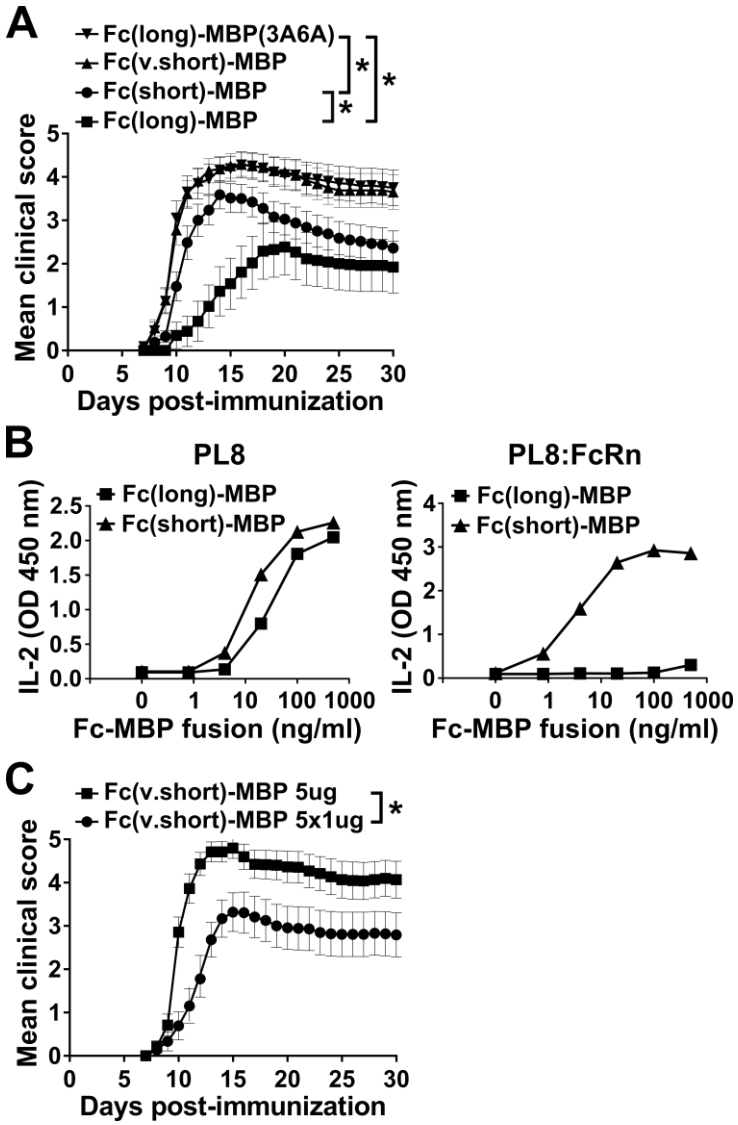

Figure 3-4. Prophylactic tolerance induction is determined by antigen persistence. (A) B10.PL mice were pretreated with 1 μg Fc-MBP fusion and immunized seven days later with MBP1-9 to induce EAE. Mean clinical scores are shown. Data are combined from at least two independent experiments (n = 13-30 mice/group). (B) IL-2 production by antigen-specific T cell hybridoma (#46^{263}) cells in response to the Fc-MBP fusions in the presence of I-A^{u}-expressing PL8 or PL8:FcRn^{257} cells. Data is representative of at least two independent experiments. (C) B10.PL mice were pretreated with either 5 doses of 1 μg of Fc(v.short)-MBP (starting at 7 days prior to immunization, at 36 hour intervals) or with a single bolus dose of 5 μg of Fc(v.short)-MBP and immunized seven days later to induce EAE. Mean clinical scores are shown. Data are combined from at least two independent experiments (n = 18-26 mice/group). Error bars indicate SEM and significant differences ($p < 0.05$; linear mixed effects model) are indicated by *****.

control mice) > Fc(short)-MBP > Fc(long)-MBP (Fig. 3-5A,B). In addition, prophylactic delivery of a single dose of 5 μg Fc(v.short)-MBP resulted in higher numbers of antigen-specific T cells compared with treatment using five repeated doses (1 μg/dose) of this Fc-MBP fusion (Fig. 3-5C). Further, there were no significant differences between the numbers of $CD4^+Foxp3^+$ Tregs in mice treated with the different Fc-MBP fusions (Fig. 3-6). Consequently, there is a correlation between antigen longevity, disease blockade and reduction in antigen-specific T cell numbers.

3.2.5 Antigen persistence regulates T cell tolerance induction during ongoing disease

To assess therapeutic tolerance induction, mice were immunized with MBP1-9 to induce EAE and treated with the different fusion proteins (1 μg/mouse; ~50 μg/kg) following the onset of disease (EAE score of 1-2). Severe disease was observed in the control group of mice within 4-5 days of disease onset, whereas treatment with Fc(long)-MBP resulted in either almost complete recovery or lowered disease to a score of 1-2 following a transient increase in disease score (Fig. 3-7A). The therapeutic effect of Fc(short)-MBP was analogous to that of Fc(long)-MBP, whereas by analogy with prophylactic tolerance, the treatment of mice with Fc(v.short)-MBP had no effect on ongoing disease. This indicates a requirement for the Fc-MBP fusion to reach a threshold level of persistence for therapeutic tolerance, with the threshold being tightly bounded by the *in vivo* dynamics of Fc(short)-MBP and Fc(v.short)-MBP (Fig. 3-1C). Importantly, the delivery of a molar equivalent of MBP1-9(4Y) peptide (33 ng/mouse), which is expected to be rapidly cleared (~ 2-30 minutes[17]) by renal filtration, was less effective in treating EAE than Fc(long)-MBP (Fig. 3-7B).

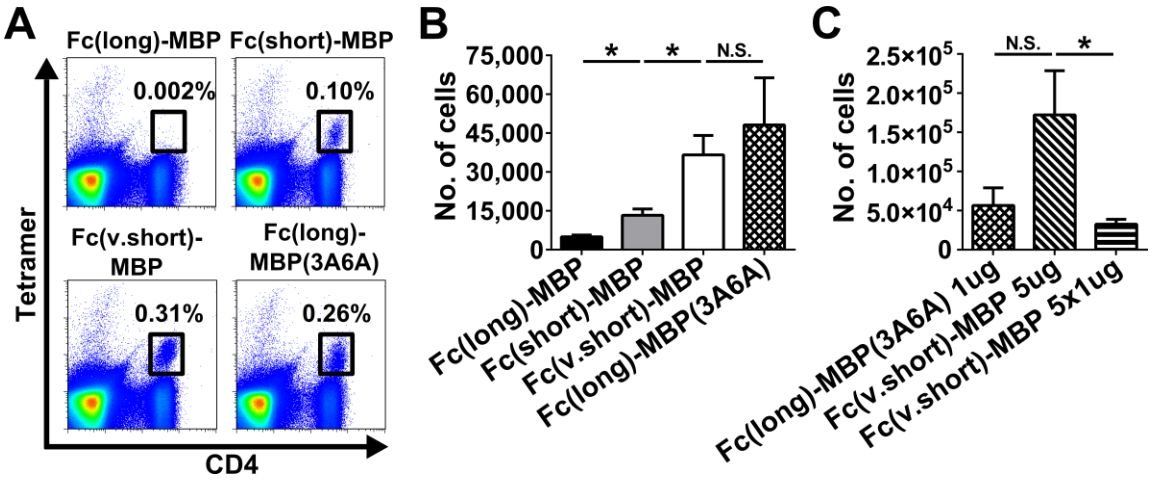

Figure 3-5. Prophylactic tolerance induction is accompanied by lower numbers of antigen-specific T cells. (A, B, C) Quantitation of antigen-specific T cells in the spleens of mice using fluorescently labeled MBP1-9(4Y):I-A^u tetramers ten days following immunization. % (boxed, A) and total numbers of $CD4^+$tetramer$^+$ T cells (B, C) are shown. Percentages (± SEM) of $CD4^+$ T cells for mice treated with the Fc-MBP fusions were: Fc(long)-MBP, 10.5 ± 0.9; Fc(short)-MBP, 11.4 ± 0.3; Fc(v.short)-MBP, 12.4 ± 0.8; Fc(long)-MBP(3A6A), 10.3 ± 0.6; 5 µg Fc(v.short)-MBP, 10.6 ± 0.7; 5 x 1 µg Fc(v.short)-MBP, 11.2 ± 0.4. Dot plots show data for one representative mouse within each group (A), and data in (B) and (C) are derived from 4-7 mice/group. Error bars indicate SEM and significant differences ($p < 0.05$; two-tailed Student's *t*-test) are indicated by *****. N.S., no significant difference.

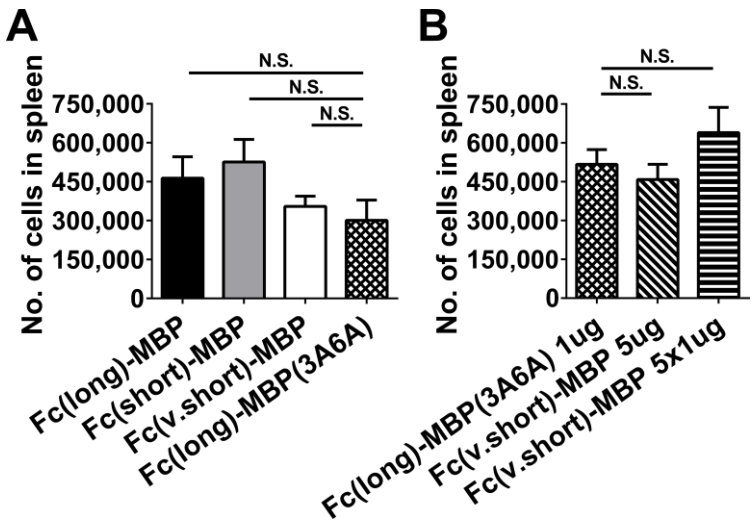

Figure 3-6. Prophylactic tolerance induction does not result in increased numbers of CD4$^+$Foxp3$^+$ T cells. B10.PL mice were treated as in Fig. 3-4. (A, B) Numbers of CD4$^+$Foxp3$^+$ T cells in the spleens were determined using flow cytometry ten days following immunization of mice with MBP1-9. Data are derived from 4-7 mice per treatment group. Error bars indicate SEM. N.S., no significant difference ($p > 0.05$; two-tailed Student's *t*-test).

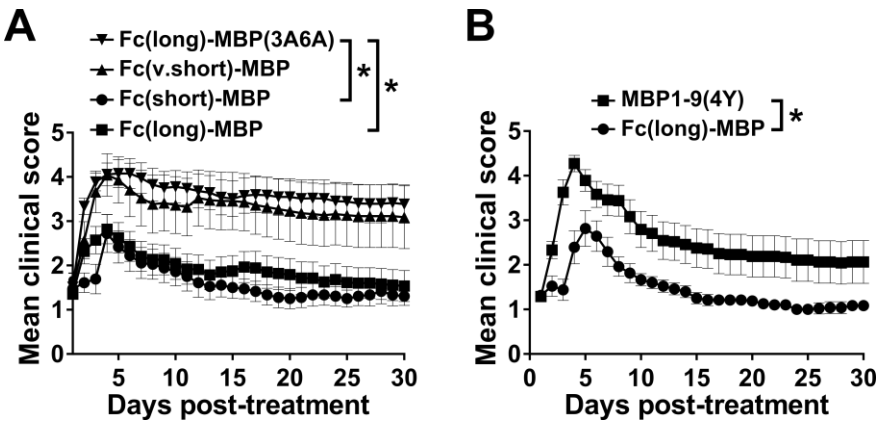

Figure 3-7. A threshold persistence level of Fc-MBP fusion is necessary for the treatment of EAE. (A, B) B10.PL mice were immunized with MBP1-9 and treated with 1 μg Fc-MBP fusion or 33 ng MBP1-9(4Y) peptide following the onset of disease symptoms (EAE score of 1-2). Mean clinical scores are shown. Data are combined from at least two independent experiments (n = 9-26 mice/group). Error bars indicate SEM and significant differences ($p < 0.05$; linear mixed effects model) are indicated by *****.

3.2.6 The mechanisms of prophylactic and therapeutic tolerance induction are distinct

To elucidate the mechanism through which Fc-MBP fusions induce therapeutic tolerance, cells from spleens and draining LNs were analyzed in mice from Fc(long)-MBP and control treatment groups six days following treatment. Unexpectedly, and by marked contrast with the prophylactic setting, the numbers of antigen-specific $CD4^+$ T cells in the spleens and LNs of tolerized mice were approximately 10- and 4-fold higher, respectively, than in control mice (Fig. 3-8A). By contrast, quantitation of the antigen-specific T cells in the brain and spinal cord revealed around 10-fold lower numbers in the spinal cord of Fc(long)-MBP-treated mice, whereas similar numbers were detected in the brain (Fig. 3-8B). In the majority of murine EAE models, inflammation predominates in the spinal cord rather than the brain[264]. Also, MBP1-9-induced EAE in B10.PL mice is primarily Th1 cell-mediated[242, 265] and it is well established that Th1 cells promote the accumulation of macrophages in the CNS during EAE[266]. Consistent with the reduced T cell infiltrates in the spinal cords of tolerized mice, macrophage numbers were also decreased at this site (Fig. 3-8C).

The increased numbers of antigen-specific T cells in the periphery of tolerized mice, combined with their reduced numbers in the CNS, prompted us to further characterize these cells by quantitating their levels of the following markers: CXCR3, α4β1, α4β7, LFA-1, CTLA-4, PD-1 and CD40L. In addition, the intracellular levels of the master regulator of Th1 lineage development, T-bet, were analyzed. T-bet and CD40L were the only molecules that were differentially expressed between the groups. T-bet levels were significantly lower in splenic antigen-specific T cells obtained from mice treated with Fc(long)-MBP (Fig. 3-8D). This trend was also seen in antigen-specific T cells obtained from draining LNs (constituting only ~ 20% of the total number of antigen-specific T cells isolated from both spleen and LNs), but the difference

was not statistically significant (Fig. 3-8D). Further, approximately threefold lower numbers of splenic antigen-specific T cells were $CD40L^{hi}$ in Fc(long)-MBP-treated mice by comparison with T cells obtained from control mice (Fig. 3-8E). Importantly, mice treated with Fc(long)-MBP had higher numbers of $CD4^{+}Foxp3^{+}$ Tregs in the spleen and draining LNs (Fig. 3-8F) which did not bind to MBP1-9(4Y):I-A^{u} tetramers. The increase in $CD4^{+}Foxp3^{+}$ Tregs, combined with decrease in $CD4^{+}$T-bet^{+} antigen-specific (Th1) T cells, resulted in higher Treg:Th1 ratios in tolerized mice (Fig. 3-8G). The treatment of mice with Fc(short)-MBP resulted in similar effects on splenic antigen-specific T cell numbers, their phenotype and $CD4^{+}Foxp3^{+}$ Treg numbers (Fig. 3-9), demonstrating antigen-specific tolerance of splenic T cells combined with the amplification of Tregs in tolerized mice.

Figure 3-8

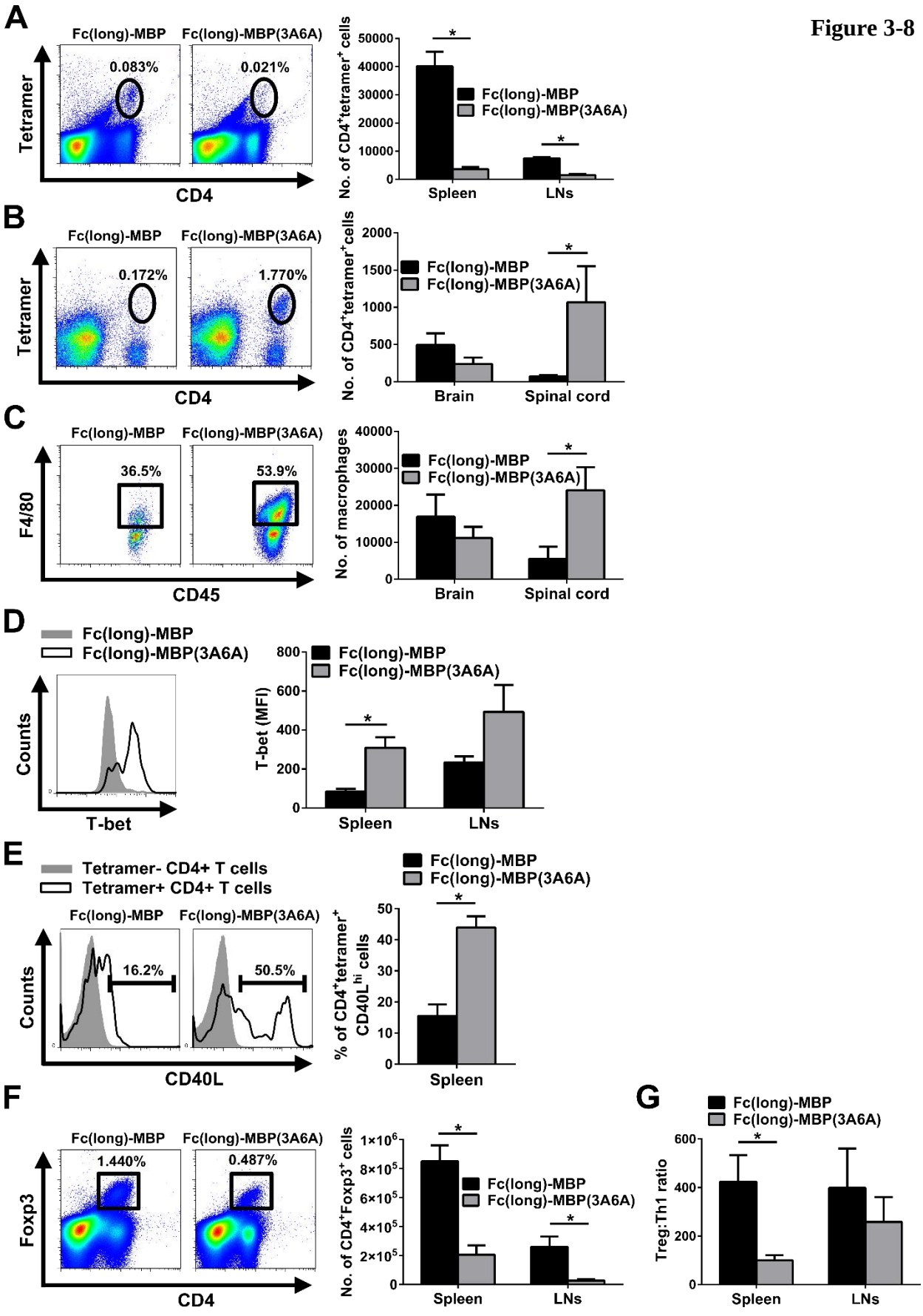
A
Fc(long)-MBP
Fc(long)-MBP(3A6A)
0.083%
0.021%
Tetramer
CD4
No. of CD4+tetramer+ cells
Spleen
LNs
B
0.172%
1.770%
Brain
Spinal cord
C
36.5%
53.9%
F4/80
CD45
No. of macrophages
D
Counts
T-bet
T-bet (MFI)
E
Tetramer- CD4+ T cells
Tetramer+ CD4+ T cells
16.2%
50.5%
CD40L
% of CD4+tetramer+ CD40Lhi cells
F
1.440%
0.487%
Foxp3
No. of CD4+Foxp3+ cells
G
Treg:Th1 ratio

Figure 3-8. Tolerance induction during ongoing EAE results in increased numbers of peripheral antigen-specific CD4$^+$ T cells with downregulated T-bet and CD40L levels combined with reduced inflammatory infiltrates in the CNS. B10.PL mice were immunized and treated with Fc(long)-MBP as in Fig. 3-7. Six days following treatment, mice were sacrificed and tissues isolated for flow cytometry analyses to determine: (A) % (in spleens) and total numbers (in spleens, LNs) of CD4$^+$tetramer$^+$ T cells; (B, C) % (in spinal cords) and total numbers (in brains, spinal cords) of mononuclear infiltrates that are CD4$^+$tetramer$^+$ T cells (B) or F4/80$^+$CD45^{hi} macrophages (C); (D) MFI levels for T-bet amongst CD4$^+$tetramer$^+$ T cells in spleens and LNs; (E) % CD4$^+$tetramer$^+$CD40L^{hi} T cells in spleens; (F) % (in spleens) and total numbers (in spleens, LNs) of CD4$^+$Foxp3$^+$ T cells; (G) Treg (CD4$^+$Foxp3$^+$ T cells):Th1 (CD4$^+$tetramer$^+$T-bet$^+$ T cells) ratios in spleens and LNs. For A-F, left panels show data for one representative mouse from each group. For A-C, F, populations of interest are indicated in dot plots by solid circles or boxes. Percentages (± SEM) of CD4$^+$ T cells for mice treated with the Fc-MBP fusions were: Fc(long)-MBP, 8.8 ± 0.4 (spleens) and 34.8 ± 1.5 (LNs); Fc(long)-MBP(3A6A), 14.7 ± 0.9 (spleens) and 37.5 ± 2.4 (LNs). Data are combined from at least two independent experiments (n = 5-8 mice/group; right panels). Error bars indicate SEM and significant differences ($p < 0.05$; two-tailed Student's *t*-test) are indicated by *****.

Figure 3-9

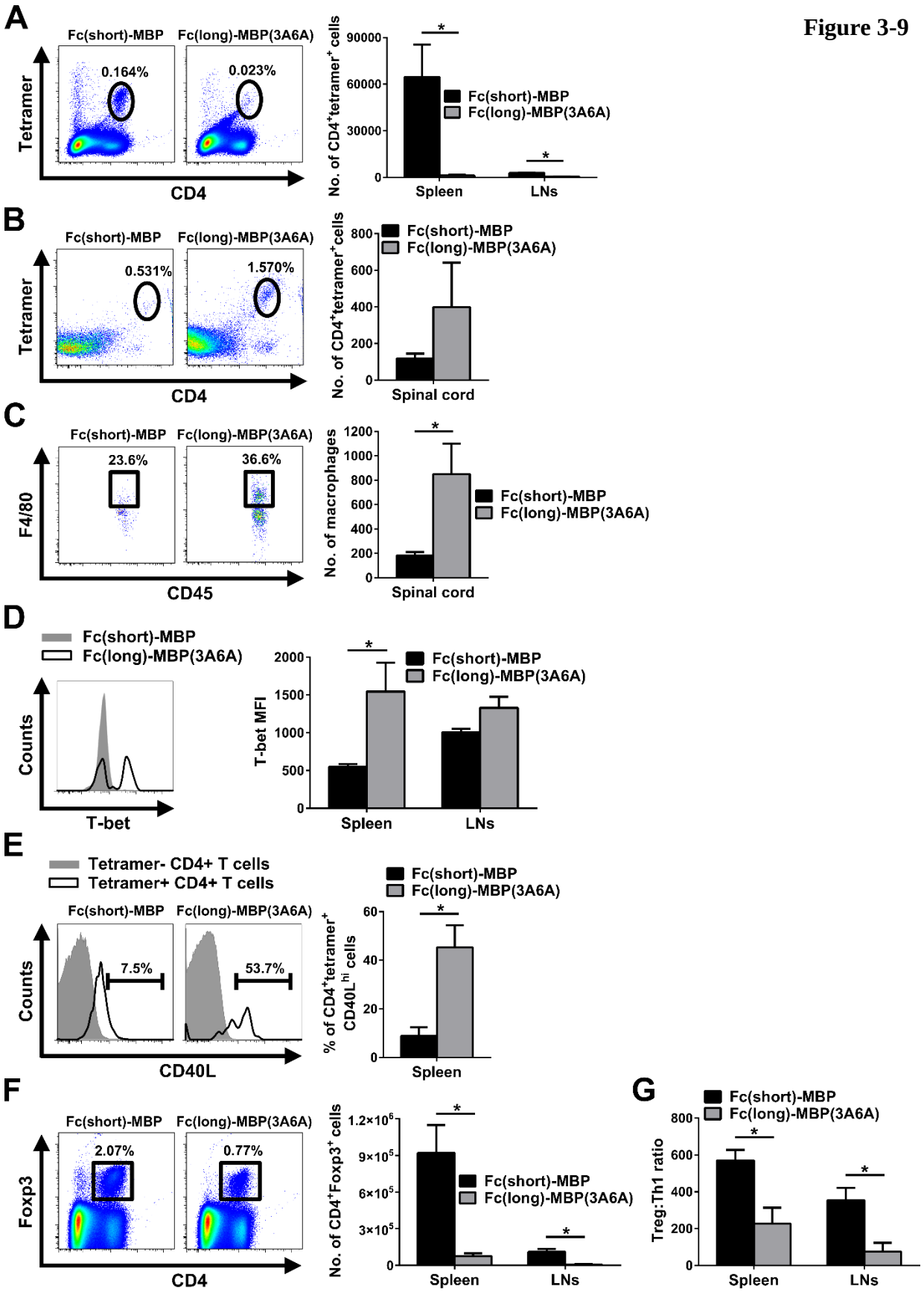
A
Fc(short)-MBP
Fc(long)-MBP(3A6A)
0.164%
0.023%
Tetramer
CD4
No. of CD4+tetramer+ cells
90000
60000
30000
0
Fc(short)-MBP
Fc(long)-MBP(3A6A)
*
*
Spleen
LNs
B
Fc(short)-MBP
Fc(long)-MBP(3A6A)
0.531%
1.570%
Tetramer
CD4
No. of CD4+tetramer+ cells
800
600
400
200
0
Fc(short)-MBP
Fc(long)-MBP(3A6A)
Spinal cord
C
Fc(short)-MBP
Fc(long)-MBP(3A6A)
23.6%
36.6%
F4/80
CD45
No. of macrophages
1200
1000
800
600
400
200
0
*
Fc(short)-MBP
Fc(long)-MBP(3A6A)
Spinal cord
D
Fc(short)-MBP
Fc(long)-MBP(3A6A)
Counts
T-bet
T-bet MFI
2000
1500
1000
500
0
*
Fc(short)-MBP
Fc(long)-MBP(3A6A)
Spleen
LNs
E
Tetramer- CD4+ T cells
Tetramer+ CD4+ T cells
Fc(short)-MBP
Fc(long)-MBP(3A6A)
Counts
7.5%
53.7%
CD40L
% of CD4+tetramer+ CD40Lhi cells
60
40
20
0
*
Fc(short)-MBP
Fc(long)-MBP(3A6A)
Spleen
F
Fc(short)-MBP
Fc(long)-MBP(3A6A)
2.07%
0.77%
Foxp3
CD4
No. of CD4+Foxp3+ cells
1.2×10^6
9×10^5
6×10^5
3×10^5
0
*
Fc(short)-MBP
Fc(long)-MBP(3A6A)
*
Spleen
LNs
G
Fc(short)-MBP
Fc(long)-MBP(3A6A)
Treg:Th1 ratio
800
600
400
200
0
*
*
Spleen
LNs

Figure 3-9. Tolerance induction during ongoing EAE results in increased numbers of peripheral antigen-specific CD4$^+$ T cells with downregulated T-bet and CD40L levels combined with reduced inflammatory infiltrates in the CNS. B10.PL mice were immunized and treated with Fc(short)-MBP as in Fig. 3-7. Six days following treatment, mice were sacrificed and tissues isolated for flow cytometry analyses to determine: (A) % (in spleens) and total numbers (in spleens, LNs) of CD4$^+$tetramer$^+$ T cells; (B, C) % and total numbers of mononuclear infiltrates in the spinal cords that are CD4$^+$tetramer$^+$ T cells (B) or F4/80$^+$CD45^{hi} macrophages (C); (D) MFI levels for T-bet amongst CD4$^+$tetramer$^+$ T cells in spleens and LNs; (E) % CD4$^+$tetramer$^+$ CD40L^{hi} T cells in spleens; (F) % (in spleens) and total numbers (in spleens, LNs) of CD4$^+$Foxp3$^+$ T cells; (G) Treg (CD4$^+$Foxp3$^+$ T cells):Th1 (CD4$^+$tetramer$^+$T-bet$^+$ T cells) ratios in spleens and LNs. For A-F, data for one representative mouse from each treatment group is presented in the left panels. For A-C, F, populations of interest are indicated in dot plots by solid circles or boxes. Percentages (± SEM) of CD4$^+$ T cells for mice treated with the Fc-MBP fusions were: Fc(short)-MBP, 9.5 ± 0.8 (spleens) and 28.8 ± 0.8 (LNs); Fc(long)-MBP(3A6A), 11.5 ± 0.6 (spleens) and 19.7 ± 2.7 (LNs). Data are derived from 3-4 mice/group (A-C, E-G) or 7 mice/group (D). Error bars indicate SEM and significant differences ($p < 0.05$; two-tailed Student's *t*-test) are indicated by *****.

3.3 DISCUSSION AND CONCLUSION

The induction of antigen-specific T cell tolerance represents a highly specific approach for the treatment of autoimmunity. However, despite extensive preclinical analyses of the efficacy of immunodominant peptides in tolerance induction, this strategy has met with limited success in the clinic[228, 247, 253, 254]. Importantly, the short half-lives of peptides necessitate the use of relatively high doses that can provoke anaphylaxis[18, 19, 267]. Here we have investigated the role of antigen dynamics in tolerance induction, by determining the tolerogenic activity of low doses (~50 μg/kg) of Fc fusions comprising an immunodominant MBP epitope linked to engineered Fc fragments with different binding properties for FcRn. These mutated Fc fragments are designed to endow different pharmacokinetic behavior on the appended antigen. Using this approach, we have established that the *in vivo* persistence of antigen is critical for tolerance induction and, in addition, have identified a requirement for a stringent threshold of persistence to achieve tolerance in both prophylactic and therapeutic settings (Fig. 3-10).

The *in vivo* persistence of Fc-MBP fusions is governed by their interactions with FcRn in endothelial cells and/or hematopoietic cells[20]. Amongst hematopoietic cells, all professional APCs express FcRn[21, 36, 257, 258]. Variations in interactions between Fc-MBP fusions and FcRn therefore also regulate epitope loading onto MHC class II molecules and cognate T cell activation. Consistent with our earlier study[257], Fc-MBP fusions that are recycled efficiently out of FcRn-expressing cells lead to poor antigen presentation *in vitro*, whereas fusions such as Fc(short)-MBP or Fc(v.short)-MBP that bind to FcRn with high affinity at near neutral and acidic pH accumulate to relatively high levels in APCs and are efficiently presented. However, recycled Fc-MBP fusions have prolonged *in vivo* persistence, whereas those that accumulate in FcRn-expressing cells have

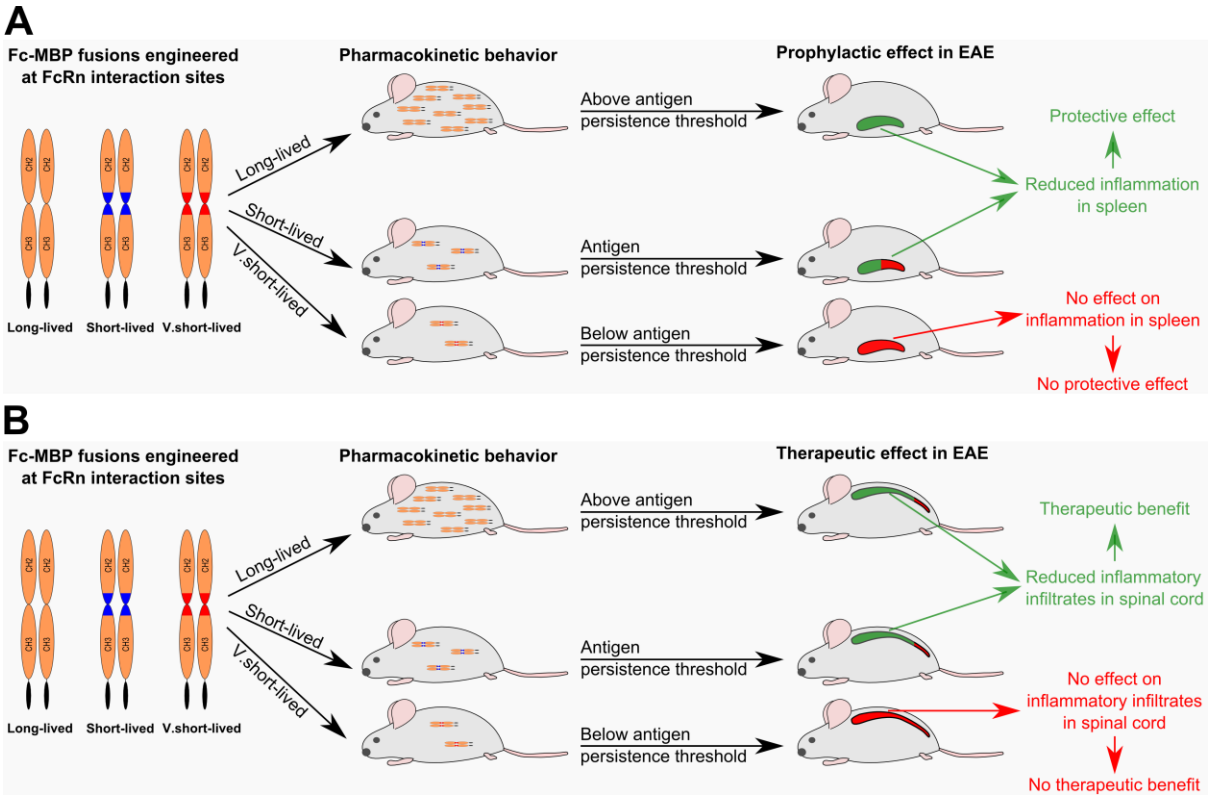

Figure 3-10. Effects of engineered Fc-MBP fusions on EAE. In a prophylactic setting (A), delivery of long-lived and short-lived Fc-MBP fusion proteins results in reduced numbers of antigen-specific $CD4^+$ T cells in the spleen and protection against the disease, whereas in a therapeutic setting (B), delivery of these fusion proteins results in reduced numbers of antigen-specific $CD4^+$ T cells and macrophages in the spinal cord and amelioration of the disease. In contrast, delivery of very short (v.short)-lived Fc-MBP fusion protein does not have an effect on inflammation and disease in either settings, indicating a requirement for stringent threshold of antigen persistence for tolerance induction.

comparatively short half-lives. Importantly, the induction of tolerance by five doses of Fc(v.short)-MBP delivered over a seven day period prior to EAE induction, combined with the lack of efficacy of an equivalent bolus dose of this fusion protein, demonstrate that the endolysosomal trafficking properties of this protein do not mitigate tolerance induction if antigen persistence is prolonged. In addition, the lack of protection by a single dose of this Fc-MBP fusion indicates a minimum threshold of persistence of low dose antigen for tolerance induction that is tightly bounded by the pharmacokinetic behavior of Fc(short)-MBP and Fc(v.short)-MBP.

Although the benefit of tolerance induction during ongoing disease is obvious, there are also clinical situations where prophylactic T cell tolerance has potential applications such as the prevention of transplant rejection and reduction of immune responses against protein-based therapeutics[268-270]. In addition, epitope spreading has been observed in patients and animal models of MS[271, 272] and T cells specific for spread epitopes can induce EAE relapses[273]. Consequently, prophylactic tolerization of naive autoreactive T cells specific to potential 'spreading' epitopes combined with tolerization of activated autoreactive T cells may result in effective treatment.

By analogy with prophylactic tolerance induction, a threshold of antigen persistence that is delimited by the behavior of Fc(short)-MBP and Fc(v.short)-MBP is also a requirement for the amelioration of ongoing disease. Analyses of the effects of Fc-MBP fusions reveal that although a fusion protein with a shorter persistence (Fc(short)-MBP) is less effective as a tolerogen in the prophylactic setting than its longer lived counterpart, Fc(long)-MBP, both fusion proteins have similar therapeutic activity during EAE. This is possibly due to the different sensitivities of naïve and primed T cells to antigenic stimulation[274]. In addition, the mechanisms of prophylactic and therapeutic tolerance are distinct: prophylactic tolerance induction results in reduced numbers of antigen-specific $CD4^+$ T cells in the periphery, indicating T cell deletion or anergy. By contrast,

in a therapeutic setting tolerance is unexpectedly accompanied by increased numbers of peripheral antigen-specific $CD4^+$ T cells. This contrasts with the induction of T cell apoptosis in mice following the delivery of multiple high doses (400 μg/mouse) of acetylated MBP1-11 following the adoptive transfer of autoreactive $CD4^+$ T cells[8].

Importantly, we observe that the increased numbers of splenic antigen-specific T cells in the tolerized mice harbor significantly reduced levels of T-bet, which is essential for the encephalitogenicity of Th1 cells[275] and has been reported to be downregulated in tolerized Th1 cells[276]. In addition, CD40L levels are substantially lower in the majority of splenic antigen-specific T cells in the tolerized mice. Studies using both CD40L knockout mice and anti-CD40L blocking antibodies support a critical role for this molecule in T cell activation and EAE induction or progression[277, 278]. Importantly, the downregulation of T-bet could be a downstream effect of reduced CD40L levels, since CD40L is required for the induction of co-stimulatory molecules such as B7.1 and B7.2 on APCs[277]. Our observation that tolerance induction during active EAE is accompanied by amplification of $CD4^+Foxp3^+$ Tregs, combined with reports that durable tolerance is dependent on the expansion of Tregs[249, 255], suggest that Fc-epitope fusions will have long term effects.

Earlier studies have demonstrated that the delivery of relatively high doses of hapten-IgG conjugates can result in immunological tolerance, although the molecular mechanism was not defined[279]. More recent analyses have revealed the presence of conserved T cell epitopes, or Tregitopes, in IgGs that activate regulatory T cells[280]. Importantly, the Tregitope sequences identified to date are not altered by the Fc mutations used to generate shorter-lived Fc-MBP fusions in the current study. However, the doses of Tregitopes typically used are substantially higher than those of Fc-MBP fusions. Although we cannot exclude a contribution of the tolerogenic properties

of Tregitopes to the amelioration of EAE, our results show that antigen persistence is a crucial factor for tolerance induction.

Polystyrene or PLG microparticles coupled with antigenic peptides have also been used to induce tolerance under both prophylactic and therapeutic conditions in murine EAE[250]. This approach has also been used with less success in an islet transplant model (e.g. administration of donor antigen-coupled PLGA microparticles induced tolerance in about 20% of recipient mice)[281]. Tolerance induction using Fc-peptide fusions differs from microparticle-based approach in several important respects: first, the amount of peptide in Fc-MBP fusions is around ~450-600-fold lower than that used with peptide-coupled microparticles. This low dose is expected to reduce the risk of anaphylactic shock and disease exacerbation. Second, the microparticles are injected intravenously and were reported to be ineffective when delivered subcutaneously[250]. By contrast, the established use of this pathway for the delivery of therapeutic antibodies or Fc fusions[282-285] indicate that tolerogenic Fc-peptide fusions can be effectively delivered via this route. Third, the persistence of Fc-antigen fusions can be modulated and even increased by Fc engineering[122, 123, 127] to optimize tolerogenic effects (the requirements for tolerance induction are predicted to vary in different pathological conditions), whereas for microparticles such tuning is not readily achievable.

MS is a very heterogeneous disease in terms of clinical course, the characteristics of demyelinating lesions and response to therapy[170]. Nevertheless, in the active lesions corresponding to the different disease types (pattern I-III), T cells and macrophages predominate in the inflammatory infiltrates[178]. Hence, in the current study we employed an EAE model for which autoreactive T cells and macrophages are drivers of demyelination[242, 266]. By contrast with the immunodominance of acetylated MBP1-9 in B10.PL mice[286], T cells specific for multiple neuroantigen-derived epitopes contribute to pathology in MS[271, 272]. Importantly, Fc fusions

harboring multiple peptides can be readily generated. In combination with the emergence of approaches to define T cell epitopes for pathological or protective immune responses in individuals[287], this provides support for the clinical translation of tolerance induction using long-lived Fc fusions.

In summary, by using Fc engineering to tune antigen dynamics, this study reveals that a stringent threshold of antigen persistence is a prerequisite for antigen-specific T cell tolerance induction. Low doses of relatively long-lived, Fc-epitope fusions are effective in ameliorating EAE in both prophylactic and therapeutic settings. Our observations not only provide mechanistic insight into tolerance induction, but also have direct relevance to the development of tunable, efficient and safer tolerogens.

3.4 MATERIALS AND METHODS

3.4.1 Mice

B10.PL (H-2^{u}) mice were purchased from the Jackson Laboratory (Bar Harbor, ME). Mice that transgenically express the 1934.4 TCR (1934.4 tg mice[288]) or clone 19 TCR (T/R^{+} tg mice[289]) were kindly provided by Dr. Hugh McDevitt (Stanford University, CA) and Dr. Juan Lafaille (New York University School of Medicine, NY), respectively. Both the 1934.4 and clone 19 TCRs are specific for MBP1-9 complexed with I-A^{u}[288, 289] and have similar affinities for antigen[290]. Mice were bred in a specific pathogen-free facility at the University of Texas Southwestern Medical Center or Texas A&M University and were handled in compliance with institutional policies and protocols approved by the Institutional Animal Care and Use Committees. 6-10 week old male or female mice were used in experiments.

3.4.2 Peptides

The N-terminal, acetylated peptide of MBP (MBP1-9, Ac-ASQKRPSQR) and MBP1-9(4Y) (Ac-ASQYRPSQR) were purchased from CS Bio (Menlo Park, CA).

3.4.3 Production of recombinant proteins

Expression constructs for the production of full length anti-lysozyme antibodies (WT, m-set-1 and m-set-2) were generated by isolating the cDNA encoding the heavy chain and light chain from the D1.3 hybridoma (mouse IgG1, anti-hen egg lysozyme)[198]. The mutations were inserted into the WT heavy chain gene using splicing by overlap extension and cloned into pOptiVEC™-TOPO® vector (Life Technologies, Grand Island, NY) for expression. The light chain gene was

cloned into pcDNA™3.3-TOPO® vector (Life Technologies, Grand Island, NY). Complete sequences of expression plasmids are available upon request. The light chain expression construct was transfected into CHO DG44 cells by electroporation. Stable clones of CHO DG44 cells were selected for light chain expression using previously described methods[194]. The light chain transfectant expressing the highest levels of recombinant protein was used as a recipient for the heavy chain constructs. Clones expressing the highest levels of anti-lysozyme antibody were selected and recombinant antibodies purified from culture supernatants using lysozyme-Sepharose[216]. Mouse IgG1 (anti-hen egg lysozyme, D1.3[198]) was purified using lysozyme-Sepharose[216] from hybridoma culture supernatants.

Expression plasmids encoding WT or mutated (m-set-2) mouse IgG1-derived Fc-hinge connected at the C-termini through a Gly-Ser-Gly-Gly linker to codons encoding the MBP1-9(4Y) epitope or MBP1-9(4Y) epitope with residues 3 and 6 of the peptide replaced by alanine have been described previously[257]. The glycine at the N-terminus of the peptide mimics the acetyl group that is necessary for T cell recognition of the MBP epitope[259]. The m-set-1 mutations were inserted into the WT Fc-MBP fusion construct using splicing by overlap extension and designed oligonucleotide primers. All Fc-MBP fusion genes were cloned into pEF6/V5-His vector (Life Technologies, Grand Island, NY). Fc-MBP fusion constructs were transfected into CHO-S cells, stable transfectants selected and recombinant proteins purified from culture supernatants as described previously[257]. Analogous methods were used to generate Fc-hinge variants (WT, m-set-1, m-set-2) without the C-terminal MBP1-9 epitope. Complete sequences of expression constructs are available upon request.

3.4.4 Recombinant peptide-MHC complexes

Soluble, recombinant MBP1–9(4Y):I-A^u complexes were generated using baculovirus-infected High Five insect cells and purified as described previously[219]. The complexes were site-specifically biotinylated and multimeric complexes ("tetramers") were generated using PE-labeled ExtrAvidin (Sigma-Aldrich, St. Louis, MO).

3.4.5 Cell lines

The MBP1–9:I-A^u-specific T cell hybridoma #46 has been described previously[263]. The I-A^u-expressing B lymphoblastoid line PL8 was generously provided by Dr. David Wraith (University of Bristol, Bristol, U.K.). PL8:FcRn cells were generated by stably transfecting PL8 cells with an expression construct encoding mouse FcRn tagged at the C-terminus with GFP, followed by selection with G418 (600 μg/ml, Life Technologies, Grand Island, NY)[257].

3.4.6 Surface plasmon resonance analyses

Equilibrium dissociation constants of WT and mutated mouse Fc-hinge fragments (IgG1-derived) for binding to recombinant mouse FcRn were determined using surface plasmon resonance and a BIAcore 2000. Mouse Fc-hinge fragments were immobilized by amine coupling chemistry (to a density of ~250-850 RU) and BIAcore experiments carried out as described previously, using soluble mouse FcRn in phosphate-buffered saline (PBS) plus 0.01% Tween pH 6.0 or 7.4 as analyte[291]. FcRn binds to two sites on IgG that are not equivalent[291]. This results in K_D estimates for two dissociation constants, and the values for the higher affinity interaction sites are presented. The data were processed as described previously[291].

3.4.7 T cell stimulation assay

Fc-MBP fusions were added to 96-well plates containing PL-8 or PL-8:FcRn cells (5×10^4 cells/well) and MBP1–9:I-A^u-specific T cell hybridoma #46 cells (5×10^4 cells/well). IL-2 levels in culture supernatants following 24 hours of incubation were assessed using a sandwich ELISA with the following reagents: rat anti-mouse IL-2 capture antibody (clone, JES6-1A12; Becton-Dickinson, San Jose, CA), biotinylated rat anti-mouse IL-2 detection antibody (clone, JES6-5H4; Becton-Dickinson, San Jose, CA) and ExtrAvidin-Peroxidase (Sigma-Aldrich, St. Louis, MO).

3.4.8 Pharmacokinetic experiments

6-10 week old female B10.PL mice were fed 0.1% Lugol (Sigma-Aldrich, St. Louis, MO) in water starting at 72 h before i.v. injection in the tail vein with ^{125}I-labeled (using Iodogen as described previously[220]) IgGs or Fc-MBP fusions (10–15 μg per mouse). Levels of radioactivity in 10 μl blood samples were determined at the indicated times by gamma counting. To determine the AUC for IgGs and Fc-MBP fusion proteins, data were fitted to a bi-exponential decay model using custom software written in MATLAB (Mathworks, Natick, MA). The area under each of these bi-exponential model curves between time t = 0 and the time at which the extrapolated curve reaches 1% of the injected dose was calculated.

To investigate whether the Fc-MBP fusions affected the activity of FcRn in regulating the clearance rate of IgG, 6-10 week old male B10.PL mice were fed 0.1% Lugol (Sigma-Aldrich, St. Louis, MO) in drinking water for 72 h prior to i.v. injection with 10–15 μg of ^{125}I-labeled mouse IgG1 (anti-hen egg lysozyme, D1.3). 24 hours later, the mice were i.v. injected with 1 μg Fc-MBP fusion or vehicle (PBS) control. Levels of radioactivity in 10 μl blood samples were analyzed at

the indicated times by gamma counting and β-phase half-lives following injection of Fc-MBP fusion or vehicle determined as described previously[20].

3.4.9 Analyses of proliferative responses of transferred antigen-specific T cells

Antigen-specific $CD4^+$ T cells were isolated from the splenocytes of MBP1–9:I-A^u-specific TCR transgenic mice (1934.4 tg[288] and T/R^+ tg[289]) through negative selection using a MACS $CD4^+$ T cell isolation kit (Miltenyi Biotec, San Diego, CA). Female B10.PL mice were i.v. injected with 1 μg Fc-MBP fusion. One hour ('Day 0'), 3 or 5 days following Fc-MBP fusion delivery, 5×10^5 CFSE-labeled $CD4^+$ T cells were injected i.v. into the mice. Three days later, splenocytes and LN cells were isolated for flow cytometry analyses.

3.4.10 Induction of EAE

8-10 week old male B10.PL mice were immunized subcutaneously at four sites in the flanks with 200 μg acetylated MBP1-9 (CS Bio, Menlo Park, CA) emulsified with complete Freund's adjuvant (Sigma Aldrich, St. Louis, MO) containing an additional 4 mg/ml heat-inactivated *Mycobacterium tuberculosis* (strain H37Ra, Becton-Dickinson, San Jose, CA). In addition, 200 ng pertussis toxin (List Biological Laboratories, Campbell, CA) was injected i.p. on days 0 (0 h) and 2 (45 h).

Scoring of disease activity was as follows: 0, no paralysis; 1, limp tail; 2, moderate hind limb weakness; 3, severe hind limb weakness; 4, complete hind limb paralysis; 5, quadriplegia; and 6, death due to disease. Clinical signs of EAE were assessed for up to 30 days after immunization.

3.4.11 Prophylactic and therapeutic treatment of mice with Fc-MBP fusions

For tolerance induction in a prophylactic setting, male B10.PL mice were injected i.v. with 1 μg Fc-MBP fusion and seven days later, immunized with MBP1-9 and treated with pertussis toxin to induce EAE. In some experiments, mice were treated with 5 doses of 1 μg Fc(v.short)-MBP (starting at 7 days prior to immunization, at 36 hour intervals) or with a single dose of 5 μg Fc(v.short)-MBP delivered 7 days prior to immunization. For tolerance induction during ongoing disease, mice were injected i.v. with 1 μg Fc-MBP fusion at the onset of EAE (mean clinical score of 1-2).

3.4.12 Antibodies and flow cytometry analyses

Single cell suspensions from spleen, draining LNs (axillary, brachial and inguinal), brain and spinal cord were obtained by mechanical disruption and forcing through 70 μm cell strainers (Becton-Dickinson, San Jose, CA). For experiments involving analyses of immune cells in the CNS, mice were perfused with heparinized PBS before collecting the organs. Splenic cell suspensions were depleted of erythrocytes using red blood cell lysis buffer.

Mononuclear cells from CNS cell suspensions were obtained using Percoll (1131 g/ml, GE Healthcare) gradients. Briefly, cells were washed with 37% Percoll and suspended in 30% Percoll which was then layered over 70% Percoll and centrifuged at 2118 g. Following centrifugation, the cells at the interface were collected, washed with PBS and used for flow cytometry analyses.

For intracellular staining to detect Foxp3 and T-bet, cells were initially surface-stained, followed by fixation and permeabilization using Foxp3 staining buffer set (eBioscience, San Diego, CA). Permeabilized cells were incubated with fluorescently labeled anti-Foxp3 or anti-T-bet antibodies and washed with PBS.

To detect antigen-specific $CD4^+$ T cells, single cell suspensions from spleens and LNs were incubated with PE-labeled MBP1–9(4Y):I-A^u tetramers for 90 minutes at 12°C, followed by washing with PBS.

Flow cytometry analyses were performed using a FACSCalibur (Becton-Dickinson, San Jose, CA) or LSRFortessa (Becton-Dickinson, San Jose, CA) and data analyzed using FlowJo (Tree Star, Ashland, OR). Antibodies specific for the following were purchased from either Becton-Dickinson (San Jose, CA), eBioscience (San Diego, CA) or Biolegend (San Diego, CA): CD4 (RM4-5), Foxp3 (FJK-16s), T-bet (4B10), CD40L (MR1), F4/80 (BM8), PD-1 (29F.1A12), CTLA-4 (UC10-4B9), LFA-1 (H155-78), CXCR3 (CXCR3-173), α4 (R1-2), β1 (HMβ1-1), α4β7 (DATK32) and CD45 (30-F11).

3.4.13 Statistical analyses

Tests for statistical significance for flow cytometric analyses of cell numbers and pharmacokinetic data were carried out using two-tailed Student's *t*-test in the statistics toolbox of MATLAB (Mathworks, Natick, MA). Due to the longitudinal nature of the measures of clinical scores over time, we compared the clinical score profiles between the groups of mice in disease experiments using the linear mixed effects model with AR(1) covariance structure with Statistical Analysis System software (SAS Institute Inc., Cary, NC). *p* values of less than 0.05 were taken to be significant.

CHAPTER FOUR
Macrophages represent an important site of FcRn-mediated IgG homeostasis

4.1 INTRODUCTION

The regulation of the levels and transport of antibodies of the immunoglobulin G (IgG) class in the body represents a fundamental aspect of humoral immunity that also has direct relevance to the effective delivery of antibody-based therapeutics and diagnostics. Although it is established that the neonatal Fc receptor, FcRn, plays a central role in these processes, the sites of FcRn activity at the organ and tissue level remain poorly defined. FcRn is a recycling or transcytotic receptor that binds to the majority of naturally occurring IgGs at acidic, endosomal pH, but with negligible affinity at near neutral pH[1]. Consequently, ligand uptake into cells bathed at physiological pH (7.3-7.4) is dependent on fluid phase rather than receptor-mediated pathways. The activity of FcRn in different cell types is therefore expected to not only to depend on FcRn expression levels and recycling or transcytotic rates, but also on pinocytic activity and local concentrations of IgG. The challenges associated with distinguishing these different factors in an *in vivo* setting have to date limited definition of the cell types that contribute to IgG homeostasis. In the current study, we have used a combination of *ex vivo* and *in vivo* approaches, including mouse strains that conditionally lack FcRn, to resolve these issues.

Although studies have demonstrated that FcRn in hematopoietic cells (HCs) and endothelial cells (ECs) contributes to IgG homeostasis[20, 24, 88, 92], the contribution of individual cell types to this process has not been delineated. Of the HCs, monocytes, macrophages, B cells and dendritic cells (DCs) express functional FcRn[20]. The expression of FcRn in these HCs is of particular

relevance to IgG homeostasis for the following reasons: firstly, the HCs in the circulation (monocytes and B cells) are exposed to relatively high concentrations of IgG, similar to vascular ECs. Secondly, macrophages, monocytes and dendritic cells are characterized by avid pinocytosis[292]. Lastly, macrophages are ubiquitous and constitute a significant fraction of cells in most organs in the body[293-296]. Further, hyperproliferative disorders that dysregulate HC numbers will modulate IgG homeostasis if the affected cell type represents a significant depot of FcRn activity. Apparently, in chronic myelomonocytic leukemia an increase in cells of the myeloid lineage (monocytosis and leukocytosis with monocytes and granulocytes in the bone marrow) is accompanied by abnormally high IgG levels in the absence of plasmacytosis[297, 298], suggesting that one or more cell types belonging to the myeloid lineage contribute to the regulation of IgG concentrations. Understanding how FcRn regulates IgG levels in different disease states through alterations in the levels of cell types with FcRn activity therefore represents an important step toward understanding pathogenesis.

Inflammation and microbial products can modulate FcRn expression in HCs. For example, tumor necrosis factor (TNF)-α, interleukin-1β, CpG oligodeoxynucleotide, lipopolysaccharide enhance the expression of FcRn in HCs of human origin[93]. In contrast, interferon-γ treatment downregulates FcRn expression in HCs of both mouse and human origin[94]. These observations indicate that IgG homeostasis mediated by FcRn in HCs might differ between steady state and inflammatory conditions. Understanding these differences would require mice that conditionally lack (or express) FcRn and could reveal new therapeutic pathways to modulate FcRn activity in pathological conditions. Further, alterations in IgG homeostasis (due to a pathological condition) can have implications for T cell-mediated immune responses since *in vivo* IgG levels or local concentrations of IgG can affect the formation of IgG-based immune complexes, which in turn

deliver the antigen to antigen presenting cells (APCs). FcRn, in combination with the classical FcγRs, also plays a role in the trafficking of immune complexes to antigen processing compartments involved in both MHC Class I and II loading in APCs, aiding T cell stimulation[258]. Observations made using mice that overexpress FcRn supports these effects of FcRn levels on the regulation of T cell immunity[299, 300].

In the current study, multiple strains of mice were generated that conditionally lack FcRn in monocytes/macrophages, B cells and DCs using the Cre/loxP technology. Importantly, the specificity of FcRn deletion was verified using an assay that indicates the levels of functional FcRn in different cell types. The effect of site-specific deletion of FcRn on IgG pharmacokinetics and steady state levels was assessed, which demonstrates that macrophages are an important site for IgG homeostasis. Interestingly, depletion of splenic macrophages does not affect IgG homeostasis but whole body depletion of macrophages significantly reduces IgG half-life. In this context, in FcRn knockout (KO) mice, alveolar macrophages and to lesser extent macrophages in the skin and liver accumulate higher levels of exogenously delivered IgG compared with macrophages in kidney, intestine, muscle, spleen and lymph nodes. Importantly, alveolar macrophages from FcRn-sufficient mice are efficient in recycling IgG in an *ex vivo* assay.

4.2 RESULTS

4.2.1 Generation and characterization of cell type-specific FcRn KO mice

Amongst HCs, FcRn is expressed in monocytes, macrophages, DCs and B cells[20, 21]. To investigate the role of FcRn in regulating IgG homeostasis in these cells, we intercrossed FcRn-floxed mice[20] with mice transgenic for LysM-Cre[301], CD11c-Cre[302] and CD19-Cre[303] with the goal of generating macrophage-, DC- and B cell-specific FcRn KO mice, respectively. To determine the specificity of FcRn deletion in these conditional FcRn KO mice, flow cytometry was used to assess the accumulation of a mutated human IgG1 (MST-HN, M252Y/S254T/T256E/H433K/N434F)[3] that binds to mouse FcRn with increased affinity at acidic and near-neutral pH (K_d = 1.2 nM at pH 6.0; K_d = 7.4 nM at pH 7.2)[3]. This mutated human IgG1 is efficiently endocytosed into FcRn-expressing cells by receptor-mediated uptake[1, 3]. As a control for both fluid phase accumulation and FcγR-mediated endocytosis, a mutated human IgG1 variant (H435A) that has substantially reduced affinity for FcRn relative to its wild type parent antibody[104] was used. Loss of FcRn was specific to monocytes/macrophages in LysM-Cre-FcRn$^{flox/flox}$ mice (M-KO mice; Fig. 4-1A,B, 4-2). By contrast with the restriction of FcRn deletion to macrophages in M-KO mice, however, in both CD11c-Cre-FcRn$^{flox/flox}$ and CD19-Cre-FcRn$^{flox/flox}$ mice FcRn deletion was not specific to DCs and B cells, respectively. In CD11c-Cre-FcRn$^{flox/flox}$ mice, FcRn activity was lost in all HCs and liver ECs (data not shown), whereas in CD19-Cre-FcRn$^{flox/flox}$ mice (B-DC-KO mice), FcRn deletion occurred in both DCs and B cells (Fig. 4-1A,B). Consequently, CD11c-Cre-FcRn$^{flox/flox}$ mice were not used in these studies, whereas B-DC-KO mice provided a model for selective loss of FcRn in both B cell and DCs.

A

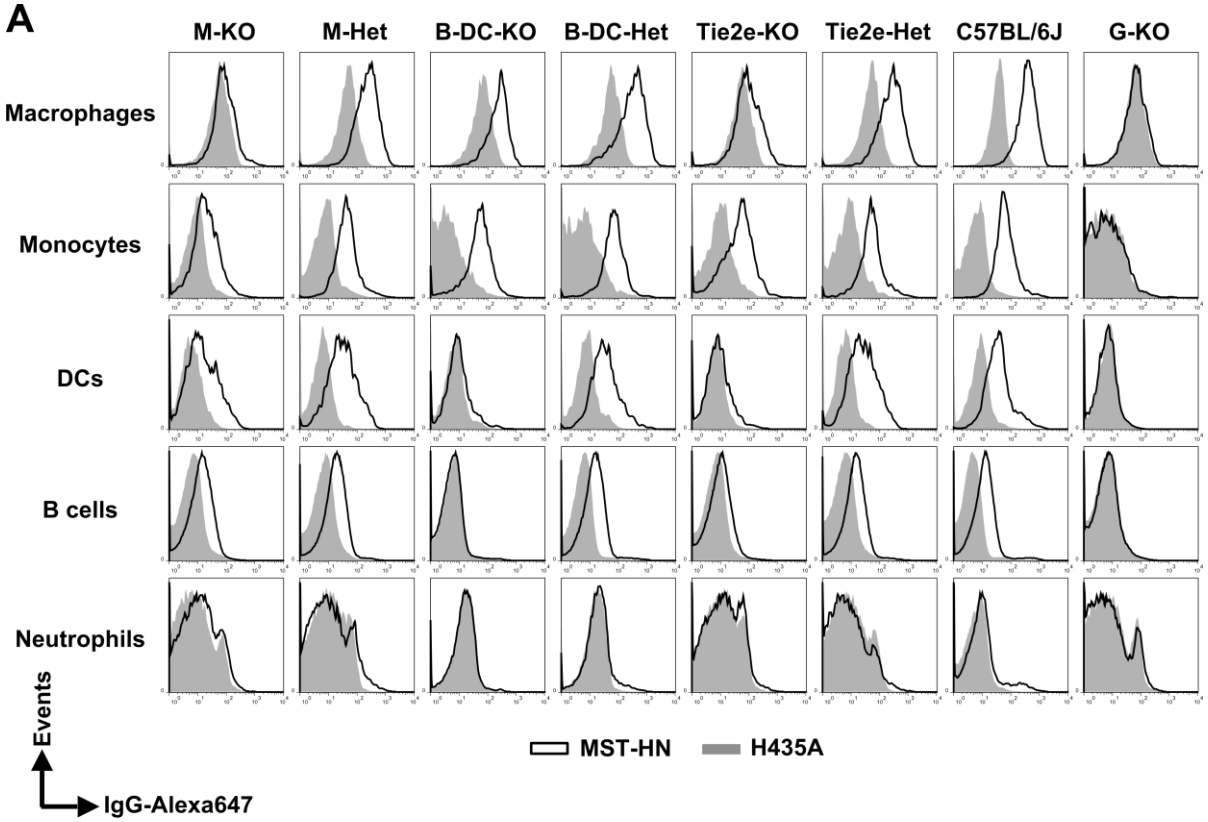

B

Cell type / Genotype	M-KO	M-Het	B-DC-KO	B-DC-Het	Tie2e-KO	Tie2e-Het	G-KO
Macrophages	Deleted	WT	WT	WT	↓↓	WT	Deleted
Monocytes	↓	WT	WT	WT	WT	WT	Deleted
DCs	↓	WT	Deleted	WT	Deleted	WT	Deleted
B cells	WT	WT	Deleted	WT	↓↓	WT	Deleted

Figure 4-1. Specificity of FcRn deletion in different FcRn KO mice. (A) Splenocytes were isolated, pooled (from 2-3 mice/genotype) and incubated with anti-FcγRIIB/III (2.4G2) antibody at 4°C followed by Alexa 647-labeled MST-HN or H435A mutant at 37°C to assess FcRn-mediated uptake. (B) Summary of FcRn expression data shown in (A). Data shown is representative of at least two independent experiments. M-KO, LysM-Cre-FcRn$^{flox/flox}$; M-Het, LysM-Cre-FcRn$^{flox/+}$; B-DC-KO, CD19-Cre-FcRn$^{flox/flox}$; B-DC-Het, CD19-Cre-FcRn$^{flox/+}$; Tie2e-KO, Tie2e-Cre-FcRn$^{flox/flox}$; Tie2e-Het, Tie2e-Cre-FcRn$^{flox/+}$; G-KO, FcRn$^{-/-}$; ↓, reduced; ↓↓, greatly reduced; WT, wild type.

To further explore the expression of FcRn in macrophages in M-KO mice, we investigated the expression of FcRn in both F4/80^{bright}CD11b^{low} [fetal hematopoietic stem cell (HSC)- or yolk sac erythro-myeloid precursors (EMPs)-derived] and F4/80^{low}CD11b^{high} [bone marrow HSC-derived] macrophages[304-306] in lung, kidney and liver (Fig. 4-3). Both cell subsets at these sites expressed FcRn in the control mice, and deletion of FcRn was observed in these cells in M-KO mice, with the exception of F4/80^{bright}CD11b^{low} macrophages in the liver.

Earlier studies in our laboratory demonstrated that the intercrossing of Tie2-Cre mice with FcRn-floxed mice resulted in a mouse strain lacking FcRn expression in all ECs and HCs[20], consistent with the observations of others that Tie2 promoter activity is not specific to EC subsets[307-309]. With the goal of assessing the contribution of ECs to the regulation of IgG levels, we therefore crossed the FcRn-floxed mice with Tie2e-Cre mice, for which Cre expression has been reported to be EC-specific[310]. However, Tie2e-Cre-FcRn$^{flox/flox}$ (Tie2e-KO) mice exhibited partial or complete deletion of FcRn in macrophages, B cells, DCs and heart ECs although this activity was retained in lung ECs (Fig. 4-1A,B, 4-2). In addition, these mice exhibited similar activity of FcRn in monocytes compared with the corresponding control mice, Tie2e-FcRn$^{flox/+}$ (Tie2e-Het; Fig. 4-1A,B). As an alternative approach toward achieving EC-specific deletion, intercrossing of the FcRn-floxed mice with tamoxifen-inducible Cdh5(PAC)-CreERT2 mice[311] resulted in only partial loss of FcRn in ECs (data not shown). Consequently, we were not able to obtain a mouse strain in which deletion of FcRn was restricted to ECs.

4.2.2 Macrophages are the predominant cell type among HCs that contribute to FcRn-mediated IgG homeostasis

We next analyzed the pharmacokinetics of mouse IgG1 (mIgG1) in M-KO, Tie2e-KO, B-DC-KO, their corresponding controls and, as a comparator, global FcRn KO (G-KO[74]) and wild

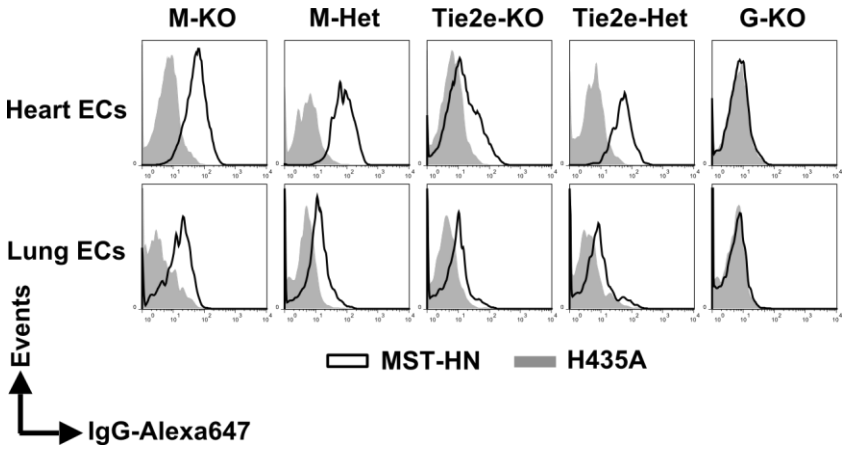

Figure 4-2. ECs express normal levels of FcRn in M-KO mice and reduced levels of FcRn in Tie2e-KO mice. Single cell suspensions from heart and lung were isolated, pooled (from 3-4 mice/genotype) and incubated with anti-FcγRIIB/III (2.4G2) antibody at 4°C followed by Alexa 647-labeled MST-HN or H435A mutant at 37°C to assess FcRn-mediated uptake. Data shown is representative of at least two independent experiments.

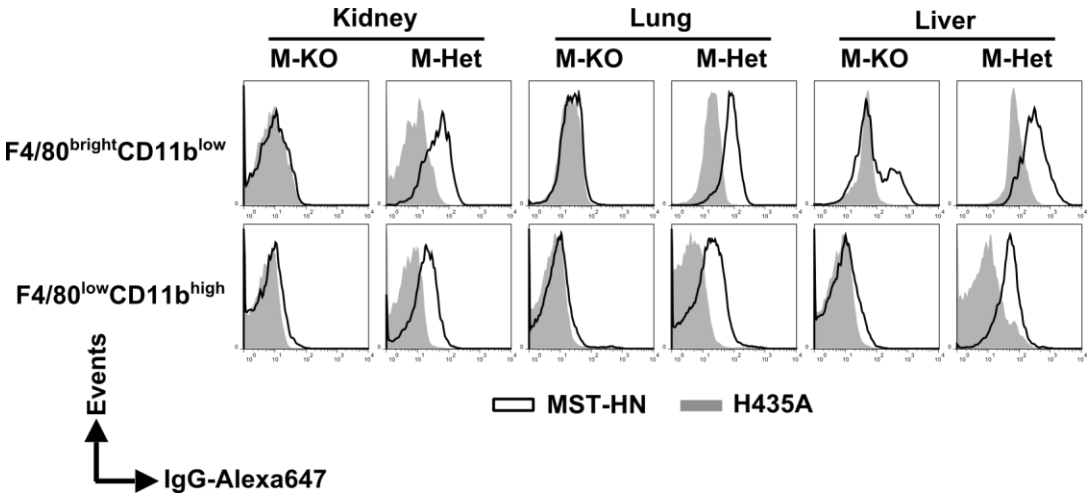

Figure 4-3. Tissue resident macrophages in M-KO mice are FcRn-deficient. Single cell suspensions from kidney, lung and liver were isolated, pooled (from 3-4 mice/genotype) and incubated with anti-FcγRIIB/III (2.4G2) antibody at 4°C followed by Alexa 647-labeled MST-HN or H435A mutant at 37°C to assess FcRn-mediated uptake. Data shown is representative of at least two independent experiments.

type (WT) C57BL/6J mice. The β-phase half-life of mIgG1 was the longest in C57BL/6J mice (~295 h). Surprisingly, the β-phase half-life of mIgG1 in M-KO mice (~42 h) was substantially reduced compared with that in control mice [LysM-Cre-FcRn$^{flox/+}$ (M-Het), ~248 h], but was only slightly longer than that observed in G-KO mice (~36 h) (Fig. 4-4). In addition, the half-life of mIgG1 in Tie2e-KO mice (~48 h) which have normal levels of FcRn in monocytes (in comparison to their corresponding controls), but greatly reduced levels in macrophages was substantially lower compared with that in control mice (Tie2e-Het, ~175 h) and was only slightly higher in comparison to M-KO mice (Fig. 4-4). By contrast, the half-life of mIgG1 in B-DC-KO mice (~203 h) was not statistically different from that observed in the control mice [CD19-Cre-FcRn$^{flox/+}$ (B-DC-Het), ~228 h] (Fig. 4-4).

The steady state levels of IgG and albumin in the serum of the different mouse strains were also determined. The IgG levels in M-KO and G-KO mice were ~0.5 mg/ml and ~0.15 mg/ml, respectively, compared with ~1.45 mg/ml in the control mice (M-Het) (Fig. 4-5A). The IgG levels in Tie2e-KO mice were ~0.55 mg/ml in comparison to 1.35 mg/ml in the control mice (Tie2e-Het) which is indicative of slightly higher IgG levels in comparison with M-KO mice (Figure 4-5A). Similar observations were made for the serum albumin levels in different conditional FcRn KO mice to those for serum IgG levels, except that the decrease in the levels relative to corresponding controls was lower (Fig. 4-5B). This difference is possibly due to feedback regulation of albumin synthesis rates[312]. These observations indicate that macrophages are a dominant cell type in regulating IgG homeostasis. In addition, the higher steady state IgG levels in M-KO mice relative to G-KO mice are most likely due to salvage of IgG by other cells such as ECs and/or epithelial cells, although the absence of an EC or epithelial cell specific KO mouse precluded direct analysis of the role of these cell types.

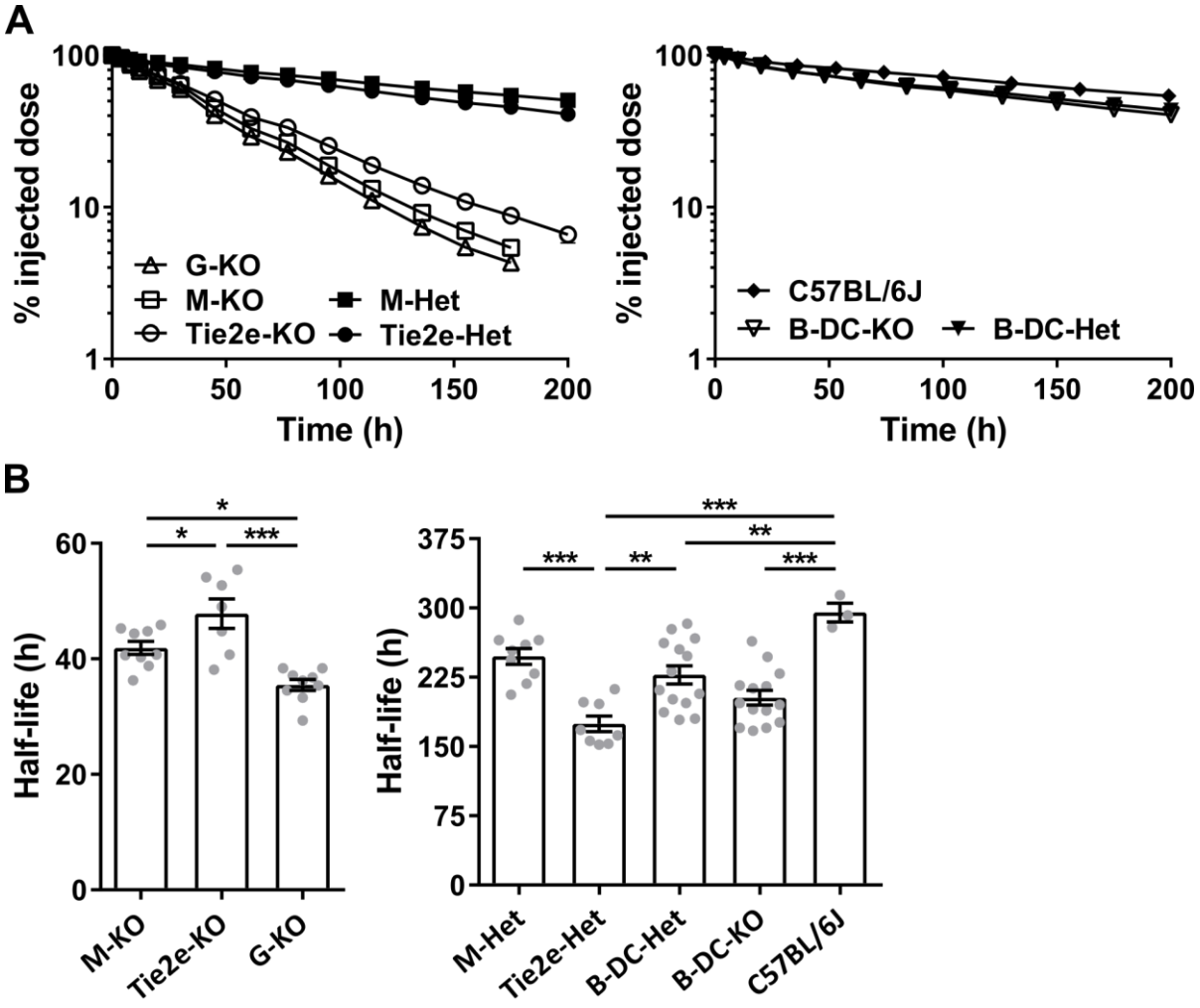

Figure 4-4. IgG1 has a short half-life in M-KO mice that is only slightly longer than the half-life in G-KO mice. (A) FcRn KO and control mice (3-6 mice/genotype) were injected (i.v.) with ^{125}I-labeled mouse WT IgG1 and whole body radioactivity levels assessed at the indicated times. Data shown is representative of at least two independent experiments, except for C57BL/6J mice. (B) Half-lives and β-phase half-lives of mIgG1 in different FcRn KO and control mice are shown which were obtained by fitting the whole body pharmacokinetic data to a decaying mono-exponential (M-KO, Tie2e-KO and G-KO) or bi-exponential model (M-Het, Tie2e-Het, B-DC-Het, B-DC-KO and C57BL/6J), respectively. Data shown is combined from at least two independent experiments (n = 7–14 mice/group), except for C57BL/6J mice (n = 3 mice). Error bars indicate SEM [obscured by the symbols in (A)]. Significant differences (*****, $p < 0.05$; ******, $p < 0.01$; *******, $p < 0.001$; one-way ANOVA) between the groups are indicated.

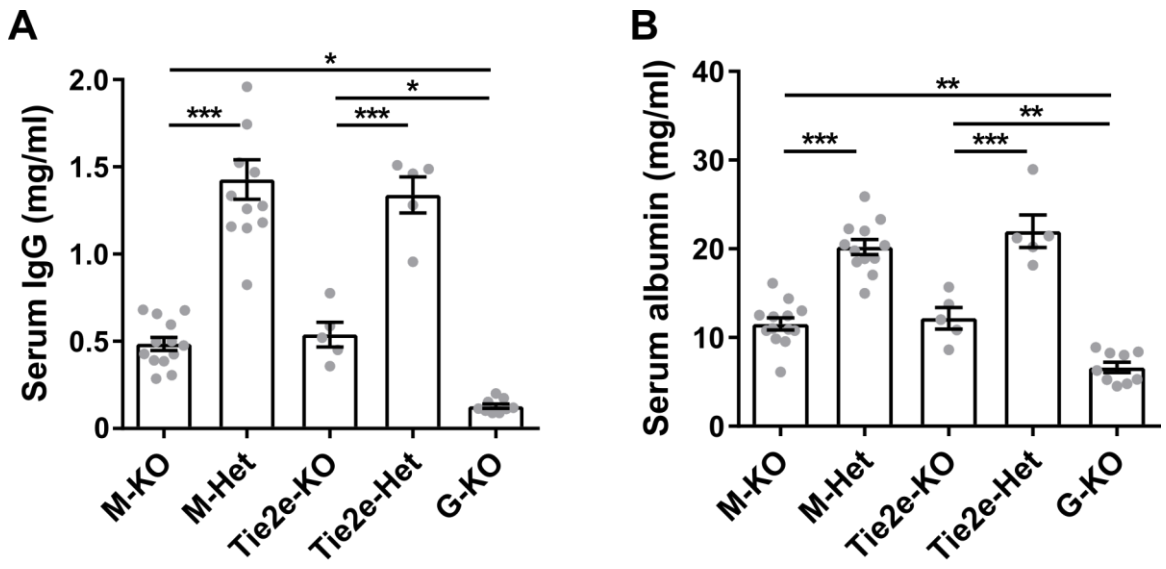

Figure 4-5. M-KO mice have reduced serum IgG and albumin levels. Serum IgG (A) and albumin (B) levels were determined using ELISA. Data shown is representative of 5-13 mice/genotype. Error bars indicate SEM. Significant differences (*****, $p < 0.05$; ******, $p < 0.01$; *******, $p < 0.001$; one-way ANOVA) between the groups are indicated.

To investigate further the residual activity of FcRn in M-KO mice, serum IgG levels in M-KO, control FcRn-sufficient and G-KO mice were determined following the treatment of mice with the MST-HN mutant (Abdeg) that inhibits FcRn binding to wild type IgGs and as such, enhances the degradation of endogenous antibodies when delivered into mice[3]. As expected, MST-HN treatment did not modulate serum IgG levels in G-KO mice (Fig. 4-6). By contrast, serum IgG levels in control, M-Het mice were reduced by ~35% and ~67% at 6 h and 24 h post-treatment, respectively and the IgG levels recovered to only ~55% of that observed in untreated mice at 120 h post-treatment. Importantly, in M-KO mice, a significant drop in serum IgG levels (~38%) was only observed at 24 h post-treatment (Fig. 4-6).

4.2.3 Systemic depletion of macrophages and depletion of splenic macrophages alone have different effects on IgG homeostasis

The deletion of FcRn in both splenic and tissue-resident macrophages in M-KO mice (Fig. 4-1A,B, 4-3), prompted us to further investigate the role of these different macrophage types in FcRn-mediated IgG homeostasis. We therefore employed the following models to systemically deplete macrophages or deplete only splenic macrophages: first, macrophage Fas-induced apoptosis (MaFIA) transgenic mice which represent the only well characterized model in which systemic macrophage depletion has been demonstrated[313]. Second, the treatment of mice with clodronate liposomes to specifically deplete splenic macrophages. MaFIA mice harbor a transgene for a cytoplasmic membrane-bound fusion of two consecutive copies of FK506 binding protein (FKBP) and cytoplasmic domain of Fas under the control of macrophage-specific macrophage colony-stimulating factor receptor (*c-fms*) promoter. FKBP preferentially binds the dimerization drug AP20187 and following the administration of AP20187 70–95% of macrophages undergo Fas-mediated apoptosis in various tissues[313]. The clearance rate of mIgG1 was significantly faster

in AP20187-treated MaFIA mice in comparison with control animals (Fig. 4-7A,B). By contrast, the pharmacokinetics of mIgG1 was not affected in mice following clodronate liposome treatment (Fig. 4-8A,B), which resulted in ~90-99% reductions in splenic macrophage numbers (Fig. 4-8C) and partial macrophage depletion in the liver (data not shown).

4.2.4 High pinocytic rates enable macrophages to play an important role in FcRn-mediated IgG recycling

We next wanted to determine the mechanism(s) through which macrophages are superior to ECs with respect to IgG homeostasis, especially because ECs also express FcRn and are present throughout the body. IgG destined for degradation or recycling is taken into the cells through fluid phase uptake/pinocytosis. Hence, the pinocytic rate is a critical factor that could govern the ability or efficiency with which the cells participate in the IgG-recycling process. We hypothesized that macrophages perform higher pinocytic uptake of IgG in comparison with ECs[292] which enable them to play a major role in IgG homeostasis. To test this hypothesis, we studied the accumulation of fluorescently-labeled, intravenously-injected mIgG1 in ECs and macrophages of various tissues (lung, kidney, liver, skin, muscle, spleen and lymph nodes) in G-KO mice. mIgG1 accumulated to very high levels within macrophages of lung (localized in the alveolus) and to lesser extent in macrophages of skin and liver (Fig. 4-9). In addition, mIgG1 accumulation was also observed within few macrophages of kidney, intestine, spleen and lymph nodes (data not shown). In contrast, liver was the only organ in which mIgG1 accumulated to detectable levels within ECs (sinusoidal) (Fig. 4-10). The accumulation of mIgG1 (on a per-cell basis) observed in sinusoidal ECs was lower in comparison with that in lung macrophages (Fig. 4-9, 4-10). Importantly, primary alveolar macrophages isolated from C57BL/6J mice efficiently accumulated and recycled mIgG1 following *in vitro* pulse and chase incubations, respectively (Fig. 4-11). In contrast, although

alveolar macrophages from G-KO mice accumulated IgG, they did not recycle this ligand (Fig. 4-11), indicating that the recycling observed in macrophages from C57BL/6J mice is FcRn-mediated. These observations confirm that macrophages are highly efficient in non-specific uptake of IgG, allowing them to make an important contribution to IgG homeostasis.

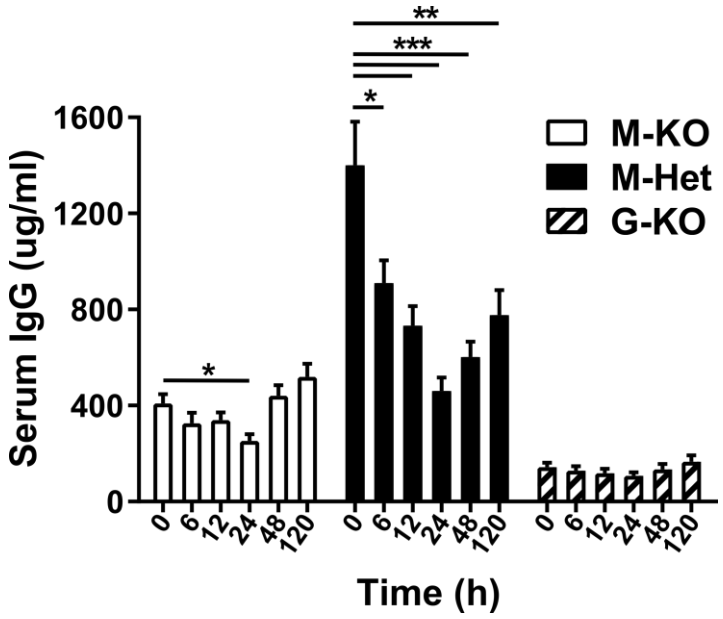

Figure 4-6. M-KO mice have very low levels of functionally active FcRn. M-KO and control mice (4-5 mice/genotype) were treated (i.v.) with 1.5 mg of MST-HN mutant (Abdegs) and serum IgG levels were determined at indicated times using ELISA. Data shown is representative of two independent experiments. Error bars indicate SEM. Significant differences (*****, $p < 0.05$; ******, $p < 0.01$; *******, $p < 0.001$; one-way ANOVA) between the groups are indicated.

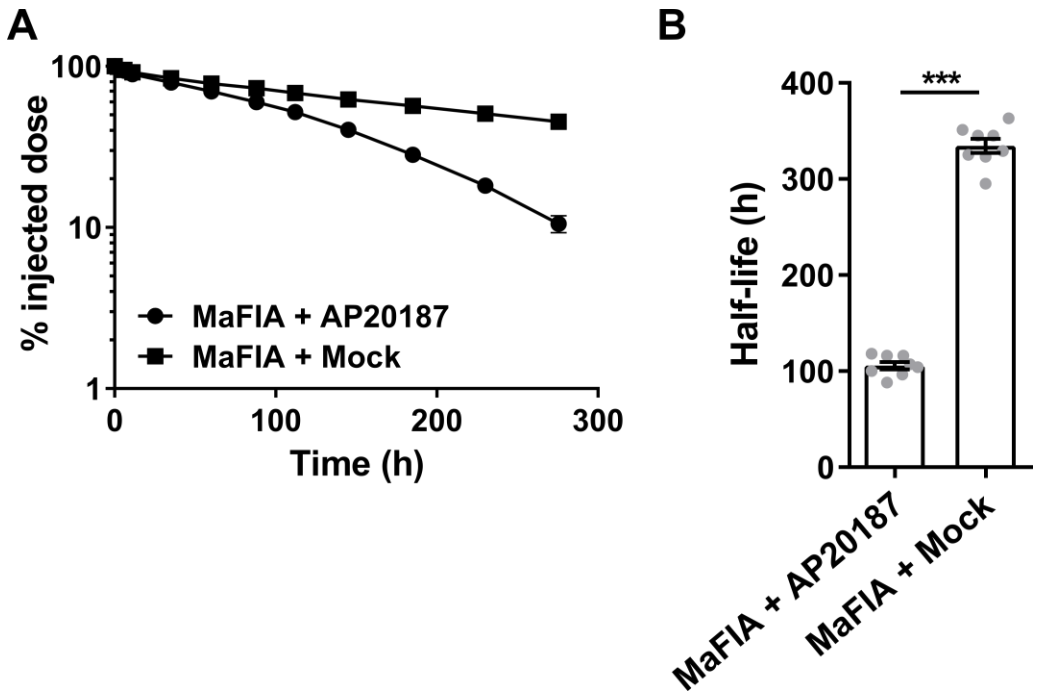

Figure 4-7. Systemic macrophage depletion results in significantly reduced persistence of mIgG1. MaFIA mice (8 mice/group) were treated with AP20187 [10 mg/kg (i.v.) on days 0, 1, 2, 3 and 4 and 1 mg/kg (i.p.) on days 7, 10, 13 and 16] or mock alone and ^{125}I-labeled mIgG1 was injected (i.v.) on day 5. (A) Whole body radioactivity levels were assessed at the indicated times. (B) β-phase half-lives of mIgG1 in different mice are shown which were obtained by fitting the data in (A) to a decaying bi-exponential model. Data shown is representative of two independent experiments. Error bars indicate SEM [obscured by the symbols in (A)]. Significant difference (*******, $p < 0.001$; two-tailed Student's *t*-test) between the groups is indicated.

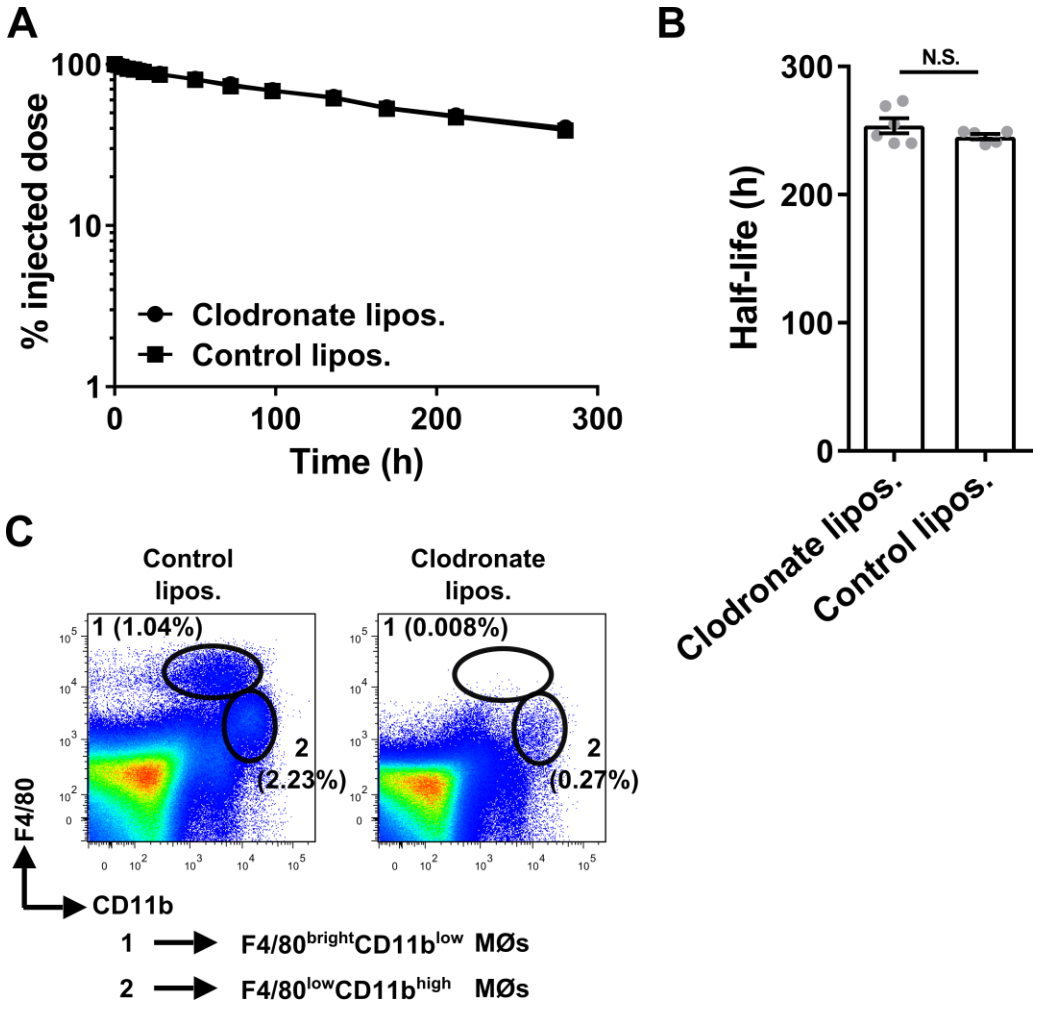

Figure 4-8. Splenic macrophage depletion does not affect the persistence of mIgG1. (A) C57BL/6J mice (5-6 mice/group) were intravenously treated with clodronate (1.5 mg/dose) or PBS (control) liposomes at 0 h and 48 h and ^{125}I-labeled mIgG1 was injected (i.v.) at 18 h, following which whole body radioactivity levels were assessed at the indicated times post-antibody injection. (B) β-phase half-lives of mIgG1 in different mice are shown which were obtained by fitting the data in (A) to a decaying bi-exponential model. (C) C57BL/6J mice (3 mice/group) were treated with clodronate or control liposomes as in (A) and splenocytes isolated at 60 h following the second injection of liposomes to quantitate the efficiency of macrophage depletion using flow cytometry. % (boxed) of F4/80^{bright}CD11b^{low} and F4/80^{low}CD11b^{high} macrophages are shown. Monocytes were gated out for this analysis. Data shown is representative of two independent experiments. Error bars indicate SEM [obscured by the symbols in (A)]. N.S., no significant difference ($p > 0.05$; two-tailed Student's *t*-test).

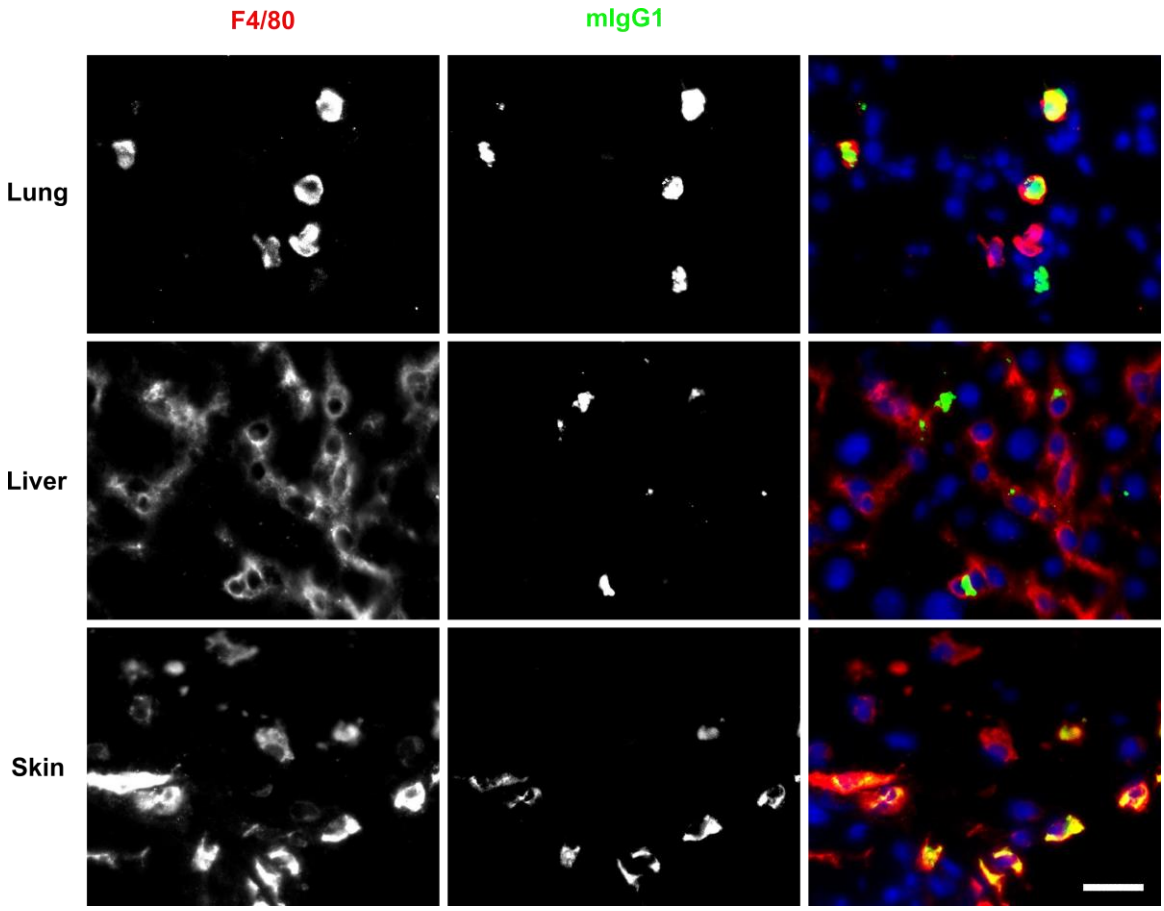

Figure 4-9. Macrophages in lung, and to a lesser degree in skin and liver, are very active in performing fluid phase uptake of intravenously injected mIgG1. G-KO mouse was injected (i.v.) with 1.5 mg of Alexa 647-labeled mIgG1 and after 50 h the mouse was perfused and different organs collected for immunohistochemistry. The localization of the injected antibody (psuedocolored in green) within macrophages (psuedocolored in red) was studied using F4/80 immunostaining. Scale bar = 20 μm. Data shown is representative of at least two independent experiments.

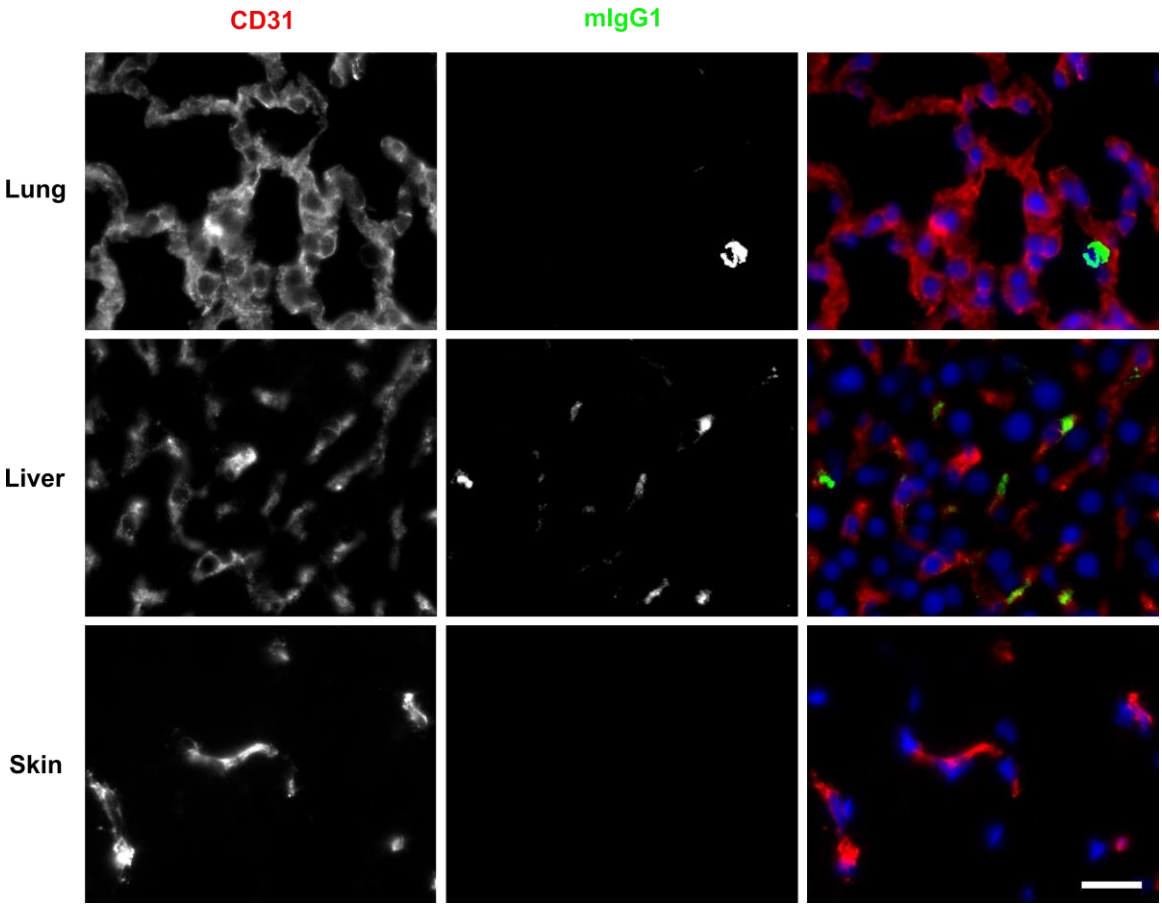

Figure 4-10. ECs in the liver pinocytose intravenously injected mIgG1. G-KO mouse was injected (i.v.) with 1.5 mg of Alexa 647-labeled mIgG1 and after 50 h the mouse was perfused and different organs collected for immunohistochemistry. The localization of the injected antibody (psuedocolored in green) within ECs (psuedocolored in red) was studied using CD31 immunostaining. Scale bar = 20 μm. Data shown is representative of at least two independent experiments.

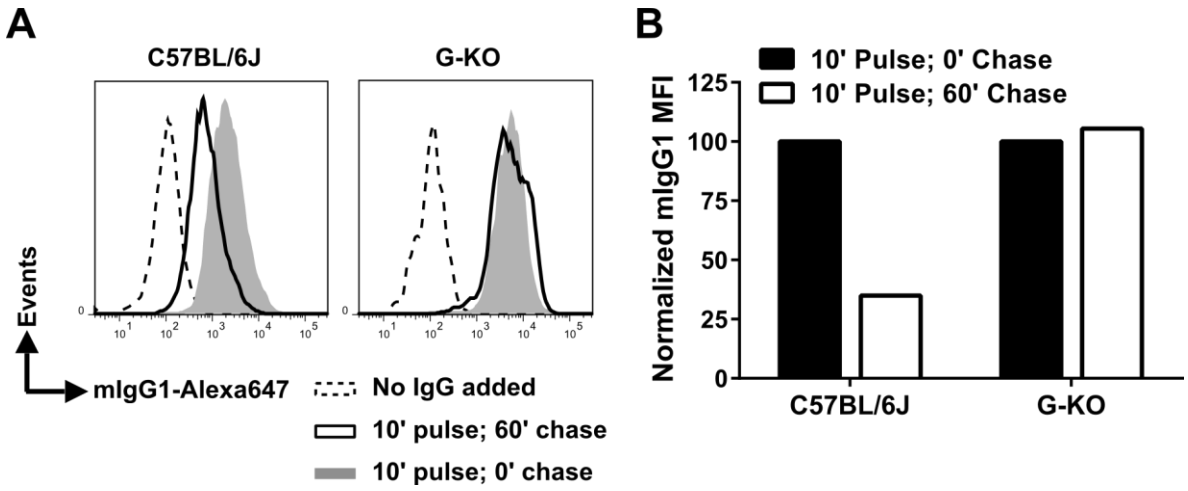

Figure 4-11. Alveolar macrophages can efficiently recycle mIgG1 *ex vivo*. (A) Bronchoalveolar lavage cells were obtained from C57BL/6J and G-KO mice, pooled (from 4 mice/genotype) and pulsed with 200 μg/ml of Alexa 647-labeled mIgG1 for 10 minutes at 37°C. The cells were subsequently chased for 0 or 45 minutes at 37°C, followed by surface staining for F4/80. Cell-associated fluorescence (Alexa 647) levels in F4/80^{+} cells was analyzed by flow cytometry and presented as histogram overlays. (B) Normalized (with respect to 0' chase values) mean fluorescence intensity (MFI) of mIgG1 for the data shown in (A).

4.3 DISCUSSION AND CONCLUSION

Monoclonal Abs, Fc-fusion protein therapeutics and Ab-drug/toxin conjugates have recently become some of the most effective drugs to treat various types of cancers, autoimmune and infectious diseases and prevent transplant rejection. One important factor responsible for the success of Ab-based therapeutics (of the IgG class) is long *in vivo* half-life or persistence, which is mediated by FcRn-dependent IgG recycling. Although the intracellular mechanism that governs IgG recycling is well understood[1], the sites of IgG homeostasis *in vivo* have not been unambiguously identified. Studies carried out using cell type-specific FcRn KO ($Tie2^{+}FcRn^{flox/flox}$) mice indicated that ECs and HCs are the primary sites where FcRn-mediated IgG recycling is carried out[20]. In order to evaluate the contribution of FcRn in macrophages, DCs and B cells in IgG salvage, we generated mice that conditionally lack FcRn in these cell types. Our results indicate that FcRn in macrophages is indispensable for the long *in vivo* half-life of IgG. These observations were also confirmed using whole body macrophage depletion. Further, our results indicate that receptor-independent uptake of IgG by FcRn-expressing cells is a crucial factor that governs the relative contribution of these cells to FcRn-mediated IgG homeostasis. Importantly, alveolar macrophages are very efficient in fluid phase uptake of intravenously-delivered IgG and are capable of performing FcRn-dependent IgG recycling. To our knowledge, this is the first study to show an important role of macrophages in regulating IgG persistence.

Cre-loxp technology was employed in the current study to generate cell type-specific FcRn KO mice. Importantly, few recent publications have revealed problems with respect to the specificity of cre expression in some of the commonly used mouse lines[314, 315]. Therefore, in order to draw conclusions from experiments performed using these genetically modified mice, we

employed a flow cytometry-based functional assay to verify the specificity and efficiency of knock down of the gene product in various KOs we generated. This assay involves comparison of the cellular uptake of an antibody has tight binding to FcRn at both acidic and near neutral pH with the uptake of an antibody that does not bind to FcRn at either pH[3, 20, 44, 45].

To generate macrophage-specific FcRn KO mice, LysM-Cre mice[301] were crossed with $FcRn^{flox/flox}$ mice[20]. It has been shown that cre expression in LysM-Cre mice is limited to macrophages and neutrophils[301]. However, neutrophils in C57BL/6J mice do not express FcRn[20]. Analysis of FcRn deletion efficiency and specificity in LysM-Cre-$FcRn^{flox/flox}$ mice revealed almost complete deletion in splenic macrophages and partial deletion in monocytes. For generating DC-specific FcRn KO mice, CD11c-Cre mice[302] were employed, however, the resultant mice lacked FcRn in multiple cell types including all HCs and ECs. Although, CD11c-Cre mice have been used in the past to delete genes of interest specifically in DCs, our results combined with recently published results of others[314] indicate that CD11c is expressed in HCs other than DCs at some stage of their development or differentiation. Further, cre-mediated recombination efficiency depends on the level of recombinase activity and the size of the gene (i.e, the distance between the loxp sites)[316] – modest cre expression might be inadequate for efficient deletion of a large gene. Hence, the specificity of gene deletion using a particular cre strain might depend on the size of the targeted gene. Interestingly, although no problems have been reported with regards to the specificity of CD19-Cre mice[303], crossing these mice with FcRn-floxed mice lead to FcRn deletion in both B cells and DCs. The observed FcRn deletion in DCs could be either due to CD19-Cre or constitutive FcRn deletion in $FcRn^{flox/flox}$ line (different from the line used for generating M-KO mice with respect to number of backcrossings to C57BL/6J mice) that was used for generating these mice. Further studies have to be carried out to identify the cause of this deletion. Finally, for

generating EC-specific FcRn KO mice, Tie2e-Cre mice[310] and tamoxifen-dependent Cdh5(PAC)-CreERT2 mice[311] were employed. Tie2e-Cre-FcRn$^{flox/flox}$ mice exhibited partial FcRn deletion in heart ECs and also in all the HCs except monocytes. Although these mice cannot be used as EC-specific KOs, these mice were used to evaluate the contribution of FcRn in monocytes in conjunction with LysM-Cre-FcRn$^{flox/flox}$ mice. In tamoxifen-treated Cdh5(PAC)-CreERT2-FcRn$^{flox/flox}$ mice, partial FcRn deletion was observed in heart ECs but no deletion was observed in the lung ECs. Hence, additional cre transgenic mice or different tamoxifen administration protocols have to be tested in order to generate EC-specific FcRn KO mice.

To evaluate the contribution of FcRn in different cellular compartments of HCs, the whole body pharmacokinetics of mIgG1 was studied in different cell type-specific FcRn KOs and G-KO mice. Surprisingly, the half-life of mIgG1 in M-KO mice was only slightly longer than that observed in G-KO mice. Since, monocytes and classical DCs in M-KO mice exhibit partial FcRn deletion it is not possible to evaluate the role of macrophages in FcRn-mediated IgG homeostasis using the M-KO mice alone. However, Tie2e-KO mice, in which many cell types including macrophages exhibit marked reduction in FcRn expression, but monocytes harbor normal levels of FcRn the half-life of mIgG1 is only slightly longer than that measured in M-KO mice. In addition, specific deletion of FcRn in DCs and B cells (B-DC-KO) does not significantly affect the half-life of mIgG1. Hence, in combination, these observations indicate that the contribution of FcRn in macrophages to IgG homeostasis greatly surpass the contribution by this receptor in other HCs. The lack of a major role for B cells in FcRn-mediated IgG homeostasis could be due to low pinocytic rate[292] and FcRn expression levels, whereas for DCs, the reason could be their relatively low numbers in the body.

Similar to the pharmacokinetic data, quantification of serum IgG and albumin levels in different KO mice indicated that among HCs, macrophages are an important site of FcRn activity in the context of IgG and albumin homeostasis. Although the half-life of mIgG1 in M-KO mice was only slightly different from that in G-KO mice, the steady state serum IgG levels in M-KO mice were only ~66% lower in comparison to the control mice as opposed to ~89% lower in GKO mice. If the synthetic rate of IgG is similar between M-KO and G-KO mice, this behavior can be explained based on the presence of residual FcRn-mediated IgG salvage activity in M-KO mice, as confirmed by IgG depletion studies using MST-HN.

IgG pharmacokinetics has been studied in the past in bone marrow chimeras of G-KO and WT mice to evaluate the relative contribution of the hematopoietic compartment and parenchymal compartment to FcRn-mediated IgG homeostasis. One such study demonstrated that the contribution of the hematopoietic compartment to IgG salvage is greater than that of the parenchymal compartment[36, 88], in agreement with the results presented here. However, two other studies based on a similar approach indicated that parenchymal cells and HCs play equal roles[24, 92]. These different results could be due to the fact that although the recovery of tissue resident macrophages (after lethal irradiation and bone marrow transplantation) occurs mostly via donor bone marrow-derived cells, the remaining irradiated host tissue resident macrophages retain the capability to self-maintain by local proliferation[317]. Thereby, the donor chimerism among tissue macrophages will not be 100%[317]. Importantly, a change in the effective irradiation dose (e.g., lethal vs sublethal) and a change in the competition from donor-derived cells to repopulate the tissues can affect the percentage of chimerism[317, 318]. In this context, different protocols were used for bone marrow transplantation in the above mentioned studies. Further, it was recently (several years after reporting of bone marrow transplantation studies described above) confirmed that tissue

resident macrophages, which self-maintain locally throughout adult life, are derived from fetal HSCs or yolk sac-derived EMPs and not from bone marrow HSCs[305, 308, 317] and the macrophages derived from these different progenitor sources are phenotypically different[318, 319]. These findings indicate that bone marrow transplantation would lead to inefficient replacement of tissue macrophages and/or modulate tissue macrophage function, thereby making this technique less accurate in evaluating the contribution of myeloid cells versus parenchymal cells to a biological process in which tissue resident macrophages participate, such as IgG homeostasis.

A role of systemic macrophages in FcRn-mediated IgG homeostasis was confirmed using mice that underwent whole body macrophage depletion, in which mIgG1 had significantly reduced half-life in comparison to control, macrophage-sufficient mice. This indicates that specific deletion of FcRn in macrophages or systemic depletion of macrophages themselves negatively impact IgG pharmacokinetics which leads to a possible hypothesis – macrophages act as a reservoir for IgG which limits the concentration of this molecule in the microenvironment around the macrophages thus minimizing the uptake and degradation of IgG by FcRn-ve cell types in that microenvironment. Interestingly, mIgG1 half-life was not affected when macrophages were depleted only from the spleen (and partially from liver) using clodronate liposomes. This lack of effect could be due to fact that splenic macrophages form only a small fraction of total macrophage count in the body[293]. Thereby, following splenic macrophage depletion, other macrophages in the body compensate for their absence in regulating IgG half-life. Alternatively, in contrast to macrophages in non-lymphoid tissues, splenic macrophages could be inefficient in IgG uptake and as a result their presence or absence do not significantly affect IgG salvage. Supporting this possibility, intravenously-delivered, fluorescently-labeled mIgG1 accumulated primarily in alveolar macrophages and to a lesser degree in skin macrophages and liver sinusoidal ECs and

macrophages. In agreement with this, a study in the past had reported that the lung environment enables mouse alveolar macrophages to exhibit high levels of spontaneous macropinocytosis[320], an endocytic process through which large volumes of extracellular fluid is ingested by the cell in a receptor-independent manner[321]. In addition, the lung is very well perfused and receives 100% of the output from heart, whereas other tissues in the body receive only a fraction of this blood supply[105] which translates into relatively higher concentrations of blood-derived macromolecules such as IgG in the lung interstitial space and especially in the lung epithelial lining fluid (ELF) where alveolar macrophages reside - the concentration of IgG in the mouse and human ELF has been reported to be ~200 and ~1600 μg/ml, respectively[322-324]. In combination with the *in vitro* experiment showing efficient IgG recycling by mouse alveolar macrophages, the above mentioned lung-specific factors indicate that alveolar macrophages contribute to FcRn-mediated IgG homeostasis. A recent report has shown that human alveolar macrophages express high levels of FcRn[325] which supports the clinical relevance of these findings.

In summary, this study underscores an important role for macrophages, that efficiently accumulate IgG by fluid phase pinocytosis, in FcRn-dependent IgG salvage. These findings not only have relevance to understanding the sites of action of IgG-based drugs and predicting their pharmacokinetics but also to the understanding of pathogenesis of disorders that involve dysregulation of macrophages.

4.4 MATERIALS AND METHODS

4.4.1 Mice

FcRn$^{-/-}$[74], LysM-Cre[301], CD11c-Cre[302], CD19-Cre[303] and MaFIA[313] mice on a C57BL/6J background and C57BL/6J mice were purchased from the Jackson Laboratory (Bar Harbor, ME). FcRn-floxed mice have been described previously[20]. Tie2e-Cre mice[310] and Cdh5(PAC)-CreERT2 mice[311] on a C57BL/6J background were a kind gift from Dr. Xiaoxia Li (Cleveland Clinic, OH) and Dr. Ralf Adams (Max Planck Institute for Molecular Biomedicine, Münster, Germany), respectively. Mice were bred in a specific pathogen-free facility at the University of Texas Southwestern Medical Center or Texas A&M University and were handled in compliance with institutional policies and protocols approved by the Institutional Animal Care and Use Committees.

4.4.2 Production of antibodies

For all experiments except *ex vivo* IgG recycling assays, mIgG1 (anti-hen egg lysozyme, D1.3[198]) was purified from hybridoma culture supernatants using lysozyme-Sepharose[216]. Recombinant mIgG1 (anti-hen egg lysozyme) was used in *ex vivo* recycling assays. In order to generate expression constructs for the production of recombinant mIgG1, cDNA encoding the heavy chain and light chain was isolated from the D1.3 hybridoma[198]. The heavy and light chain genes were subsequently cloned into pcDNA^{TM}3.4-TOPO® vector (Life Technologies, Grand Island, NY) for expression. Expi293^{TM} expression system kit (Life Technologies, Grand Island, NY) was used for transient transfection of heavy and light chain expression constructs into Expi293F^{TM} cells (Life Technologies, Grand Island, NY) and protein expression. The recombinant

antibody was purified from culture supernatants using lysozyme-Sepharose[216]. Binding properties of the antibodies were confirmed using surface plasmon resonance (BIAcore) analyses.

NS0 transfectants expressing mutated derivatives of humanized anti-hen egg lysozyme IgG1 (HuLys10)[216], MST-HN (M252Y/S254T/T256E/ H433K/N434F) and H435A, were generated and cultured as described previously[3, 104]. The recombinant antibodies were purified from culture supernatants using lysozyme-Sepharose[216].

4.4.3 Antibody labeling

Iodination (^{125}I) of mIgG1 was carried out using Iodogen as previously described[220]. mIgG1, MST-HN and H435A were labeled with Alexa Fluor 647 (Alexa 647) carboxylic acid (succimidyl ester; Life Technologies, Grand Island, NY) using previously described methods[54]. The activity of Alexa 647-labeled antibodies was verified by carrying out BIAcore analyses.

4.4.4 Pharmacokinetic experiments

6-10 week old male and female mice were fed 0.1% Lugol (Sigma-Aldrich, St. Louis, MO) in water starting at 72 h before i.v. injection in the tail vein with ^{125}I-labeled mIgG1 (10–15 μg per mouse). Levels of whole body radioactivity were measured at the indicated times using Atom Lab 100 dose calibrator (Biodex Medical Systems, Shirley, NY).

To analyze the effects of systemic depletion of macrophages on the pharmacokinetics of mIgG1, the above described experimental procedure was followed except that MaFIA mice[313] were treated with 10 mg/kg (i.v.) of AP20187 on days 0, 1, 2, 3 and 4, followed by 1 mg/kg (i.p.) of AP20187 on days 7, 10, 13 and 16 and ^{125}I-labeled mIgG1 was injected (i.v.) on day 5. AP20187 was either a gift from ARIAD Pharmaceuticals or was purchased from Clontech (Mountain View,

CA). Lyophilized AP20187 was dissolved in 100% ethanol at a concentration of 13.75 mg/ml, and stored at -20°C in dark. All injections of AP20187 were carried out within 30 minutes after dilution into injection vehicle (4% ethanol, 10% PEG-400, and 1.7% Tween in water). Control MaFIA mice were treated with mock (4% ethanol, 10% PEG-400, and 1.7% Tween in water) only.

To investigate the effects of splenic macrophage depletion on mIgG1 pharmacokinetics, C57BL/6J mice were intravenously injected with clodronate (1.5 mg/dose) or phosphate-buffered saline (PBS; control) liposomes (Encapsula NanoSciences, Brentwood, TN) at 0 h and 48 h, and ^{125}I-labeled mIgG1 was injected (i.v.) at 18 h, followed by above described experimental procedure.

A two-compartment model is one of the most commonly used approaches for pharmacokinetic modeling of antibodies in the plasma or circulation. In this model, one compartment represents the plasma or circulation and the second compartment refers to the interstitial space in the organs or tissues. The plasma antibody levels initially decrease rapidly due to redistribution of the antibody from the plasma compartment to the tissue compartment and the degradation of aggregated or misfolded antibody molecules or fragments, with the former usually dominating. This phase is referred to as the α-phase and for antibodies typically lasts around 24 hours. Once the antibody distribution between the compartments reaches an equilibrium, the decrease in plasma antibody levels is due to elimination from the body which is usually slower relative to the clearance during the α-phase and is called the β-phase. In contrast to the above, the pharmacokinetic modeling of antibodies in the whole body involves only one compartment (body). However, the antibody clearance from the body also involves an initial rapid α-phase, followed by a slower β-phase. The α-phase in this case is believed to be due to the degradation of aggregated or misfolded antibody molecules or fragments.

To calculate the half-lives of injected mIgG1 in mice that exhibit relatively slow clearance of injected antibody (M-Het, Tie2e-Het, B-DC-Het, B-DC-KO, C57BL/6J and MaFIA), the whole body counts (*y*) and times of their measurement (*t*) were fit to a biexponential (1) decay curve as mentioned below. In mice that exhibit rapid physiological decay of injected mIgG1 (M-KO, Tie2e-KO and G-KO), the α- and β-phases cannot be clearly defined. Consequently, the whole body counts obtained from these mice and times of their measurement were fit to a monoexponential (2) decay curve as mentioned below.

$$y = C_1 e^{-k_1 t} + C_2 e^{-k_2 t} \ (1)$$

$$y = C e^{-kt} \ (2)$$

The values of *C* and *k* that best fit these equations to the data are found using a non-linear least squares minimization method implemented using custom scripts written in MATLAB (Mathworks, Natick, MA). The half-life values for the phase(s) are then calculated from the *k* as *ln(2)/k*.

4.4.5 Antibodies and flow cytometry analyses

For analyzing functional FcRn levels in different hematopoietic cell types in the spleen, the animals were euthanized and spleens harvested. Single cell suspensions from spleen were obtained by mechanical disruption and forcing through 70 μm cell strainers (Becton-Dickinson, San Jose, CA). The cell suspensions were depleted of erythrocytes using red blood cell lysis buffer and washed with PBS. Subsequently, the cells were incubated with anti-FcγRIIB/III (2.4G2) antibody for 15 minutes at 4°C, followed by another incubation in IgG-depleted[54] phenol red-free cDMEM

(pH 7.2) containing 5 μg/ml Alexa 647-labeled MST-HN or H435A mutants for 45 minutes at 37°C. Following a PBS wash, the cells were incubated on ice with fluorescently-labeled antibodies to identify the following cell types: macrophages ($F4/80^{bright}CD11b^{low}$), monocytes ($Ly6C^{high}CD11b^{int}$), classical DCs ($CD11c^{+}CD11b^{+}$), follicular B cells ($CD23^{high}CD21^{low}$) and neutrophils ($Ly6C^{int}CD11b^{high}$).

To evaluate functional FcRn levels in heart and lung ECs, modified version of a previously described protocol[326] was followed to prepare single cell suspensions from these tissues. Briefly, the animals were euthanized, heart and lungs harvested and washed with calcium- and magnesium-free Hank's Balanced Salt Solution (HBSS; Life Technologies, Grand Island, NY) to remove excess blood. The washed tissues were mechanically dissociated into small pieces and to obtain single cell suspensions, the diced tissues were incubated in calcium- and magnesium-free HBSS containing 1 mg/ml of collagenase type I (Worthington Biochemical Corp., Lakewood, NJ) and 2.4 mg/ml of dispase (Life Technologies, Grand Island, NY) for 45 minutes at 37°C. Following incubation, the tissue homogenates were filtered through a 100 μm cell strainer (Becton-Dickinson, San Jose, CA) and resultant cell suspensions were depleted of erythrocytes using red blood cell lysis buffer. After a wash with HBSS, the cells were incubated with anti-FcγRIIB/III (2.4G2) antibody for 15 minutes at 4°C, followed by another incubation in IgG-depleted[54] phenol red-free cDMEM (pH 7.2) containing 5 μg/ml Alexa 647-labeled MST-HN or H435A mutants for 45 minutes at 37°C. The cells were subsequently washed and stained with fluorescently-labeled isolectin B4 (Vector Laboratories, Burlingame, CA) and antibodies to identify ECs ($CD31^{+}CD105^{+}$isolectin $B4^{+}$). Analysis of functional FcRn expression in tissue resident macrophages was carried out using the protocol described above, except that the animals were anesthetized and intracardially perfused with 10-20 mls of 10 U/ml heparin in PBS before the

collection of organs (kidneys, lungs and liver) and all the washes were performed with calcium- and magnesium-free PBS. Fetal HSC- (or yolk sac EMPs-) and bone marrow HSC-derived macrophages were identified as $CD45^{+}F4/80^{bright}CD11b^{low}$ and $CD45^{+}F4/80^{low}CD11b^{high}$, respectively.

For *ex vivo* recycling assays, bronchoalveolar cells were obtained by performing bronchoalveolar lavage with 4 x 1 ml of ice cold calcium- and magnesium-free PBS containing 0.6 mM of EDTA (Fisher Scientific, Fair Lawn, NJ) [PBS-EDTA]. Bronchoalveolar cells isolated from multiple mice were pooled, treated with red blood cell lysis buffer to deplete erythrocytes and washed with PBS-EDTA. The cells were then pulsed with 200 μg/ml of Alexa 647-labeled mIgG1 in IgG-depleted[54] phenol red-free cRPMI (pH 7.2) for 10 minutes at 37°C. Subsequently, the cells were washed with PBS-EDTA and chased for 0 or 45 minutes at 37°C. After washing with PBS-EDTA, the bronchoalveolar cells were surface stained on ice with F4/80 to identify macrophages.

Flow cytometry analyses were performed using a FACSCalibur (Becton-Dickinson, San Jose, CA) or LSRFortessa (Becton-Dickinson, San Jose, CA) and data analyzed using FlowJo (Tree Star, Ashland, OR). Antibodies specific for the following were purchased from either Becton-Dickinson (San Jose, CA), eBioscience (San Diego, CA) or Biolegend (San Diego, CA): F4/80 (BM8), CD11b (M1/70), Ly6C (AL-21), CD11c (HL3), CD23 (B3B4), CD21 (7G6), CD31 (390), CD105 (MJ7/18) and CD45 (30-F11).

4.4.6 Quantification of serum IgG and albumin levels

Serum IgG and albumin levels were assessed using sandwich ELISAs using previously described methods[3]. Coating antibodies included polyclonal rabbit anti-mouse IgG (gamma chain

specific; Life Technologies, Grand Island, NY) and polyclonal goat anti-mouse albumin (Abacm, Cambridge, MA). Secondary antibodies included horseradish peroxidase (HRP)-conjugated polyclonal rabbit anti-mouse IgG (heavy and light chain specific; Life Technologies, Grand Island, NY) and HRP-conjugated polyclonal goat anti-mouse albumin (Abacm, Cambridge, MA). Mouse IgG and albumin standards were obtained from Jackson ImmunoResearch Laboratories (West Grove, PA) and Sigma-Aldrich (St. Louis, MO), respectively.

4.4.7 Tissue collection, staining and immunofluorescence analyses

To analyze the accumulation of intravenously-administered mIgG1 *in vivo*, 6-10 weeks old male and female mice were injected (i.v.) with 1.5 mg of Alexa 647-labeled mIgG1. 50 hours later, mice were anesthetized and intracardially perfused with 10-20 mls of 10 U/ml heparin in PBS, following which organs [lung, liver, kidney, skin (dorsal area), muscle (gastrocnemius, soleus and plantaris), intestine (small and large), spleen and inguinal, mesenteric, axillary and brachial lymph nodes] were excised. The tissues were immediately embedded in Tissue-Tek® OCT compound (Sakura Finetek USA, Torrance, CA), flash-frozen in liquid N_2 and stored at -80ºC until sectioning. Sections of 5 µm thickness from different tissue depths were made and stored at -80ºC for subsequent staining. Frozen sections were fixed in acetone (-20˚C) and air-dried overnight. After washing with PBS, sections were blocked using 5% goat serum (Sigma-Aldrich, St. Louis, MO), followed by incubation with rat anti-mouse CD31 (clone 390; Biolegend, San Diego, CA) or rat anti-mouse F4/80 (clone CI:A3-1; Abcam, Cambridge, MA). Bound primary antibody was detected using Alexa 555-labeled polyclonal goat anti-rabbit IgG (Life Technologies, Grand Island, NY). Following washing, coverslips were mounted using Vectashield mounting medium containing DAPI (Vector Laboratories, Burlingame, CA).

Sections were imaged using a Zeiss Axiovert 200M inverted microscope equipped with a Zeiss 20X, 0.5 NA Plan-Neofluar objective and an ORCA CCD camera (Hamamatsu). Images were acquired with filtersets specific for Alexa 555 Fluor (TRITC-B-000-ZERO; Semrock), Alexa 647 Fluor (Cy5-4040C-ZERO; Semrock) and DAPI (Part No 31013v2; Chroma Technologies). The data were processed and displayed using the microscopy image analysis tool (MIATool) software package (www4.utsouthwestern.edu/wardlab/miatool.asp) in MATLAB (Mathworks). The acquired images were embedded in 16-bit grayscale format and overlaid for presentation. For comparative purposes, the intensities of the Alexa 647 Fluor channel were adjusted in an analogous manner across the datasets. Images were exported into Inkscape for final composition of the figures.

4.4.8 Statistical analyses

Statistical analyses of data were carried out using two-tailed Student's *t*-test or one-way ANOVA (GraphPad Software, La Jolla, CA). *p* values of less than 0.05 were taken to be significant.

CHAPTER FIVE
Future studies and caveats

Studies described in Chapter II demonstrate that FcRn-blockade using Abdegs is effective in ameliorating disease in a passive, autoantibody-dependent EAE model. These studies underscore the therapeutic potential of Abdegs for the treatment of MS or other autoimmune diseases involving autoreactive antibodies. Importantly, MST-HN Abdegs bind to mouse FcRn with higher affinity than to human FcRn at both pH 6.0 and 7.4[3]. Thus, Abedgs would be expected to result in reduced competition with endogenous IgG in the presence of human FcRn, although this behavior is expected to result in longer *in vivo* half-lives of Abdegs. Hence, a future study of potential interest will include studying the effects of Abdegs on disease following the transfer of humanized MOG-specific antibodies into mice that transgenically express human FcRn[74]. In addition, it will be of interest to test the therapeutic effects of Abdegs in EAE models involving the active or spontaneous generation of encephalitogenic antibodies. In this context, although, CNS antigen-specific antibodies are generated in several EAE models, their role in disease pathogenesis is limited or not well characterized[192, 327, 328]. Hence, future studies will involve the identification of a suitable actively-induced or spontaneous autoantibody-dependent EAE model, in which the therapeutic effects of Abdegs will be tested. Finally, since the EAE model employed in this study is dependent on both autoantibodies and autoreactive T cells, the effect of Abdegs on such T cells will be evaluated.

As mentioned earlier, autoreactive $CD4^+$ T cells are drivers of autoimmune diseases[6]. Consequently, safe and effective treatments for autoimmune diseases would include therapeutic strategies that lead to specific deletion or inhibition of autoreactive T cell activity. Studies presented in Chapter III demonstrate that administration of long-lived Fc-antigen fusion proteins

tolerize autoreactive T cells and consequently ameliorate disease in an EAE model involving the immunization of H-2^u mice with the immunodominant epitope, MBP1-9. However, T cells contributing to pathology in MS patients are specific for multiple epitopes[14, 329, 330]. Further, the specificity of these T cells can spread to additional epitopes during the progression of the disease[271, 272]. In the current study, Fc-epitope fusions containing MBP1-9 were employed, since this is the only epitope relevant to disease in H-2^u mice[286]. Nevertheless, Fc fusions containing multiple epitopes can be readily generated. For example, eight different epitopes could be linked as epitope dimers to the N- and C-termini of a heterodimeric Fc fragment (using 'knobs-into-holes' technology[331] to produce Fc heterodimers). It will be of interest to test the efficacy of Fc-antigen fusions containing more than one immunodominant epitope in relevant EAE models. Further, MBP1-9-induced EAE in H-2^u mice is primarily Th1 cell-mediated with little or no contribution from Th17 cells[242, 332], which are believed to play an important role in disease in many EAE models and MS[6]. However, the downregulation of T-bet in Th1 cells following the delivery of Fc-antigen fusions observed in the current study, combined with a recent study indicating that T-bet expression by encephalitogenic Th17 cells is required for their accumulation in the CNS[333], indicate that Fc-antigen fusions could be effective in ameliorating disease in Th17-mediated EAE models. In addition to tolerization of antigen-specific T cells, $Foxp3^+$ Treg numbers were amplified by the delivery of Fc-antigen fusions. However, the relative contribution of Tregs in fusion protein-induced amelioration of disease remains to be tested. Finally, therapeutic strategies combining Abdegs and Fc-antigen fusions could lead to greater efficacy than either agent alone, especially in patients with active lesions belonging to the type II pattern of disease[133] (refer to section 1.3.3).

Abdegs and Fc-antigen fusions both function by targeting FcRn. In order to gain an improved understanding of the mechanism of action of these IgG-based therapeutics, it is essential to identify

the sites of FcRn-mediated IgG homeostasis. As a result, studies described in Chapter IV were carried out which indicate that macrophages represent an important cell type responsible for FcRn-mediated IgG salvage. This conclusion is largely based on the IgG clearance rates and serum IgG levels observed in macrophage-specific FcRn KO mice. A complementary study of potential interest would include analysis of IgG pharmacokinetics and levels in mice that conditionally lack FcRn in ECs. Previous attempts to generate such mice were unsuccessful due to the lack of specificity and efficiency of cre-mediated gene deletion (refer to section 4.3). Therefore, future studies will include the identification of a suitable transgenic mouse line harboring EC-specific cre. Further, in contrast to the effect of systemic depletion of macrophages on IgG pharmacokinetics, splenic depletion of macrophages in FcRn-sufficient mice did not affect the half-life or IgG. This lack of effect could be related to the relatively low contribution of splenic macrophages to pinocytosis of IgG in comparison to macrophages at other sites in the body. To investigate this, future studies will include pharmacokinetic studies of IgG in splenic macrophage-depleted FcRn-deficient (G-KO) mice.

BIBLIOGRAPHY

1. Ward, E.S. & Ober, R.J. Multitasking by exploitation of intracellular transport functions: the many faces of FcRn. *Adv. Immunol.* **103**, 77-115 (2009).

2. Challa, D.K., Velmurugan, R., Ober, R.J. & Sally Ward, E. FcRn: from molecular interactions to regulation of IgG pharmacokinetics and functions. *Curr. Top. Microbiol. Immunol.* **382**, 249-272 (2014).

3. Vaccaro, C., Zhou, J., Ober, R.J. & Ward, E.S. Engineering the Fc region of immunoglobulin G to modulate *in vivo* antibody levels. *Nat. Biotechnol.* **23**, 1283-1288 (2005).

4. Krumbholz, M., Derfuss, T., Hohlfeld, R. & Meinl, E. B cells and antibodies in multiple sclerosis pathogenesis and therapy. *Nat. Rev. Neurol.* **8**, 613-623 (2012).

5. Weber, M.S., Hemmer, B. & Cepok, S. The role of antibodies in multiple sclerosis. *Biochim. Biophys. Acta* **1812**, 239-245 (2011).

6. Dendrou, C.A., Fugger, L. & Friese, M.A. Immunopathology of multiple sclerosis. *Nat. Rev. Immunol.* **15**, 545-558 (2015).

7. Steward-Tharp, S.M., Song, Y.J., Siegel, R.M. & O'Shea, J.J. New insights into T cell biology and T cell-directed therapy for autoimmunity, inflammation, and immunosuppression. *Ann. NY Acad. Sci.* **1183**, 123-148 (2010).

8. Critchfield, J.M. *et al.* T cell deletion in high antigen dose therapy of autoimmune encephalomyelitis. *Science* **263**, 1139-1143 (1994).

9. Jiang, Z., Li, H., Fitzgerald, D.C., Zhang, G.X. & Rostami, A. MOG(35-55) i.v suppresses experimental autoimmune encephalomyelitis partially through modulation of Th17 and JAK/STAT pathways. *Eur. J. Immunol.* **39**, 789-799 (2009).

10. Racke, M.K. *et al.* Intravenous antigen administration as a therapy for autoimmune demyelinating disease. *Ann. Neurol.* **39**, 46-56 (1996).

11. Samson, M.F. & Smilek, D.E. Reversal of acute experimental autoimmune encephalomyelitis and prevention of relapses by treatment with a myelin basic protein peptide analogue modified to form long-lived peptide-MHC complexes. *J. Immunol.* **155**, 2737-2746 (1995).

12. Devaux, B., Enderlin, F., Wallner, B. & Smilek, D.E. Induction of EAE in mice with recombinant human MOG, and treatment of EAE with a MOG peptide. *J. Neuroimmunol.* **75**, 169-173 (1997).

13. Leadbetter, E.A. *et al.* Experimental autoimmune encephalomyelitis induced with a combination of myelin basic protein and myelin oligodendrocyte glycoprotein is ameliorated by administration of a single myelin basic protein peptide. *J. Immunol.* **161**, 504-512 (1998).

14. Streeter, H.B., Rigden, R., Martin, K.F., Scolding, N.J. & Wraith, D.C. Preclinical development and first-in-human study of ATX-MS-1467 for immunotherapy of MS. *Neurol. Neuroimmunol. Neuroinflamm.* **2**, e93 (2015).

15. Steinman, L. The re-emergence of antigen-specific tolerance as a potential therapy for MS. *Mult. Scler.* **21**, 1223-1238 (2015).

16. Lutterotti, A. & Martin, R. Antigen-specific tolerization approaches in multiple sclerosis. *Expert Opin. Investig. Drugs* **23**, 9-20 (2014).

17. Penchala, S.C. *et al.* A biomimetic approach for enhancing the *in vivo* half-life of peptides. *Nat. Chem. Biol.* **11**, 793-798 (2015).

18. Smith, C.E., Eagar, T.N., Strominger, J.L. & Miller, S.D. Differential induction of IgE-mediated anaphylaxis after soluble vs. cell-bound tolerogenic peptide therapy of autoimmune encephalomyelitis. *Proc. Natl. Acad. Sci. USA* **102**, 9595-9600 (2005).

19. Pedotti, R. *et al.* An unexpected version of horror autotoxicus: anaphylactic shock to a self-peptide. *Nat. Immunol.* **2**, 216-222 (2001).

20. Perez-Montoyo, H. *et al.* Conditional deletion of the MHC Class I-related receptor, FcRn, reveals the sites of IgG homeostasis in mice. *Proc. Natl. Acad. Sci. USA* **106**, 2788-2793 (2009).

21. Zhu, X. *et al.* MHC class I-related neonatal Fc receptor for IgG is functionally expressed in monocytes, intestinal macrophages, and dendritic cells. *J. Immunol.* **166**, 3266-3276 (2001).

22. Brambell, F.W.R. *The Transmission of Passive Immunity from Mother to Young*. North Holland Publ Corp: Amsterdam, 1970.

23. Simister, N.E. & Mostov, K.E. An Fc receptor structurally related to MHC class I antigens. *Nature* **337**, 184-187 (1989).

24. Akilesh, S., Christianson, G.J., Roopenian, D.C. & Shaw, A.S. Neonatal FcR expression in bone marrow-derived cells functions to protect serum IgG from catabolism. *J. Immunol.* **179**, 4580-4588 (2007).

25. Borvak, J. *et al.* Functional expression of the MHC class I-related receptor, FcRn, in endothelial cells of mice. *Int. Immunol.* **10**, 1289-1298 (1998).

26. Nimmerjahn, F. & Ravetch, J.V. Fcγ receptors as regulators of immune responses. *Nat. Rev. Immunol.* **8**, 34-47 (2008).

27. Hogarth, P.M. & Pietersz, G.A. Fc receptor-targeted therapies for the treatment of inflammation, cancer and beyond. *Nat. Rev. Drug Discov.* **11**, 311-331 (2012).

28. Kuo, T.T. *et al.* N-glycan moieties in neonatal Fc receptor determine steady-state membrane distribution and directional transport of IgG. *J. Biol. Chem.* **284**, 8292-8300 (2009).

29. Roopenian, D.C. & Akilesh, S. FcRn: the neonatal Fc receptor comes of age. *Nat. Rev. Immunol.* **7**, 715-725 (2007).

30. Kuo, T.T. *et al.* Neonatal Fc receptor: from immunity to therapeutics. *J. Clin. Immunol.* **30**, 777-789 (2010).

31. Chaudhury, C. *et al.* The major histocompatibility complex-related Fc receptor for IgG (FcRn) binds albumin and prolongs its lifespan. *J. Exp. Med.* **197**, 315-322 (2003).

32. Andersen, J.T., Dee Qian, J. & Sandlie, I. The conserved histidine 166 residue of the human neonatal Fc receptor heavy chain is critical for the pH-dependent binding to albumin. *Eur. J. Immunol.* **36**, 3044-3051 (2006).

33. Oganesyan, V. *et al.* Structural insights into neonatal Fc receptor-based recycling mechanisms. *J. Biol. Chem.* **289**, 7812-7824 (2014).

34. Akilesh, S. *et al.* Podocytes use FcRn to clear IgG from the glomerular basement membrane. *Proc. Natl. Acad. Sci. USA* **105**, 967-972 (2008).

35. Sarav, M. *et al.* Renal FcRn reclaims albumin but facilitates elimination of IgG. *J. Am. Soc. Nephrol.* **20**, 1941-1952 (2009).

36. Qiao, S.W. *et al.* Dependence of antibody-mediated presentation of antigen on FcRn. *Proc. Natl. Acad. Sci. USA* **105**, 9337-9342 (2008).

37. Baker, K. *et al.* Neonatal Fc receptor for IgG (FcRn) regulates cross-presentation of IgG immune complexes by $CD8^{-}CD11b^{+}$ dendritic cells. *Proc. Natl. Acad. Sci. USA* **108**, 9927-9932 (2011).

38. Naparstek, Y. & Plotz, P.H. The role of autoantibodies in autoimmune disease. *Annu. Rev. Immunol.* **11**, 79-104 (1993).

39. Chan, A.C. & Carter, P.J. Therapeutic antibodies for autoimmunity and inflammation. *Nat. Rev. Immunol.* **10**, 301-316 (2010).

40. Scott, A.M., Wolchok, J.D. & Old, L.J. Antibody therapy of cancer. *Nat. Rev. Cancer* **12**, 278-287 (2012).

41. Claypool, S.M., Dickinson, B.L., Yoshida, M., Lencer, W.I. & Blumberg, R.S. Functional reconstitution of human FcRn in Madin-Darby canine kidney cells requires co-expressed human β2-microglobulin. *J. Biol. Chem.* **277**, 28038-28050 (2002).

42. Martin, W.L., West, A.P., Jr., Gan, L. & Bjorkman, P.J. Crystal structure at 2.8 Å of an FcRn/heterodimeric Fc complex: mechanism of pH dependent binding. *Mol. Cell* **7**, 867-877 (2001).

43. Raghavan, M., Bonagura, V.R., Morrison, S.L. & Bjorkman, P.J. Analysis of the pH dependence of the neonatal Fc receptor/immunoglobulin G interaction using antibody and receptor variants. *Biochemistry* **34**, 14649-14657 (1995).

44. Shields, R.L. *et al.* High resolution mapping of the binding site on human IgG1 for FcγRI, FcγRII, FcγRIII, and FcRn and design of IgG1 variants with improved binding to the FcγR. *J. Biol. Chem.* **276**, 6591-6604 (2001).

45. Kim, J.K. *et al.* Mapping the site on human IgG for binding of the MHC class I-related receptor, FcRn. *Eur. J. Immunol.* **29**, 2819-2825 (1999).

46. Medesan, C., Matesoi, D., Radu, C., Ghetie, V. & Ward, E.S. Delineation of the amino acid residues involved in transcytosis and catabolism of mouse IgG1. *J. Immunol.* **158**, 2211-2217 (1997).

47. Sanchez, L.M., Penny, D.M. & Bjorkman, P.J. Stoichiometry of the interaction between the major histocompatibility complex-related Fc receptor and its Fc ligand. *Biochemistry* **38**, 9471-9476 (1999).

48. Schuck, P., Radu, C.G. & Ward, E.S. Sedimentation equilibrium analysis of recombinant mouse FcRn with murine IgG1. *Mol. Immunol.* **36**, 1117-1125 (1999).

49. Raghavan, M., Gastinel, L.N. & Bjorkman, P.J. The class I major histocompatibility complex related Fc receptor shows pH-dependent stability differences correlating with immunoglobulin binding and release. *Biochemistry* **32**, 8654-8660 (1993).

50. Popov, S. *et al.* The stoichiometry and affinity of the interaction of murine Fc fragments with the MHC class I-related receptor, FcRn. *Mol. Immunol.* **33**, 521-530 (1996).

51. Newton, E.E., Wu, Z. & Simister, N.E. Characterization of basolateral-targeting signals in the neonatal Fc receptor. *J. Cell Sci.* **118**, 2461-2469 (2005).

52. Dickinson, B.L. *et al.* Ca^{2+}-dependent calmodulin binding to FcRn affects immunoglobulin G transport in the transcytotic pathway. *Mol. Biol. Cell* **19**, 414-423 (2008).

53. Ober, R.J., Martinez, C., Lai, X., Zhou, J. & Ward, E.S. Exocytosis of IgG as mediated by the receptor, FcRn: An analysis at the single-molecule level. *Proc. Natl. Acad. Sci. USA* **101**, 11076-11081 (2004).

54. Ober, R.J., Martinez, C., Vaccaro, C., Zhou, J. & Ward, E.S. Visualizing the site and dynamics of IgG salvage by the MHC class I-related receptor, FcRn. *J. Immunol.* **172**, 2021-2029 (2004).

55. Prabhat, P. *et al.* Elucidation of intracellular recycling pathways leading to exocytosis of the Fc receptor, FcRn, by using multifocal plane microscopy. *Proc. Natl. Acad. Sci. USA* **104**, 5889-5894 (2007).

56. Gan, Z., Ram, S., Vaccaro, C., Ober, R.J. & Ward, E.S. Analyses of the recycling receptor, FcRn, in live cells reveal novel pathways for lysosomal delivery. *Traffic* **10**, 600-614 (2009).

57. Gan, Z., Ram, S., Ober, R.J. & Ward, E.S. Using multifocal plane microscopy to reveal novel trafficking processes in the recycling pathway. *J. Cell Sci.* **126**, 1176-1188 (2013).

58. Claypool, S.M. *et al.* Bidirectional transepithelial IgG transport by a strongly polarized basolateral membrane Fc-γ receptor. *Mol. Biol. Cell* **15**, 1746-1759 (2004).

59. Tesar, D.B., Tiangco, N.E. & Bjorkman, P.J. Ligand valency affects transcytosis, recycling and intracellular trafficking mediated by the neonatal Fc receptor. *Traffic* **7**, 1127-1142 (2006).

60. Jahn, R., Lang, T. & Sudhof, T.C. Membrane fusion. *Cell* **112**, 519-533 (2003).

61. Miaczynska, M. & Zerial, M. Mosaic organization of the endocytic pathway. *Exp. Cell Res.* **272**, 8-14 (2002).

62. Somsel, R.J. & Wandinger-Ness, A. Rab GTPases coordinate endocytosis. *J. Cell Sci.* **113**, 183-192 (2000).

63. Stenmark, H. Rab GTPases as coordinators of vesicle traffic. *Nat. Rev. Mol. Cell Biol.* **10**, 513-525 (2009).

64. Agola, J.O., Jim, P.A., Ward, H.H., Basuray, S. & Wandinger-Ness, A. Rab GTPases as regulators of endocytosis, targets of disease and therapeutic opportunities. *Clin. Genet.* **80**, 305-318 (2011).

65. Hammer, J.A., 3rd & Sellers, J.R. Walking to work: roles for class V myosins as cargo transporters. *Nat. Rev. Mol. Cell Biol.* **13**, 13-26 (2012).

66. Ward, E.S. *et al.* From sorting endosomes to exocytosis: association of Rab4 and Rab11 GTPases with the Fc receptor, FcRn, during recycling. *Mol. Biol. Cell* **16**, 2028-2038 (2005).

67. Tzaban, S. *et al.* The recycling and transcytotic pathways for IgG transport by FcRn are distinct and display an inherent polarity. *J. Cell Biol.* **185**, 673-684 (2009).

68. Dati, F. *et al.* Consensus of a group of professional societies and diagnostic companies on guidelines for interim reference ranges for 14 proteins in serum based on the standardization against the IFCC/BCR/CAP Reference Material (CRM 470). International Federation of Clinical Chemistry. Community Bureau of Reference of the Commission of the European Communities. College of American Pathologists. *Eur. J. Clin. Chem. Clin. Biochem.* **34**, 517-520 (1996).

69. Spiegelberg, H.L. & Fishkin, B.G. The catabolism of human G immunoglobulins of different heavy chain subclasses. 3. The catabolism of heavy chain disease proteins and of Fc fragments of myeloma proteins. *Clin. Exp. Immunol.* **10**, 599-607 (1972).

70. Vieira, P. & Rajewsky, K. The half-lives of serum immunoglobulins in adult mice. *Eur. J. Immunol.* **18**, 313-316 (1988).

71. Ghetie, V. *et al.* Abnormally short serum half-lives of IgG in β2-microglobulin-deficient mice. *Eur. J. Immunol.* **26**, 690-696 (1996).

72. Junghans, R.P. & Anderson, C.L. The protection receptor for IgG catabolism is the β_2-microglobulin-containing neonatal intestinal transport receptor. *Proc. Natl. Acad. Sci. USA* **93**, 5512-5516 (1996).

73. Israel, E.J., Wilsker, D.F., Hayes, K.C., Schoenfeld, D. & Simister, N.E. Increased clearance of IgG in mice that lack β_2-microglobulin: possible protective role of FcRn. *Immunology* **89**, 573-578 (1996).

74. Roopenian, D.C. *et al.* The MHC class I-like IgG receptor controls perinatal IgG transport, IgG homeostasis, and fate of IgG-Fc-coupled drugs. *J. Immunol.* **170**, 3528-3533 (2003).

75. Wani, M.A. *et al.* Familial hypercatabolic hypoproteinemia caused by deficiency of the neonatal Fc receptor, FcRn, due to a mutant β_2-microglobulin gene. *Proc. Natl. Acad. Sci. USA* **103**, 5084-5089 (2006).

76. Antohe, F., Radulescu, L., Gafencu, A., Ghetie, V. & Simionescu, M. Expression of functionally active FcRn and the differentiated bidirectional transport of IgG in human placental endothelial cells. *Hum. Immunol.* **62**, 93-105 (2001).

77. Powner, M.B., McKenzie, J.A., Christianson, G.J., Roopenian, D.C. & Fruttiger, M. Expression of Neonatal Fc Receptor in the eye. *Invest. Ophthalmol. Vis. Sci.* **55**, 1607-1615 (2014).

78. van Bilsen, K. *et al.* The neonatal Fc receptor is expressed by human lymphocytes. *J. Transl. Med.* **8**, P1 (2010).

79. Cauza, K. *et al.* Expression of FcRn, the MHC class I-related receptor for IgG, in human keratinocytes. *J. Invest. Dermatol.* **124**, 132-139 (2005).

80. Andersen, J.T. *et al.* Anti-carcinoembryonic antigen single-chain variable fragment antibody variants bind mouse and human neonatal Fc receptor with different affinities that reveal distinct cross-species differences in serum half-life. *J. Biol. Chem.* **287**, 22927-22937 (2012).

81. Israel, E.J. *et al.* Expression of the neonatal Fc receptor, FcRn, on human intestinal epithelial cells. *Immunology* **92**, 69-74 (1997).

82. Dickinson, B.L. *et al.* Bidirectional FcRn-dependent IgG transport in a polarized human intestinal epithelial cell line. *J. Clin. Invest.* **104**, 903-911 (1999).

83. Cianga, P., Cianga, C., Cozma, L., Ward, E.S. & Carasevici, E. The MHC class I related Fc receptor, FcRn, is expressed in the epithelial cells of the human mammary gland. *Hum. Immunol.* **64**, 1152-1159 (2003).

84. Haymann, J.P. *et al.* Characterization and localization of the neonatal Fc receptor in adult human kidney. *J. Am. Soc. Nephrol.* **11**, 632-639 (2000).

85. Spiekermann, G.M. *et al.* Receptor-mediated immunoglobulin G transport across mucosal barriers in adult life: functional expression of FcRn in the mammalian lung. *J. Exp. Med.* **196**, 303-310 (2002).

86. Li, Z. *et al.* Transfer of IgG in the female genital tract by MHC class I-related neonatal Fc receptor (FcRn) confers protective immunity to vaginal infection. *Proc. Natl. Acad. Sci. USA* **108**, 4388-4393 (2011).

87. Kim, H. *et al.* Mapping of the neonatal Fc receptor in the rodent eye. *Invest. Ophthalmol. Vis. Sci.* **49**, 2025-2029 (2008).

88. Rath, T. *et al.* Fc-fusion proteins and FcRn: structural insights for longer-lasting and more effective therapeutics. *Crit. Rev. Biotechnol.* **35**, 235-254 (2013).

89. Kuo, T.T. & Aveson, V.G. Neonatal Fc receptor and IgG-based therapeutics. *MAbs* **3**, 422-430 (2011).

90. Desoubeaux, G., Daguet, A. & Watier, H. Therapeutic antibodies and infectious diseases, Tours, France, November 20-22, 2012. *MAbs* **5**, 626-632 (2013).

91. Gatta, A., Verardo, A. & Bolognesi, M. Hypoalbuminemia. *Intern. Emerg. Med.* **7**, 193-199 (2012).

92. Kobayashi, K. *et al.* An FcRn-dependent role for anti-flagellin immunoglobulin G in pathogenesis of colitis in mice. *Gastroenterology* **137**, 1746-1756 (2009).

93. Liu, X. *et al.* NF-κB signaling regulates functional expression of the MHC class I-related neonatal Fc receptor for IgG via intronic binding sequences. *J. Immunol.* **179**, 2999-3011 (2007).

94. Liu, X. *et al.* Activation of the JAK/STAT-1 signaling pathway by IFN-γ can down-regulate functional expression of the MHC class I-related neonatal Fc receptor for IgG. *J. Immunol.* **181**, 449-463 (2008).

95. Medesan, C., Radu, C., Kim, J.K., Ghetie, V. & Ward, E.S. Localization of the site of the IgG molecule that regulates maternofetal transmission in mice. *Eur. J. Immunol.* **26**, 2533-2536 (1996).

96. Appleby, P. & Catty, D. Transmission of immunoglobulin to foetal and neonatal mice. *J. Reprod. Immunol.* **5**, 203-213 (1983).

97. Jones, E.A. & Waldmann, T.A. The mechanism of intestinal uptake and transcellular transport of IgG in the neonatal rat. *J. Clin. Invest.* **51**, 2916-2927 (1972).

98. Rodewald, R. & Abrahamson, D.R. Receptor-mediated transport of IgG across the intestinal epithelium of the neonatal rat. *Ciba. Found. Symp.* **92,** 209-232 (1982).

99. Rodewald, R. & Kraehenbuhl, J.P. Receptor-mediated transport of IgG. *J. Cell Biol.* **99**, 159s-164s (1984).

100. Martin, M.G., Wu, S.V. & Walsh, J.H. Ontogenetic development and distribution of antibody transport and Fc receptor mRNA expression in rat intestine. *Dig. Dis. Sci.* **42**, 1062-1069 (1997).

101. Salimonu, L.S., Ladipo, O.A., Adeniran, S.O. & Osukoya, B.O. Serum immunoglobulin levels in normal, premature and postmature newborns and their mothers. *Int. J. Gynaecol. Obstet.* **16**, 119-123 (1978).

102. Leach, J.L. *et al.* Isolation from human placenta of the IgG transporter, FcRn, and localization to the syncytiotrophoblast: implications for maternal-fetal antibody transport. *J. Immunol.* **157**, 3317-3322 (1996).

103. Simister, N.E., Story, C.M., Chen, H.L. & Hunt, J.S. An IgG-transporting Fc receptor expressed in the syncytiotrophoblast of human placenta. *Eur. J. Immunol.* **26**, 1527-1531 (1996).

104. Firan, M. *et al.* The MHC class I related receptor, FcRn, plays an essential role in the maternofetal transfer of gammaglobulin in humans. *Int. Immunol.* **13**, 993-1002 (2001).

105. Fox, S.I. *Human physiology*, 12 edn. McGraw-Hill: New York, NY, 2011.

106. Pavenstadt, H., Kriz, W. & Kretzler, M. Cell biology of the glomerular podocyte. *Physiol. Rev.* **83**, 253-307 (2003).

107. Wartiovaara, J. *et al.* Nephrin strands contribute to a porous slit diaphragm scaffold as revealed by electron tomography. *J. Clin. Invest.* **114**, 1475-1483 (2004).

108. Russo, L.M. *et al.* The normal kidney filters nephrotic levels of albumin retrieved by proximal tubule cells: retrieval is disrupted in nephrotic states. *Kidney Int.* **71**, 504-513 (2007).

109. Kobayashi, N. *et al.* FcRn-mediated transcytosis of immunoglobulin G in human renal proximal tubular epithelial cells. *Am. J. Physiol. Renal Physiol.* **282**, F358-F365 (2002).

110. Neefjes, J., Jongsma, M.L., Paul, P. & Bakke, O. Towards a systems understanding of MHC class I and MHC class II antigen presentation. *Nat. Rev. Immunol.* **11**, 823-836 (2011).

111. Joffre, O.P., Segura, E., Savina, A. & Amigorena, S. Cross-presentation by dendritic cells. *Nat. Rev. Immunol.* **12**, 557-569 (2012).

112. Schuette, V. & Burgdorf, S. The ins-and-outs of endosomal antigens for cross-presentation. *Curr. Opin. Immunol.* **26**, 63-68 (2014).

113. Kurts, C., Robinson, B.W. & Knolle, P.A. Cross-priming in health and disease. *Nat. Rev. Immunol.* **10**, 403-414 (2010).

114. Asano, K. *et al.* CD169-positive macrophages dominate antitumor immunity by crosspresenting dead cell-associated antigens. *Immunity* **34**, 85-95 (2011).

115. Houde, M. *et al.* Phagosomes are competent organelles for antigen cross-presentation. *Nature* **425**, 402-406 (2003).

116. Guilliams, M., Bruhns, P., Saeys, Y., Hammad, H. & Lambrecht, B.N. The function of Fcγ receptors in dendritic cells and macrophages. *Nat. Rev. Immunol.* **14**, 94-108 (2014).

117. Simmons, D.P. *et al.* Type I IFN drives a distinctive dendritic cell maturation phenotype that allows continued class II MHC synthesis and antigen processing. *J. Immunol.* **188**, 3116-3126 (2012).

118. Ye, L. *et al.* The MHC class II-associated invariant chain interacts with the neonatal Fcγ receptor and modulates its trafficking to endosomal/lysosomal compartments. *J. Immunol.* **181**, 2572-2585 (2008).

119. Hildner, K. *et al.* Batf3 deficiency reveals a critical role for $CD8\alpha^+$ dendritic cells in cytotoxic T cell immunity. *Science* **322**, 1097-1100 (2008).

120. Reichert, J.M. Which are the antibodies to watch in 2013? *MAbs* **5**, 1-4 (2013).

121. Mahmud, N., Klipa, D. & Ahsan, N. Antibody immunosuppressive therapy in solid-organ transplant: Part I. *MAbs* **2**, 148-156 (2010).

122. Ghetie, V. *et al.* Increasing the serum persistence of an IgG fragment by random mutagenesis. *Nat. Biotechnol.* **15**, 637-640 (1997).

123. Dall'Acqua, W.F., Kiener, P.A. & Wu, H. Properties of human IgG1s engineered for enhanced binding to the neonatal Fc receptor (FcRn). *J. Biol. Chem.* **281**, 23514-23524 (2006).

124. Hinton, P.R. *et al.* Engineered human IgG antibodies with longer serum half-lives in primates. *J. Biol. Chem.* **279**, 6213-6216 (2004).

125. Hinton, P.R. *et al.* An engineered human IgG1 antibody with longer serum half-life. *J. Immunol.* **176**, 346-356 (2006).

126. Yeung, Y.A. *et al.* Engineering human IgG1 affinity to human neonatal Fc receptor: impact of affinity improvement on pharmacokinetics in primates. *J. Immunol.* **182**, 7663-7671 (2009).

127. Vaccaro, C., Bawdon, R., Wanjie, S., Ober, R.J. & Ward, E.S. Divergent activities of an engineered antibody in murine and human systems have implications for therapeutic antibodies. *Proc. Natl. Acad. Sci. USA* **103**, 18709-18714 (2006).

128. Zalevsky, J. *et al.* Enhanced antibody half-life improves *in vivo* activity. *Nat. Biotechnol.* **28**, 157-159 (2010).

129. Dall'Acqua, W. *et al.* Increasing the affinity of a human IgG1 to the neonatal Fc receptor: biological consequences. *J. Immunol.* **169**, 5171-5180 (2002).

130. Sherer, Y., Gorstein, A., Fritzler, M.J. & Shoenfeld, Y. Autoantibody explosion in systemic lupus erythematosus: more than 100 different antibodies found in SLE patients. *Semin. Arthritis Rheum.* **34**, 501-537 (2004).

131. Jarius, S. & Wildemann, B. AQP4 antibodies in neuromyelitis optica: diagnostic and pathogenetic relevance. *Nat. Rev. Neurol.* **6**, 383-392 (2010).

132. Conti-Fine, B.M., Milani, M. & Kaminski, H.J. Myasthenia gravis: past, present, and future. *J. Clin. Invest.* **116**, 2843-2854 (2006).

133. Popescu, B.F. & Lucchinetti, C.F. Pathology of demyelinating diseases. *Annu. Rev. Pathol.* **7**, 185-217 (2012).

134. Colvin, R.B. & Smith, R.N. Antibody-mediated organ-allograft rejection. *Nat. Rev. Immunol.* **5**, 807-817 (2005).

135. Winters, J.L. Plasma exchange: concepts, mechanisms, and an overview of the American Society for Apheresis guidelines. *Hematology Am. Soc. Hematol. Educ. Program* **2012**, 7-12 (2012).

136. Orange, J.S. *et al.* Use of intravenous immunoglobulin in human disease: a review of evidence by members of the Primary Immunodeficiency Committee of the American Academy of Allergy, Asthma and Immunology. *J. Allergy Clin. Immunol.* **117**, S525-S553 (2006).

137. Winters, J.L., Brown, D., Hazard, E., Chainani, A. & Andrzejewski, C., Jr. Cost-minimization analysis of the direct costs of TPE and IVIg in the treatment of Guillain-Barre syndrome. *BMC Health Serv. Res.* **11**, 101 (2011).

138. Heatwole, C., Johnson, N., Holloway, R. & Noyes, K. Plasma exchange versus intravenous immunoglobulin for myasthenia gravis crisis: an acute hospital cost comparison study. *J. Clin. Neuromuscul. Dis.* **13**, 85-94 (2011).

139. Li, N. *et al.* Complete FcRn dependence for intravenous Ig therapy in autoimmune skin blistering diseases. *J. Clin. Invest.* **115**, 3440-3450 (2005).

140. Hansen, R.J. & Balthasar, J.P. Effects of intravenous immunoglobulin on platelet count and antiplatelet antibody disposition in a rat model of immune thrombocytopenia. *Blood* **100**, 2087-2093 (2002).

141. Patel, D.A. *et al.* Neonatal Fc receptor blockade by Fc engineering ameliorates arthritis in a murine model. *J. Immunol.* **187**, 1015-1022 (2011).

142. Challa, D.K. *et al.* Autoantibody depletion ameliorates disease in murine experimental autoimmune encephalomyelitis. *MAbs* **5**, 655-659 (2013).

143. Swiercz, R. *et al.* Use of Fc-engineered antibodies as clearing agents to increase contrast during PET. *J. Nucl. Med.* **55**, 1204-1207 (2014).

144. Getman, K.E. & Balthasar, J.P. Pharmacokinetic effects of 4C9, an anti-FcRn antibody, in rats: implications for the use of FcRn inhibitors for the treatment of humoral autoimmune and alloimmune conditions. *J. Pharm. Sci.* **94**, 718-729 (2005).

145. Christianson, G.J. *et al.* Monoclonal antibodies directed against human FcRn and their applications. *MAbs* **4**, 208-216 (2012).

146. Liu, L. *et al.* Amelioration of experimental autoimmune myasthenia gravis in rats by neonatal FcR blockade. *J. Immunol.* **178**, 5390-5398 (2007).

147. Mezo, A.R. *et al.* Reduction of IgG in nonhuman primates by a peptide antagonist of the neonatal Fc receptor FcRn. *Proc. Natl. Acad. Sci. USA* **105**, 2337-2342 (2008).

148. Mezo, A.R., Low, S.C., Hoehn, T. & Palmieri, H. PEGylation enhances the therapeutic potential of peptide antagonists of the neonatal Fc receptor, FcRn. *Bioorg. Med. Chem. Lett.* **21**, 6332-6335 (2011).

149. Hafler, D.A. *et al.* Multiple sclerosis. *Immunol. Rev.* **204**, 208-231 (2005).

150. Milo, R. & Miller, A. Revised diagnostic criteria of multiple sclerosis. *Autoimmun. Rev.* **13**, 518-524 (2014).

151. Whitacre, C.C. Sex differences in autoimmune disease. *Nat. Immunol.* **2**, 777-780 (2001).

152. Ngo, S.T., Steyn, F.J. & McCombe, P.A. Gender differences in autoimmune disease. *Front. Neuroendocrinol.* **35**, 347-369 (2014).

153. Compston, A. & Coles, A. Multiple sclerosis. *Lancet* **372**, 1502-1517 (2008).

154. Ramagopalan, S.V., Dobson, R., Meier, U.C. & Giovannoni, G. Multiple sclerosis: risk factors, prodromes, and potential causal pathways. *Lancet Neurol.* **9**, 727-739 (2010).

155. Miller, D., Barkhof, F., Montalban, X., Thompson, A. & Filippi, M. Clinically isolated syndromes suggestive of multiple sclerosis, part I: natural history, pathogenesis, diagnosis, and prognosis. *Lancet Neurol.* **4**, 281-288 (2005).

156. Lublin, F.D. *et al.* Defining the clinical course of multiple sclerosis: the 2013 revisions. *Neurology* **83**, 278-286 (2014).

157. Weinshenker, B.G. *et al.* The natural history of multiple sclerosis: a geographically based study I. Clinical course and disability. *Brain* **112**, 133-146 (1989).

158. Hu, W. & Lucchinetti, C.F. The pathological spectrum of CNS inflammatory demyelinating diseases. *Semin. Immunopathol.* **31**, 439-453 (2009).

159. Hermans, G. *et al.* Cytokine profile of myelin basic protein-reactive T cells in multiple sclerosis and healthy individuals. *Ann. Neurol.* **42**, 18-27 (1997).

160. Ota, K. *et al.* T-cell recognition of an immunodominant myelin basic protein epitope in multiple sclerosis. *Nature* **346**, 183-187 (1990).

161. Burns, J., Rosenzweig, A., Zweiman, B. & Lisak, R.P. Isolation of myelin basic protein-reactive T-cell lines from normal human blood. *Cell. Immunol.* **81**, 435-440 (1983).

162. Pette, M. *et al.* Myelin basic protein-specific T lymphocyte lines from MS patients and healthy individuals. *Neurology* **40**, 1770-1776 (1990).

163. Scholz, C., Patton, K.T., Anderson, D.E., Freeman, G.J. & Hafler, D.A. Expansion of autoreactive T cells in multiple sclerosis is independent of exogenous B7 costimulation. *J. Immunol.* **160**, 1532-1538 (1998).

164. Zhang, J. *et al.* Increased frequency of interleukin 2-responsive T cells specific for myelin basic protein and proteolipid protein in peripheral blood and cerebrospinal fluid of patients with multiple sclerosis. *J. Exp. Med.* **179**, 973-984 (1994).

165. Harkiolaki, M. *et al.* T cell-mediated autoimmune disease due to low-affinity crossreactivity to common microbial peptides. *Immunity* **30**, 348-357 (2009).

166. Tejada-Simon, M.V., Zang, Y.C., Hong, J., Rivera, V.M. & Zhang, J.Z. Cross-reactivity with myelin basic protein and human herpesvirus-6 in multiple sclerosis. *Ann. Neurol.* **53**, 189-197 (2003).

167. Wucherpfennig, K.W. & Strominger, J.L. Molecular mimicry in T cell-mediated autoimmunity: viral peptides activate human T cell clones specific for myelin basic protein. *Cell* **80**, 695-705 (1995).

168. Ji, Q., Perchellet, A. & Goverman, J.M. Viral infection triggers central nervous system autoimmunity via activation of $CD8^+$ T cells expressing dual TCRs. *Nat. Immunol.* **11**, 628-634 (2010).

169. Shechter, R., London, A. & Schwartz, M. Orchestrated leukocyte recruitment to immune-privileged sites: absolute barriers versus educational gates. *Nat. Rev. Immunol.* **13**, 206-218 (2013).

170. Metz, I. *et al.* Pathologic heterogeneity persists in early active multiple sclerosis lesions. *Ann. Neurol.* **75**, 728-738 (2014).

171. Link, H. & Huang, Y.M. Oligoclonal bands in multiple sclerosis cerebrospinal fluid: an update on methodology and clinical usefulness. *J. Neuroimmunol.* **180**, 17-28 (2006).

172. Chu, A.B. *et al.* Oligoclonal IgG bands in cerebrospinal fluid in various neurological diseases. *Ann. Neurol.* **13**, 434-439 (1983).

173. Owens, G.P. *et al.* Restricted use of VH4 germline segments in an acute multiple sclerosis brain. *Ann. Neurol.* **43**, 236-243 (1998).

174. Baranzini, S.E. *et al.* B cell repertoire diversity and clonal expansion in multiple sclerosis brain lesions. *J. Immunol.* **163**, 5133-5144 (1999).

175. Owens, G.P. *et al.* VH4 gene segments dominate the intrathecal humoral immune response in multiple sclerosis. *J. Immunol.* **179**, 6343-6351 (2007).

176. Winges, K.M. *et al.* Analysis of multiple sclerosis cerebrospinal fluid reveals a continuum of clonally related antibody-secreting cells that are predominantly plasma blasts. *J. Neuroimmunol.* **192**, 226-234 (2007).

177. Qin, Y. *et al.* Clonal expansion and somatic hypermutation of V(H) genes of B cells from cerebrospinal fluid in multiple sclerosis. *J. Clin. Invest.* **102**, 1045-1050 (1998).

178. Frischer, J.M. *et al.* The relation between inflammation and neurodegeneration in multiple sclerosis brains. *Brain* **132**, 1175-1189 (2009).

179. Zhou, D. *et al.* Identification of a pathogenic antibody response to native myelin oligodendrocyte glycoprotein in multiple sclerosis. *Proc. Natl. Acad. Sci. USA* **103**, 19057-19062 (2006).

180. Lalive, P.H. *et al.* Antibodies to native myelin oligodendrocyte glycoprotein are serologic markers of early inflammation in multiple sclerosis. *Proc. Natl. Acad. Sci. USA* **103**, 2280-2285 (2006).

181. O'Connor, K.C. *et al.* Myelin basic protein-reactive autoantibodies in the serum and cerebrospinal fluid of multiple sclerosis patients are characterized by low-affinity interactions. *J. Neuroimmunol.* **136**, 140-148 (2003).

182. Fraussen, J., Claes, N., de Bock, L. & Somers, V. Targets of the humoral autoimmune response in multiple sclerosis. *Autoimmun. Rev.* **13**, 1126-1137 (2014).

183. Weinshenker, B.G. Plasma exchange for severe attacks of inflammatory demyelinating diseases of the central nervous system. *J. Clin. Apher.* **16**, 39-42 (2001).

184. Trebst, C., Reising, A., Kielstein, J.T., Hafer, C. & Stangel, M. Plasma exchange therapy in steroid-unresponsive relapses in patients with multiple sclerosis. *Blood Purif.* **28**, 108-115 (2009).

185. Koziolek, M.J. *et al.* Immunoadsorption therapy in patients with multiple sclerosis with steroid-refractory optical neuritis. *J. Neuroinflammation* **9**, 80 (2012).

186. Heigl, F. *et al.* Immunoadsorption in steroid-refractory multiple sclerosis: clinical experience in 60 patients. *Atheroscler. Suppl.* **14**, 167-173 (2013).

187. Keegan, M. *et al.* Relation between humoral pathological changes in multiple sclerosis and response to therapeutic plasma exchange. *Lancet* **366**, 579-582 (2005).

188. Zettl, U.K. *et al.* Lesion pathology predicts response to plasma exchange in secondary progressive MS. *Neurology* **67**, 1515-1516 (2006).

189. Pedotti, R. *et al.* Exacerbation of experimental autoimmune encephalomyelitis by passive transfer of IgG antibodies from a multiple sclerosis patient responsive to immunoadsorption. *J. Neuroimmunol.* **262**, 19-26 (2013).

190. Johns, T.G. & Bernard, C.C. The structure and function of myelin oligodendrocyte glycoprotein. *J. Neurochem.* **72**, 1-9 (1999).

191. Nave, K.A. & Werner, H.B. Myelination of the nervous system: mechanisms and functions. *Annu. Rev. Cell Dev. Biol.* **30**, 503-533 (2014).

192. Pollinger, B. *et al.* Spontaneous relapsing-remitting EAE in the SJL/J mouse: MOG-reactive transgenic T cells recruit endogenous MOG-specific B cells. *J. Exp. Med.* **206**, 1303-1316 (2009).

193. Petkova, S.B. *et al.* Enhanced half-life of genetically engineered human IgG1 antibodies in a humanized FcRn mouse model: potential application in humorally mediated autoimmune disease. *Int. Immunol.* **18**, 1759-1769 (2006).

194. Bansal, P. *et al.* The encephalitogenic, human myelin oligodendrocyte glycoprotein-induced antibody repertoire is directed toward multiple epitopes in C57BL/6-immunized mice. *J. Immunol.* **191**, 1091-1101 (2013).

195. Lyons, J.A., Ramsbottom, M.J. & Cross, A.H. Critical role of antigen-specific antibody in experimental autoimmune encephalomyelitis induced by recombinant myelin oligodendrocyte glycoprotein. *Eur. J. Immunol.* **32**, 1905-1913 (2002).

196. Linnington, C., Webb, M. & Woodhams, P.L. A novel myelin-associated glycoprotein defined by a mouse monoclonal antibody. *J. Neuroimmunol.* **6**, 387-396 (1984).

197. Schluesener, H.J., Sobel, R.A., Linington, C. & Weiner, H.L. A monoclonal antibody against a myelin oligodendrocyte glycoprotein induces relapses and demyelination in central nervous system autoimmune disease. *J. Immunol.* **139**, 4016-4021 (1987).

198. Amit, A.G., Mariuzza, R.A., Phillips, S.E. & Poljak, R.J. Three-dimensional structure of an antigen-antibody complex at 2.8 Å resolution. *Science* **233**, 747-753 (1986).

199. Nimmerjahn, F. & Ravetch, J.V. Anti-inflammatory actions of intravenous immunoglobulin. *Annu. Rev. Immunol.* **26**, 513-533 (2008).

200. Baerenwaldt, A., Biburger, M. & Nimmerjahn, F. Mechanisms of action of intravenous immunoglobulins. *Expert Rev. Clin. Immunol.* **6**, 425-434 (2010).

201. Haas, J., Maas-Enriquez, M. & Hartung, H.P. Intravenous immunoglobulins in the treatment of relapsing remitting multiple sclerosis--results of a retrospective multicenter observational study over five years. *Mult. Scler.* **11**, 562-567 (2005).

202. Hershko, A.Y. & Naparstek, Y. Removal of pathogenic autoantibodies by immunoadsorption. *Ann. NY Acad. Sci.* **1051**, 635-646 (2005).

203. Bleeker, W.K., Teeling, J.L. & Hack, C.E. Accelerated autoantibody clearance by intravenous immunoglobulin therapy: studies in experimental models to determine the magnitude and time course of the effect. *Blood* **98**, 3136-3142 (2001).

204. Bayry, J., Kazatchkine, M.D. & Kaveri, S.V. Shortage of human intravenous immunoglobulin - reasons and possible solutions. *Nat. Clin. Pract. Neurol.* **3**, 120-121 (2007).

205. Zhang, Y.Y. *et al.* Comparison of double filtration plasmapheresis with immunoadsorption therapy in patients with anti-glomerular basement membrane nephritis. *BMC Nephrol.* **15**, 128 (2014).

206. Yeh, J.H., Chen, W.H. & Chiu, H.C. Complications of double-filtration plasmapheresis. *Transfusion* **44**, 1621-1625 (2004).

207. Kronbichler, A., Brezina, B., Quintana, L.F. & Jayne, D.R. Efficacy of plasma exchange and immunoadsorption in systemic lupus erythematosus and antiphospholipid syndrome: A systematic review. *Autoimmun. Rev.* **15**, 38-49 (2016).

208. Hauser, S.L. *et al.* B-cell depletion with rituximab in relapsing-remitting multiple sclerosis. *N. Engl. J. Med.* **358**, 676-688 (2008).

209. Cross, A.H., Stark, J.L., Lauber, J., Ramsbottom, M.J. & Lyons, J.A. Rituximab reduces B cells and T cells in cerebrospinal fluid of multiple sclerosis patients. *J. Neuroimmunol.* **180**, 63-70 (2006).

210. Cross, A.H., Klein, R.S. & Piccio, L. Rituximab combination therapy in relapsing multiple sclerosis. *Ther. Adv. Neurol. Disord.* **5**, 311-319 (2012).

211. Huang, H., Benoist, C. & Mathis, D. Rituximab specifically depletes short-lived autoreactive plasma cells in a mouse model of inflammatory arthritis. *Proc. Natl. Acad. Sci. USA* **107**, 4658-4663 (2010).

212. Kappos, L. *et al.* Ocrelizumab in relapsing-remitting multiple sclerosis: a phase 2, randomised, placebo-controlled, multicentre trial. *Lancet* **378**, 1779-1787 (2011).

213. Marta, C.B., Oliver, A.R., Sweet, R.A., Pfeiffer, S.E. & Ruddle, N.H. Pathogenic myelin oligodendrocyte glycoprotein antibodies recognize glycosylated epitopes and perturb oligodendrocyte physiology. *Proc. Natl. Acad. Sci. USA* **102**, 13992-13997 (2005).

214. Kinzel, S. *et al.* Myelin-reactive antibodies initiate T cell-mediated CNS autoimmune disease by opsonization of endogenous antigen. *Acta Neuropathol.* **132**, 43-58 (2016).

215. Flach, A.C. *et al.* Autoantibody-boosted T-cell reactivation in the target organ triggers manifestation of autoimmune CNS disease. *Proc. Natl. Acad. Sci. USA* **113**, 3323-3328 (2016).

216. Foote, J. & Winter, G. Antibody framework residues affecting the conformation of the hypervariable loops. *J. Mol. Biol.* **224**, 487-499 (1992).

217. Breithaupt, C. *et al.* Structural insights into the antigenicity of myelin oligodendrocyte glycoprotein. *Proc. Natl. Acad. Sci. USA* **100**, 9446-9451 (2003).

218. Lyons, J.A., San, M., Happ, M.P. & Cross, A.H. B cells are critical to induction of experimental allergic encephalomyelitis by protein but not by a short encephalitogenic peptide. *Eur. J. Immunol.* **29**, 3432-3439 (1999).

219. Radu, C.G., Anderton, S.M., Firan, M., Wraith, D.C. & Ward, E.S. Detection of autoreactive T cells in H-2^{u} mice using peptide-MHC multimers. *Int. Immunol.* **12**, 1553-1560 (2000).

220. Kim, J.K., Tsen, M.F., Ghetie, V. & Ward, E.S. Localization of the site of the murine IgG1 molecule that is involved in binding to the murine intestinal Fc receptor. *Eur. J. Immunol.* **24**, 2429-2434 (1994).

221. English, C. & Aloi, J.J. New FDA-Approved Disease-Modifying Therapies for Multiple Sclerosis. *Clin. Ther.* **37**, 691-715 (2015).

222. Sloan-Lancaster, J. & Allen, P.M. Altered peptide ligand-induced partial T cell activation: molecular mechanisms and role in T cell biology. *Annu. Rev. Immunol.* **14**, 1-27 (1996).

223. Turley, D.M. & Miller, S.D. Prospects for antigen-specific tolerance based therapies for the treatment of multiple sclerosis. *Results Probl. Cell Differ.* **51**, 217-235 (2010).

224. Karin, N., Mitchell, D.J., Brocke, S., Ling, N. & Steinman, L. Reversal of experimental autoimmune encephalomyelitis by a soluble peptide variant of a myelin basic protein epitope: T cell receptor antagonism and reduction of interferon gamma and tumor necrosis factor alpha production. *J. Exp. Med.* **180**, 2227-2237 (1994).

225. Gaur, A. *et al.* Amelioration of relapsing experimental autoimmune encephalomyelitis with altered myelin basic protein peptides involves different cellular mechanisms. *J. Neuroimmunol.* **74**, 149-158 (1997).

226. Nicholson, L.B., Greer, J.M., Sobel, R.A., Lees, M.B. & Kuchroo, V.K. An altered peptide ligand mediates immune deviation and prevents autoimmune encephalomyelitis. *Immunity* **3**, 397-405 (1995).

227. Brocke, S. *et al.* Treatment of experimental encephalomyelitis with a peptide analogue of myelin basic protein. *Nature* **379**, 343-346 (1996).

228. Bielekova, B. *et al.* Encephalitogenic potential of the myelin basic protein peptide (amino acids 83-99) in multiple sclerosis: results of a phase II clinical trial with an altered peptide ligand. *Nat. Med.* **6**, 1167-1175 (2000).

229. Kappos, L. *et al.* Induction of a non-encephalitogenic type 2 T helper-cell autoimmune response in multiple sclerosis after administration of an altered peptide ligand in a placebo-controlled, randomized phase II trial. The Altered Peptide Ligand in Relapsing MS Study Group. *Nat. Med.* **6**, 1176-1182 (2000).

230. Bitar, D.M. & Whitacre, C.C. Suppression of experimental autoimmune encephalomyelitis by the oral administration of myelin basic protein. *Cell. Immunol.* **112**, 364-370 (1988).

231. Whitacre, C.C., Gienapp, I.E., Orosz, C.G. & Bitar, D.M. Oral tolerance in experimental autoimmune encephalomyelitis. III. Evidence for clonal anergy. *J. Immunol.* **147**, 2155-2163 (1991).

232. Chen, Y., Kuchroo, V.K., Inobe, J., Hafler, D.A. & Weiner, H.L. Regulatory T cell clones induced by oral tolerance: suppression of autoimmune encephalomyelitis. *Science* **265**, 1237-1240 (1994).

233. Khoury, S.J., Hancock, W.W. & Weiner, H.L. Oral tolerance to myelin basic protein and natural recovery from experimental autoimmune encephalomyelitis are associated with downregulation of inflammatory cytokines and differential upregulation of transforming growth factor β, interleukin 4, and prostaglandin E expression in the brain. *J. Exp. Med.* **176**, 1355-1364 (1992).

234. Miller, A., Lider, O., Roberts, A.B., Sporn, M.B. & Weiner, H.L. Suppressor T cells generated by oral tolerization to myelin basic protein suppress both *in vitro* and *in vivo* immune responses by the release of transforming growth factor β after antigen-specific triggering. *Proc. Natl. Acad. Sci. USA* **89**, 421-425 (1992).

235. Burkhart, C., Liu, G.Y., Anderton, S.M., Metzler, B. & Wraith, D.C. Peptide-induced T cell regulation of experimental autoimmune encephalomyelitis: a role for IL-10. *Int. Immunol.* **11**, 1625-1634 (1999).

236. Karpus, W.J., Kennedy, K.J., Smith, W.S. & Miller, S.D. Inhibition of relapsing experimental autoimmune encephalomyelitis in SJL mice by feeding the immunodominant PLP139-151 peptide. *J. Neurosci. Res.* **45**, 410-423 (1996).

237. Benson, J.M. *et al.* Oral administration of myelin basic protein is superior to myelin in suppressing established relapsing experimental autoimmune encephalomyelitis. *J. Immunol.* **162**, 6247-6254 (1999).

238. Kennedy, K.J., Smith, W.S., Miller, S.D. & Karpus, W.J. Induction of antigen-specific tolerance for the treatment of ongoing, relapsing autoimmune encephalomyelitis: a comparison between oral and peripheral tolerance. *J. Immunol.* **159**, 1036-1044 (1997).

239. Meyer, A.L., Benson, J.M., Gienapp, I.E., Cox, K.L. & Whitacre, C.C. Suppression of murine chronic relapsing experimental autoimmune encephalomyelitis by the oral administration of myelin basic protein. *J. Immunol.* **157**, 4230-4238 (1996).

240. Metzler, B. & Wraith, D.C. Inhibition of experimental autoimmune encephalomyelitis by inhalation but not oral administration of the encephalitogenic peptide: influence of MHC binding affinity. *Int. Immunol.* **5**, 1159-1165 (1993).

241. Metzler, B. & Wraith, D.C. Mucosal tolerance in a murine model of experimental autoimmune encephalomyelitis. *Ann. NY Acad. Sci.* **778**, 228-242 (1996).

242. Gabrysova, L. & Wraith, D.C. Antigenic strength controls the generation of antigen-specific IL-10-secreting T regulatory cells. *Eur. J. Immunol.* **40**, 1386-1395 (2010).

243. Xiao, B.G. & Link, H. Mucosal tolerance: a two-edged sword to prevent and treat autoimmune diseases. *Clin. Immunol. Immunopathol.* **85**, 119-128 (1997).

244. al-Sabbagh, A., Nelson, P.A., Akselband, Y., Sobel, R.A. & Weiner, H.L. Antigen-driven peripheral immune tolerance: suppression of experimental autoimmmune encephalomyelitis and collagen-induced arthritis by aerosol administration of myelin basic protein or type II collagen. *Cell. Immunol.* **171**, 111-119 (1996).

245. Weiner, H.L. *et al.* Double-blind pilot trial of oral tolerization with myelin antigens in multiple sclerosis. *Science* **259**, 1321-1324 (1993).

246. Faria, A.M. & Weiner, H.L. Oral tolerance: therapeutic implications for autoimmune diseases. *Clin. Dev. Immunol.* **13**, 143-157 (2006).

247. Miller, S.D., Turley, D.M. & Podojil, J.R. Antigen-specific tolerance strategies for the prevention and treatment of autoimmune disease. *Nat. Rev. Immunol.* **7**, 665-677 (2007).

248. Turley, D.M. & Miller, S.D. Peripheral tolerance induction using ethylenecarbodiimide-fixed APCs uses both direct and indirect mechanisms of antigen presentation for prevention of experimental autoimmune encephalomyelitis. *J. Immunol.* **178**, 2212-2220 (2007).

249. Getts, D.R. *et al.* Tolerance induced by apoptotic antigen-coupled leukocytes is induced by PD-L1$^+$ and IL-10-producing splenic macrophages and maintained by T regulatory cells. *J. Immunol.* **187**, 2405-2417 (2011).

250. Getts, D.R. *et al.* Microparticles bearing encephalitogenic peptides induce T-cell tolerance and ameliorate experimental autoimmune encephalomyelitis. *Nat. Biotechnol.* **30**, 1217-1224 (2012).

251. Larche, M. & Wraith, D.C. Peptide-based therapeutic vaccines for allergic and autoimmune diseases. *Nat. Med.* **11**, S69-S76 (2005).

252. Gaur, A., Wiers, B., Liu, A., Rothbard, J. & Fathman, C.G. Amelioration of autoimmune encephalomyelitis by myelin basic protein synthetic peptide-induced anergy. *Science* **258**, 1491-1494 (1992).

253. Warren, K.G., Catz, I., Ferenczi, L.Z. & Krantz, M.J. Intravenous synthetic peptide MBP8298 delayed disease progression in an HLA Class II-defined cohort of patients with progressive multiple sclerosis: results of a 24-month double-blind placebo-controlled clinical trial and 5 years of follow-up treatment. *Eur. J. Neurol.* **13**, 887-895 (2006).

254. Freedman, M.S. *et al.* A phase III study evaluating the efficacy and safety of MBP8298 in secondary progressive MS. *Neurology* **77**, 1551-1560 (2011).

255. Rosenblum, M.D. *et al.* Response to self antigen imprints regulatory memory in tissues. *Nature* **480**, 538-542 (2011).

256. Wherry, E.J. T cell exhaustion. *Nat. Immunol.* **12**, 492-499 (2011).

257. Mi, W. *et al.* Targeting the neonatal Fc receptor for antigen delivery using engineered Fc fragments. *J. Immunol.* **181**, 7550-7561 (2008).

258. Baker, K., Rath, T., Pyzik, M. & Blumberg, R.S. The Role of FcRn in Antigen Presentation. *Front. Immunol.* **5**, 408 (2014).

259. He, X. *et al.* Structural snapshot of aberrant antigen presentation linked to autoimmunity: the immunodominant epitope of MBP complexed with I-A^u. *Immunity* **17**, 83-94 (2002).

260. Liu, G.Y. *et al.* Low avidity recognition of self-antigen by T cells permits escape from central tolerance. *Immunity* **3**, 407-415 (1995).

261. Seamons, A. *et al.* Competition between two MHC binding registers in a single peptide processed from myelin basic protein influences tolerance and susceptibility to autoimmunity. *J. Exp. Med.* **197**, 1391-1397 (2003).

262. Wraith, D.C., Bruun, B. & Fairchild, P.J. Cross-reactive antigen recognition by an encephalitogenic T cell receptor. Implications for T cell biology and autoimmunity. *J. Immunol.* **149**, 3765-3770 (1992).

263. Huang, J.C. *et al.* T cell recognition of distinct peptide:I-A^u conformers in murine experimental autoimmune encephalomyelitis. *J. Immunol.* **171**, 2467-2477 (2003).

264. Wensky, A.K. *et al.* IFN-γ determines distinct clinical outcomes in autoimmune encephalomyelitis. *J. Immunol.* **174**, 1416-1423 (2005).

265. Ando, D.G., Clayton, J., Kono, D., Urban, J.L. & Sercarz, E.E. Encephalitogenic T cells in the B10.PL model of experimental allergic encephalomyelitis (EAE) are of the Th-1 lymphokine subtype. *Cell. Immunol.* **124**, 132-143 (1989).

266. Huang, D.R., Wang, J., Kivisakk, P., Rollins, B.J. & Ransohoff, R.M. Absence of monocyte chemoattractant protein 1 in mice leads to decreased local macrophage recruitment and antigen-specific T helper cell type 1 immune response in experimental autoimmune encephalomyelitis. *J. Exp. Med.* **193**, 713-726 (2001).

267. Liu, E. *et al.* Anti-peptide autoantibodies and fatal anaphylaxis in NOD mice in response to insulin self-peptides B:9-23 and B:13-23. *J. Clin. Invest.* **110**, 1021-1027 (2002).

268. De Groot, A.S. & Scott, D.W. Immunogenicity of protein therapeutics. *Trends Immunol.* **28**, 482-490 (2007).

269. Bluestone, J.A. *et al.* The Immune Tolerance Network at 10 years: tolerance research at the bedside. *Nat. Rev. Immunol.* **10**, 797-803 (2010).

270. Krishnamoorthy, S. *et al.* Recombinant factor VIII Fc (rFVIIIFc) fusion protein reduces immunogenicity and induces tolerance in hemophilia A mice. *Cell. Immunol.* **301**, 30-39 (2015).

271. Tuohy, V.K., Yu, M., Yin, L., Kawczak, J.A. & Kinkel, R.P. Spontaneous regression of primary autoreactivity during chronic progression of experimental autoimmune encephalomyelitis and multiple sclerosis. *J. Exp. Med.* **189**, 1033-1042 (1999).

272. Goebels, N. *et al.* Repertoire dynamics of autoreactive T cells in multiple sclerosis patients and healthy subjects: epitope spreading versus clonal persistence. *Brain* **123**, 508-518 (2000).

273. Bailey, S.L., Schreiner, B., McMahon, E.J. & Miller, S.D. CNS myeloid DCs presenting endogenous myelin peptides 'preferentially' polarize $CD4^+$ T_H-17 cells in relapsing EAE. *Nat. Immunol.* **8**, 172-180 (2007).

274. Iezzi, G., Karjalainen, K. & Lanzavecchia, A. The duration of antigenic stimulation determines the fate of naive and effector T cells. *Immunity* **8**, 89-95 (1998).

275. Yang, Y. *et al.* T-bet is essential for encephalitogenicity of both Th1 and Th17 cells. *J. Exp. Med.* **206**, 1549-1564 (2009).

276. Long, M. *et al.* T-bet down-modulation in tolerized Th1 effector CD4 cells confers a TCR-distal signaling defect that selectively impairs IFN-γ expression. *J. Immunol.* **176**, 1036-1045 (2006).

277. Grewal, I.S. *et al.* Requirement for CD40 ligand in costimulation induction, T cell activation, and experimental allergic encephalomyelitis. *Science* **273**, 1864-1867 (1996).

278. Gerritse, K. *et al.* CD40-CD40 ligand interactions in experimental allergic encephalomyelitis and multiple sclerosis. *Proc. Natl. Acad. Sci. USA* **93**, 2499-2504 (1996).

279. Venkataraman, M., Aldo-Benson, M., Borel, Y. & Scott, D.W. Persistence of antigen-binding cells with surface tolerogen: isologous versus heterologous immunoglobulin carriers. *J. Immunol.* **119**, 1006-1009 (1977).

280. Cousens, L.P. *et al.* Tregitope update: mechanism of action parallels IVIg. *Autoimmun. Rev.* **12**, 436-443 (2013).

281. Bryant, J. *et al.* Nanoparticle delivery of donor antigens for transplant tolerance in allogeneic islet transplantation. *Biomaterials* **35**, 8887-8894 (2014).

282. Sekeres, M.A. *et al.* Subcutaneous or intravenous administration of romiplostim in thrombocytopenic patients with lower risk myelodysplastic syndromes. *Cancer* **117**, 992-1000 (2011).

283. Kavanaugh, A. *et al.* Golimumab, a new human tumor necrosis factor α antibody, administered every four weeks as a subcutaneous injection in psoriatic arthritis: Twenty-four-week efficacy and safety results of a randomized, placebo-controlled study. *Arthritis Rheum.* **60**, 976-986 (2009).

284. Hanauer, S.B. *et al.* Human anti-tumor necrosis factor monoclonal antibody (adalimumab) in Crohn's disease: the CLASSIC-I trial. *Gastroenterology* **130**, 323-333 (2006).

285. Papp, K.A. *et al.* A global phase III randomized controlled trial of etanercept in psoriasis: safety, efficacy, and effect of dose reduction. *Br. J. Dermatol.* **152**, 1304-1312 (2005).

286. Zamvil, S.S. *et al.* T-cell epitope of the autoantigen myelin basic protein that induces encephalomyelitis. *Nature* **324**, 258-260 (1986).

287. Furman, D. & Davis, M.M. New approaches to understanding the immune response to vaccination and infection. *Vaccine* **33**, 5271-5281 (2015).

288. Pearson, C.I. & McDevitt, H.O. Induction of apoptosis and T helper 2 (Th2) responses correlates with peptide affinity for the major histocompatibility complex in self-reactive T cell receptor transgenic mice. *J. Exp. Med.* **185**, 583-599 (1997).

289. Lafaille, J.J., Nagashima, K., Katsuki, M. & Tonegawa, S. High incidence of spontaneous autoimmune encephalomyelitis in immunodeficient anti-myelin basic protein T cell receptor transgenic mice. *Cell* **78**, 399-408 (1994).

290. Feng, D., Bond, C.J., Ely, L.K., Maynard, J. & Garcia, K.C. Structural evidence for a germline-encoded T cell receptor-major histocompatibility complex interaction 'codon'. *Nat. Immunol.* **8**, 975-983 (2007).

291. Zhou, J., Mateos, F., Ober, R.J. & Ward, E.S. Conferring the binding properties of the mouse MHC class I-related receptor, FcRn, onto the human ortholog by sequential rounds of site-directed mutagenesis. *J. Mol. Biol.* **345**, 1071-1081 (2005).

292. Weissleder, R., Nahrendorf, M. & Pittet, M.J. Imaging macrophages with nanoparticles. *Nat. Mater.* **13**, 125-138 (2014).

293. Lee, S.H., Starkey, P.M. & Gordon, S. Quantitative analysis of total macrophage content in adult mouse tissues. Immunochemical studies with monoclonal antibody F4/80. *J. Exp. Med.* **161**, 475-489 (1985).

294. Hume, D.A., Halpin, D., Charlton, H. & Gordon, S. The mononuclear phagocyte system of the mouse defined by immunohistochemical localization of antigen F4/80: macrophages of endocrine organs. *Proc. Natl. Acad. Sci. USA* **81**, 4174-4177 (1984).

295. van oud Alblas, A.B. & van Furth, R. Origin, Kinetics, and characteristics of pulmonary macrophages in the normal steady state. *J. Exp. Med.* **149**, 1504-1518 (1979).

296. Crofton, R.W., Diesselhoff-den Dulk, M.M. & van Furth, R. The origin, kinetics, and characteristics of the Kupffer cells in the normal steady state. *J. Exp. Med.* **148**, 1-17 (1978).

297. Barnard, D.L. *et al.* Chronic myelomonocytic leukemia with paraproteinemia but no detectable plasmacytosis: a detailed cytological and immunological study. *Cancer* **44**, 927-936 (1979).

298. Solal-Celigny, P. *et al.* Chronic myelomonocytic leukemia according to FAB classification: analysis of 35 cases. *Blood* **63**, 634-638 (1984).

299. Cervenak, J. *et al.* Neonatal FcR overexpression boosts humoral immune response in transgenic mice. *J. Immunol.* **186**, 959-968 (2011).

300. Schneider, Z. *et al.* Overexpression of bovine FcRn in mice enhances T-dependent immune responses by amplifying T helper cell frequency and germinal center enlargement in the spleen. *Front. Immunol.* **6**, 357 (2015).

301. Clausen, B.E., Burkhardt, C., Reith, W., Renkawitz, R. & Forster, I. Conditional gene targeting in macrophages and granulocytes using LysMcre mice. *Transgenic Res.* **8**, 265-277 (1999).

302. Caton, M.L., Smith-Raska, M.R. & Reizis, B. Notch-RBP-J signaling controls the homeostasis of $CD8^-$ dendritic cells in the spleen. *J. Exp. Med.* **204**, 1653-1664 (2007).

303. Rickert, R.C., Roes, J. & Rajewsky, K. B lymphocyte-specific, Cre-mediated mutagenesis in mice. *Nucleic Acids Res.* **25**, 1317-1318 (1997).

304. Schulz, C. *et al.* A lineage of myeloid cells independent of Myb and hematopoietic stem cells. *Science* **336**, 86-90 (2012).

305. Sheng, J., Ruedl, C. & Karjalainen, K. Most Tissue-resident macrophages except microglia are derived from fetal hematopoietic stem cells. *Immunity* **43**, 382-393 (2015).

306. Sheng, J., Ruedl, C. & Karjalainen, K. Fetal HSCs versus EMP2s. *Immunity* **43**, 1025 (2015).

307. El Kasmi, K.C. *et al.* Toll-like receptor-induced arginase 1 in macrophages thwarts effective immunity against intracellular pathogens. *Nat. Immunol.* **9**, 1399-1406 (2008).

308. Gomez Perdiguero, E. *et al.* Tissue-resident macrophages originate from yolk-sac-derived erythro-myeloid progenitors. *Nature* **518**, 547-551 (2015).

309. Tang, Y., Harrington, A., Yang, X., Friesel, R.E. & Liaw, L. The contribution of the $Tie2^+$ lineage to primitive and definitive hematopoietic cells. *Genesis* **48**, 563-567 (2010).

310. Kano, A. *et al.* Endothelial cells require STAT3 for protection against endotoxin-induced inflammation. *J. Exp. Med.* **198**, 1517-1525 (2003).

311. Wang, Y. *et al.* Ephrin-B2 controls VEGF-induced angiogenesis and lymphangiogenesis. *Nature* **465**, 483-486 (2010).

312. Kim, J. *et al.* Albumin turnover: FcRn-mediated recycling saves as much albumin from degradation as the liver produces. *Am. J. Physiol. Gastrointest. Liver Physiol.* **290**, G352-G360 (2006).

313. Burnett, S.H. *et al.* Conditional macrophage ablation in transgenic mice expressing a Fas-based suicide gene. *J. Leukoc. Biol.* **75**, 612-623 (2004).

314. Abram, C.L., Roberge, G.L., Hu, Y. & Lowell, C.A. Comparative analysis of the efficiency and specificity of myeloid-Cre deleting strains using ROSA-EYFP reporter mice. *J. Immunol. Methods* **408**, 89-100 (2014).

315. Schmidt-Supprian, M. & Rajewsky, K. Vagaries of conditional gene targeting. *Nat. Immunol.* **8**, 665-668 (2007).

316. Zheng, B., Sage, M., Sheppeard, E.A., Jurecic, V. & Bradley, A. Engineering mouse chromosomes with Cre-loxP: range, efficiency, and somatic applications. *Mol. Cell. Biol.* **20**, 648-655 (2000).

317. Hashimoto, D. *et al.* Tissue-resident macrophages self-maintain locally throughout adult life with minimal contribution from circulating monocytes. *Immunity* **38**, 792-804 (2013).

318. Epelman, S. *et al.* Embryonic and adult-derived resident cardiac macrophages are maintained through distinct mechanisms at steady state and during inflammation. *Immunity* **40**, 91-104 (2014).

319. Gundra, U.M. *et al.* Alternatively activated macrophages derived from monocytes and tissue macrophages are phenotypically and functionally distinct. *Blood* **123**, e110-122 (2014).

320. Guth, A.M. *et al.* Lung environment determines unique phenotype of alveolar macrophages. *Am. J. Physiol. Lung Cell. Mol. Physiol.* **296**, L936-946 (2009).

321. Lim, J.P. & Gleeson, P.A. Macropinocytosis: an endocytic pathway for internalising large gulps. *Immunol. Cell Biol.* **89**, 836-843 (2011).

322. Sedor, J. *et al.* Cathepsin-G interferes with clearance of *Pseudomonas aeruginosa* from mouse lungs. *Pediatr. Res.* **61**, 26-31 (2007).

323. Karnak, D., Beder, S., Kayacan, O. & Karaca, L. IgG subclass levels in ELF in COPD. *Turk. J. Med. Sci.* **31**, 235-241 (2001).

324. Fahy, R.J., Diaz, P.T., Hart, J. & Wewers, M.D. BAL and serum IgG levels in healthy asymptomatic HIV-infected patients. *Chest* **119**, 196-203 (2001).

325. Dalloneau, E. *et al.* Downregulation of the neonatal Fc receptor expression in non-small cell lung cancer tissue is associated with a poor prognosis. *Oncotarget* **7**, 54415-54429 (2016).

326. Marelli-Berg, F.M., Peek, E., Lidington, E.A., Stauss, H.J. & Lechler, R.I. Isolation of endothelial cells from murine tissue. *J. Immunol. Methods* **244**, 205-215 (2000).

327. Molnarfi, N. *et al.* MHC class II-dependent B cell APC function is required for induction of CNS autoimmunity independent of myelin-specific antibodies. *J. Exp. Med.* **210**, 2921-2937 (2013).

328. Weber, M.S. *et al.* B-cell activation influences T-cell polarization and outcome of anti-CD20 B-cell depletion in central nervous system autoimmunity. *Ann. Neurol.* **68**, 369-383 (2010).

329. Cao, Y. *et al.* Functional inflammatory profiles distinguish myelin-reactive T cells from patients with multiple sclerosis. *Sci. Transl. Med.* **7**, 287ra274 (2015).

330. Lutterotti, A. *et al.* Antigen-specific tolerance by autologous myelin peptide-coupled cells: a phase 1 trial in multiple sclerosis. *Sci. Transl. Med.* **5**, 188ra175 (2013).

331. Moore, G.L. *et al.* A novel bispecific antibody format enables simultaneous bivalent and monovalent co-engagement of distinct target antigens. *MAbs* **3**, 546-557 (2011).

332. Gabrysova, L. *et al.* Negative feedback control of the autoimmune response through antigen-induced differentiation of IL-10-secreting Th1 cells. *J. Exp. Med.* **206**, 1755-1767 (2009).

333. Grifka-Walk, H.M. & Segal, B.M. T-bet promotes the accumulation of encephalitogenic Th17 cells in the CNS. *J. Neuroimmunol.* (2016) [DOI: http://dx.doi.org/10.1016/j.jneuroim.2016.05.007].